NUREG/CR-1953
BNL-NUREG-51345

MULTIPLE DNB EVENTS

Amir N. Nahavandi, Carlos F. Fighetti,
Devuni G. Reddy, Tsun Chiu L. Poon

Date Published - January 1981

DEPARTMENT OF NUCLEAR ENERGY BROOKHAVEN NATIONAL LABORATORY
UPTON, N.Y. 11973

Prepared for the U.S. Nuclear Regulatory Commission
Office of Nuclear Reactor Regulation
Contract No. DE-AC02-76CH00016

NUREG/CR-1953
BNL-NUREG-51345
AN, R-2

MULTIPLE DNB EVENTS

Prepared by
Amir N. Nahavandi, Carlos F. Fighetti,
Devuni G. Reddy, Tsun Chiu L. Poon

HEAT TRANSFER RESEARCH FACILITY
DEPARTMENT OF CHEMICAL ENGINEERING
COLUMBIA UNIVERSITY, NEW YORK, NEW YORK

Under BNL Contract Number 500944-S

DEPARTMENT OF NUCLEAR ENERGY
BROOKHAVEN NATIONAL LABORATORY
ASSOCIATED UNIVERSITIES, INC.
UPTON, LONG ISLAND, N.Y. 11973
FIN A-3353

ABSTRACT

The phenomenon of multiple DNB events in rod bundle heat transfer tests, referring to the occurrence of departure from nucleate boiling (DNB) on more than one heating rod or at more than one location on one heating rod, is examined. This phenomenon is characterized by the deterioration of heat transfer due to the transition from nucleate boiling to film boiling at low steam qualities or due to dryout at high steam qualities. The deterioration of heat transfer is observed by recording the temperature excursion of the heating rod thermocouples located in the region where DNB is anticipated. The available rod bundle test data at Columbia University, Heat Transfer Research Facility, are examined for multiple DNB events using a combination of parametric studies, statistical analyses and predictive correlation approach. The parametric studies involve: 1) the plots of the bundle average mass velocity contours in the plane of the bundle average DNB heat flux versus bundle inlet temperature for individual test sections at specified test pressures; and 2) the plots of constant pressure contours in the plane of the bundle average DNB heat flux versus steam energy flow for a large number of test sections and test conditions. The statistical analyses include: 1) the plots of the percent number of the multiple DNB events versus pressure, bundle average mass velocity or the bundle inlet subcooling and their comparison with the overall trend; and 2) the plots of the relative cumulative frequency distribution of the multiple DNB events at constant pressure, bundle average mass velocity or bundle inlet subcooling and their comparison with the overall trend. The predictive correlation studies show the capability of an available DNB correlation (Bowring Correlation) in the prediction of multiple DNB events together with the associated statistical data. The combination of the above analyses were applied to the study of three data sets of rod bundle heat transfer tests performed at Columbia University,

Heat Transfer Research Facility, simulating both PWR and BWR reactor cores as well as uniform and non-uniform axial flux distribution. Examination of the above results indicate that: 1) the number of multiple DNB events of higher rank than one are significant as compared to the first DNB: 2) the characteristic behavior of DNB events of higher rank than one are essentially close to those of the first DNB; and 3) the presently available DNB correlations for the first DNB, based on the bundle average conditions, are useful in the prediction of DNB events of higher rank. These correlations could predict the DNB events of higher rank with the same degree of accuracy as the first DNB. It is recommended that studies be conducted to ascertain the adequacy of predictive correlations based on local conditions at first DNB, for the prediction of DNB events of higher rank. The above conclusions are valid for rod bundle DNB tests operating under steady state conditions. Multiple DNB events occurring under transient test conditions, such as flow decay, have also been addressed in this report. The information needed by a subchannel computer code, such as COBRA-IIIC, for the determination of the rod bundle local conditions during flow decay tests have also been compiled. This information will further serve to ascertain the adequacy of predictive correlations based on local conditions at first DNB, for the prediction of DNB events of higher rank during transient conditions.

TABLE OF CONTENT

LIST OF FIGURES

LIST OF FIGURES

LIST OF FIGURES

LIST OF FIGURES

LIST OF TABLES

NOMENCLATURE

A	A parameter defined by Eqs (A-2) and (A-8)
A_1, A_2	Parameters defined by Eqs (A-9) and (A-10) respectively
B, C	Parameters defined by Eqs (A-3) and (A-4) respectively
D_h	Channel hydraulic diameter, in
D_w	Channel heated diameter, in
F_p	Radial heat flux peaking factor
F_1, F_2	Parameters defined by Eqs (A-6) and (A-7) respectively
G	Mass velocity (mass flux), million lbs/hr-sq.ft
h	Enthalpy, btu/lb
p	Pressure, psia
p_T	A parameter defined by Eq (A-5)
q	Heat flux, million btu/hr-sq.ft
SEF	Steam energy flow defined by Eqs (1), (2) and (3), million btu/hr-sq.ft (Note: The scale of x-axis in Figures 7a, 7b, 7c and 7d is 0.5 + SEF/500. for convenience)
x	Steam quality
Y	Ratio of average heat flux over the heated length to local radially averaged heat flux at DNB point (Note: Y=1 for axially uniform heat flux)
Z	Bundle heated length, in

Subscripts

DNB	Refers to departure from nucleate boiling
f	Refers to saturated liquid or final whichever applicable
fg	Refers to latent heat evaporation
i	Refers to initial
in	Refers to inlet to the rod bundle

1. INTRODUCTION

One of the most important limits in the design of water cooled reactors is the condition at which the boiling heat transfer coefficient in the core begins to deteriorate. This condition, often referred to as the departure from nucleate boiling (DNB), is accompanied by a change in fuel rod to coolant heat transfer mechanism which results in a significant decrease in heat transfer capability, and excessive clad temperatures.

Heat transfer tests to investigate DNB are performed in rod bundle test facilities, in which an array of electrically-heated rods is installed in a vertical pressure housing with the loop water flowing through the rod assembly.

The Columbia University rod bundle test facility consist of four major installations: two high pressure flow loops, a low pressure loop and an emergency core cooling system simulation loop. Each loop is composed of the following elements: the primary coolant circulation loop, the test section, the DC power supply, the process instrumentation and control system and the auxiliary gas, air and water systems. A comprehensive measurement and computer-controlled high speed data acquisition system records the heat transfer test data (1)*.

Two types of DNB heat transfer tests are conducted at Columbia rod bundle test facility:

1) Steady state DNB tests

2) Transient DNB tests

1.1 Steady State DNB Tests

During steady state DNB heat transfer tests, heat is applied to the test section to determine the heat flux and lo-

*Underlined numerals in parenthesis designate references at the end of this study

cations at which DNB occur for various test sections, heat flux distribution and test conditions.

The test section geometry may have a square pitch consisting of a square array of 3 x 3 to 6 x 6 rods or a triangular pitch with 19 to 37 rods. The rod diameter varies between 0.374" to 0.56" and the test section length is between 4' to 14'.

The heat flux distribution may have one of the following forms: axially and radially uniform, axially and radially non-uniform, axially uniform radially non-uniform and axially non-uniform radially uniform. The non-uniform axial heat flux distribution may be chopped cosine, top skewed, bottom skewed or spiked.

The range of the test conditions are tabulated hereunder:

Bundle Parameter	Range	Units
Inlet temperature	300 to 650	Deg. F
Average mass velocity	0.5 to 4.	$\frac{\text{M lb}}{\text{Hr ft}^2}$
Average heat flux	0.1 to 1.2	$\frac{\text{M Btu}}{\text{Hr ft}^2}$
Pressure	500 to 2400	Psia

The DNB data are obtained by raising the bundle average heat flux incrementally while keeping the bundle inlet temperature, average mass velocity and pressure constant, as closely as possible. At certain value of the bundle average heat flux, heat transfer deteriorates either due to the transition from nucleate boiling to film boiling at low steam qualities or due to dryout at high steam qualities. The deterioration of heat transfer, referred to as DNB, is observed by noticing the temperature excursion of the strip chart recorder showing the temperature of the rod thermocouples located in the region where DNB is anticipated. The data acquisition

computer system monitors the status of the test loop and records the test conditions at each incremental bundle average heat flux. Upon noticing the strip chart recorder excursion, the bundle average heat flux is reduced and the operator records both the locations of the thermocouples undergoing DNB and the order of occurrence of DNB, to his best judgement. The test section geometry, typically shown in Figure 1, the test conditions (i.e., bundle inlet temperature, average mass velocity, average heat flux and pressure) and the location as well as the order of occurrence of DNB, typically shown in Figure 2, constitute the record of steady state DNB tests used for further processing. A comprehensive documentation of the test sections geometry and test conditions together with the location and the order of occurrence of DNB for all available DNB data points obtained at the Columbia University, Heat Transfer Research Facility, is being compiled under the auspices of Electric Power Research Institute RP-813-1 entitled, "Parametric Study of CHF Data". Topical reports on this study are being prepared and will be released later.

An examination of these records reveals that many DNB tests involve the occurrence of departure from nucleate boiling on more than one rod or at more than one location on one rod. The order of occurrence of DNB in the printout sheets (Figure 2) is from left to right. Digits to the left of the decimal point designate the rod number and digits to the right of the decimal point designate the axial or circumferential location of the thermocouple on the rod as shown in Figures 3a and 3b. For example, for a uniform axial heat flux distribution (Figure 3a) the following indications:

20.1	20.4	21.1	21.4
.0	.0	.0	.0

mean that there are two DNB events observed on rod number 20 at circumferential positions 1 and 4 and two DNB events on rod rumber 21 at positions 1 and 4. The sequence of the ob-

CE TEST SECTION # 37.0

TOTAL NUMBER OF RODS	:	22
HEATED RODS	:	21
ROD PITCH(INCH)	:	.580
H.R. DIAMETER(INCH)	:	.440
G.T. DIAMETER(INCH)	:	1.12
HEATED LENGTH(INCH)	:	84.00
ROD TO WALL GAP(INCH)	:	.135
FLOW AREA(SQ.INCH)	:	4.835
CORNER RADIUS(INCH)	:	.00
BLOCKAGE LENGTH(INCH)	:	1.00

NUMBER OF AXIAL FLUX DISRIBUTION POINTS: 0

NUMBER OF GRIDS: 4
TYPE OF GRIDS : 1

GRID TYPES AND GRID LOCATION:
(DISTANCE FROM INLET (INCH))

1 11.75 1 30.00 1 48.25 1 66.50

ROD PATTERN

1	2	3	4	5
14	15	16	17	6
13	20	21	18	7
12	19	0	0	8
11	10	0	0	9

RADIAL POWER DISTRIBUTION:

.9806	.9673	.9692	.9774	.9704
1.1562	.9806	.9686	.9717	.9749
.9692	.9870	1.1526	1.1597	.9711
.9437	.9838	.0000	.0000	.9787
.9877	.9692	.0000	.0000	.9806

DISTANCE BETWEEN PRESSURE TAPS : 98.00
NUMBER OF GRIDS BETWEEN PRESSURE TAPS: 5

FIGURE 1 TYPICAL TEST SECTION GEOMETRY FOR STEADY STATE DNB TESTS

FIGURE 2 SAMPLE OF TEST CONDITIONS FOR STEADY STATE DNB TESTS

TEST SECTION NUMBER = 37

SERIAL NO.	RUN NO.	PRESSURE (PSIA)	INLET TEMP (°F)	AVE. G	AVE. Q	DNB RODS			
1	14	2300.	625.0	1.959	.368	20.1	20.4	.0	.0
						.0	.0	.0	.0
2	15	2000.	602.0	2.074	.384	20.1	20.4	21.1	21.4
						.0	.0	.0	.0
3	16	2300.	624.0	2.001	.367	20.1	20.4	.0	.0
						.0	.0	.0	.0
4	17	1800.	601.0	2.002	.337	20.3	20.4	20.2	21.4
						.0	.0	.0	.0
5	18	2300.	581.0	1.978	.465	18.1	18.4	20.1	20.4
						21.1	.0	.0	.0
6	19	2005.	565.0	1.983	.470	21.1	21.4	20.1	20.3
						20.4	.0	.0	.0
7	20	1800.	560.0	1.985	.459	18.1	18.4	20.1	20.3
						20.4	.0	.0	.0
8	21	2290.	541.0	2.001	.555	21.1	20.1	20.4	18.1
						.0	.0	.0	.0
9	22	2000.	522.0	1.988	.551	21.1	21.4	18.1	.0
						.0	.0	.0	.0
10	23	1800.	525.0	1.991	.515	21.1	21.4	18.1	18.4
						.0	.0	.0	.0
11	24	2300.	508.0	1.994	.622	18.1	21.1	20.1	.0
						.0	.0	.0	.0
12	25	2000.	489.0	1.994	.620	18.1	18.4	21.1	21.4
						.0	.0	.0	.0
13	26	1800.	483.0	1.992	.605	21.1	21.4	18.1	18.4
						.0	.0	.0	.0
14	27	2300.	481.0	1.972	.677	18.1	20.1	20.4	21.1
						.0	.0	.0	.0
15	28	2005.	467.0	1.981	.663	18.1	20.1	20.4	21.1
						.0	.0	.0	.0
16	29	1800.	442.0	2.010	.692	18.1	21.1	.0	.0
						.0	.0	.0	.0
17	34	2315.	621.0	3.053	.512	18.1	18.4	20.1	20.4
						.0	.0	.0	.0
18	35	2300.	550.0	2.959	.475	18.1	18.4	20.1	20.4
						.0	.0	.0	.0
19	36	2305.	613.0	2.980	.531	18.1	18.4	20.1	20.4
						.0	.0	.0	.0
20	37	2300.	590.0	2.983	.607	18.1	18.4	20.1	20.3
						.0	.0	.0	.0
21	38	2000.	614.0	3.015	.440	20.4	20.1	20.3	21.4
						.0	.0	.0	.0
22	39	1995.	602.0	2.968	.471	20.4	20.1	20.3	21.4
						.0	.0	.0	.0
23	40	1805.	596.0	3.014	.435	20.4	20.3	20.1	21.4
						.0	.0	.0	.0
24	41	2300.	555.0	2.961	.650	18.1	18.4	20.1	20.4
						.0	.0	.0	.0
25	42	1995.	574.0	3.036	.550	18.1	18.4	20.1	20.3
						.0	.0	.0	.0

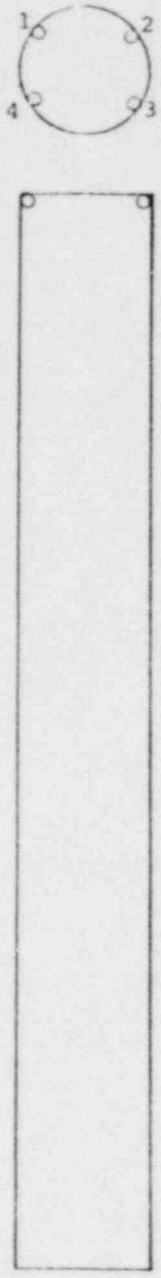

FIGURE 3a CIRCUMFERENTIAL LOCATIONS OF ROD THERMOCOUPLES FOR RODS WITH UNIFORM AXIAL HEAT FLUX DISTRIBUTION

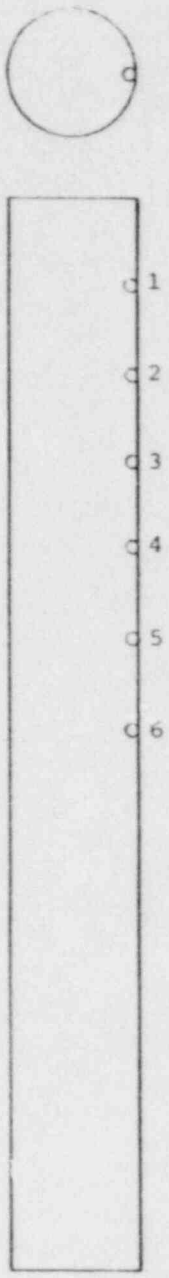

FIGURE 3b AXIAL LOCATIONS OF ROD THERMOCOUPLES FOR RODS WITH NON-UNIFORM AXIAL HEAT FLUX DISTRIBUTION

served DNB events is as follows:

Rod 20	location 1	first DNB
Rod 20	location 4	second DNB
Rod 21	location 1	third DNB
Rod 21	location 4	fourth DNB

The zeros indicate that no further DNB events were observed.

It should be further noted that for rods with uniform axial heat flux distribution, DNB occurs at the end of the rod where four thermocouples are installed circumferentially as shown in Figure 3a. For rods with non-uniform axial heat flux distribution, DNB occurs generally between the rod end and midlength where several thermocouples are installed axially as shown in Figure 3b.

Generally speaking, the second observed DNB falls within one of the following categories:

Category	Description
A	Second DNB occurs on the same rod at the same elevation as the first DNB
B	Second DNB occurs on the same rod as the first DNB but at a different elevation
C	Second DNB occurs on a different rod from the first DNB

Similarly, the third observed DNB falls within one of the following categories:

Category	Description
A	Third DNB occurs on the same rod at the same elevation as the first DNB
B	Third DNB occurs on the same rod as the first DNB but at a different elevation
C	Third DNB occurs on a different rod from the first DNB

Extending the above definition, multiple DNB events of

high rank (4th, 5th, -------) can be defined in terms of the first DNB. Since most DNB studies and the resulting correlations have been developed for the first DNB, it is logical to compare the multiple DNB events of higher rank to the first DNB.

For rods with uniform axial heat flux distribution, only DNB categories A and C are recorded. For rods with non-uniform axial heat flux distribution, only DNB categories B and C are recorded.

1.2 Transient DNB Tests

The transient DNB tests are performed on rod bundles with the same geometric configuration, heat flux distribution and test conditions as the steady state DNB tests. Two types of tests are conducted, namely, flow decay and loss-of-coolant tests. In the flow decay tests, all test conditions including the bundle inlet temperature, average heat flux and pressure are held constant, as closely as possible, while lowering the bundle average mass velocity until DNB is observed by noticing the rod thermocouples temperature excursions on the strip chart recorder. In the loss-of-coolant tests, following a simulated rupture in the test loop, all test conditions including the bundle inlet temperature, average heat flux and average mass velocity vary with time. The loss-of-coolant tests result in flow oscillations and reversal in the test section which lead to DNB. The loss-of-coolant multiple DNB events are beyond the scope of this study and will not be further discussed.

The data acquisition computer system monitors the test conditions during the flow decay tests and records the test conditions. Upon noticing the strip chart recorder excursion, the bundle average heat flux is reduced. The locations and the order of occurrence of DNB, in flow decay tests are determined by a careful examination of the computer records which will be discussed later in this report.

Typical test conditions, the location and the order of occurrence of DNB for flow decay tests are shown on Figures 4 and 5. An examination of these records reveals the occurrence of multiple DNB events, similar to those discussed earlier in the steady state DNB tests.

TEST SECTION EXACT PEAK CLAD

```
TOTAL NUMBER OF RODS :    16
HEATED RODS          :    16
ROD PITCH(INCH)      :  .642
H.R. DIAMETER(INCH)  :  .490
G.T. DIAMETER(INCH)  :   .49
HEATED LENGTH(INCH)  :144.00
ROD TO WALL GAP(INCH):  .142
FLOW AREA(SQ.INCH)   : 7.198
CORNER RADIUS(INCH)  :   .40
BLOCKAGE LENGTH(INCH):   .00

NUMBER OF AXIAL FLUX DISTRIBUTION POINTS:     7

DISTRIBUTION (X,Y) :

 .000   .580   .200   .000   .400   .900   .600  1.450   .700  1.500
 .800  1.400  1.000   .400   .000   .000   .000   .000   .000   .000
 .000   .000   .000   .000   .000   .000   .000   .000   .000   .000
 .000   .000

THERMOCOUPLE LOCATIONS :
 94.400 106.000 110.000 114.000 125.500 129.500 133.500 143.500

NUMBER OF GRIDS:     8
TYPE OF GRIDS  :     1

GRID TYPES AND GRID LOCATION:
(DISTANCE FROM INLET (INCH) )

 1  -2.80  1  15.70  1  35.20  1  55.80  1  75.50  1  94.80
 1 114.40  1 133.90
```

ROD PATTERN

1	2	3	4
12	13	14	5
11	16	15	6
10	9	8	7

RADIAL POWER DISTRIBUTION: 0

1.0600	1.0600	1.2400	1.0600
.8400	.8400	1.0600	1.2400
.8400	1.0600	.8400	1.0600
.8400	.8400	.8400	1.0600

FIGURE 4 TYPICAL TEST SECTION GEOMETRY FOR FLOW DECAY DNB TESTS

RUN NUMBER 15

F00038

FIGURE 5 SAMPLE OF TEST CONDITIONS FOR FLOW DECAY DNB TESTS

PRESSURE (PSIA)	INLET TEMPERATURE (DEGREE F)	INITIAL MASS FLUX (MLB/HR-FT2)	HEAT FLUX (MBTU/HR-FT2)
1000.00	516.00	.80	.20

ORDER OF OCCURRENCE OF DNB

3.6 5.5 5.6 5.8 3.8

TRANSIENT CONDITIONS:

TIME (SEC) VERSUS MASS FLUX (MBTU/HR/FT2)

2.670	.803	2.970	.805	3.060	.805	3.150	.805	3.250	.806
3.340	.805	3.430	.805	3.520	.801	3.620	.803	3.710	.758
3.800	.753	3.900	.755	3.990	.746	4.080	.727	4.170	.724
4.270	.715	4.360	.698	4.450	.689	4.550	.679	4.640	.665
4.730	.655	4.820	.643	4.920	.633	5.010	.624	5.100	.610
5.200	.600	5.290	.588	5.380	.576	5.470	.571	5.570	.562
5.660	.552	5.750	.538	5.850	.531	5.940	.516	6.030	.505
6.120	.500	6.220	.495	6.310	.483	6.400	.478	6.500	.469
6.590	.453	6.680	.447	6.770	.438	6.870	.432	6.960	.421
7.050	.413	7.150	.406	7.240	.401	7.330	.397	7.420	.385
7.520	.383	7.610	.377	7.700	.368	7.800	.364	7.890	.354
7.980	.351	8.070	.347	8.170	.342	8.260	.337	8.350	.335
8.450	.328	8.540	.327	8.630	.322	8.720	.318	8.820	.320
8.910	.322	9.000	.322	9.100	.325	9.190	.328	9.280	.332
9.370	.334	9.470	.337	9.560	.344	9.650	.349	9.750	.359
9.840	.371	9.930	.385	10.020	.397	10.120	.399	10.210	.407
10.300	.407	10.390	.407	10.490	.402	10.580	.387	10.670	.373
10.770	.363	10.860	.339	10.950	.316	11.040	.294	11.140	.273
11.230	.263	11.320	.259	11.420	.217	11.510	.193	11.600	.174
11.690	.156	11.790	.144	11.880	.126	11.970	.105	12.070	.083
12.160	.070	12.250	.05[illegible]	12.340	.036	12.440	.055	12.530	.066
12.620	.026	12.720	.033	.810	.009	12.900	.031	12.990	.019
13.090	.019	13.180	.005	13.270	.006	13.360	.015	13.460	.009
13.550	.007	13.640	.200	13.740	.003	13.830	.005	13.920	.000
14.010	.043	14.110	.007	14.200	.024	14.290	.0 9	14.390	.000
14.480	.046	14.570	.034	14.660	.319	14.760	.036	14.850	.053
14.940	.041	15.110	.029	15.210	.066	15.300	.071	15.390	.012
15.480	.177	15.560	.028	15.670	.050	15.760	.115	15.860	.005
15.950	.026	16.040	.005	16.130	.021	16.230	.000	16.320	.124
16.410	.019	16.510	.000	16.600	.083	16.690	.030	16.780	.046
16.880	.021	16.970	.060	17.060	.021	17.150	.046	17.250	.002
17.340	.005	17.430	.005	17.530	.002	17.620	.000	17.710	.046
17.800	.005	17.900	.029	17.990	.014	18.080	.005	18.180	.057
18.270	.126	18.360	.000	18.450	.022	18.550	.115	18.640	.124
18.730	.026	18.830	.050	18.920	.028	19.010	.000	19.100	.014
19.200	.040	19.290	.026	19.380	.021	19.480	.055	19.570	.041
19.660	.014	19.750	.009	19.850	.012	19.940	.036	20.030	.009
20.130	.031	20.220	.074	20.310	.062	20.400	.012	20.500	.033

20.590	.002	20.680	.000	20.780	.000	20.870	.007	20.960	.060
21.050	.007	21.150	.000	21.240	.002	21.330	.019	21.420	.007
21.520	.043	21.610	.000	21.700	.026	21.800	.033	21.890	.146
21.980	.009	22.070	.002	22.170	.062	22.260	.007	22.350	.007
22.450	.000	22.540	.009	22.630	.148	22.720	.024	22.820	.012
22.910	.031	23.000	.000	23.090	.009	23.190	.002	23.280	.000
23.370	-.003	23.47[illegible]	.047	23.560	.024	23.650	.048	23.740	.005
23.840	.074	23.[illegible]30	.010	24.020	.016	24.120	.067	24.210	.012
24.300	-.003	24.390	.007	24.490	.012	24.580	-.003	24.670	-.003
24.770	.182	24.860	.000	24.950	.014	25.040	-.003	25.140	.164
25.230	-.003	25.320	.009	25.410	.047	25.510	.012	25.600	.048
25.690	.022	25.790	.003	25.880	-.003	25.970	.014	26.060	-.003

1.3 Relevance of the Multiple DNB Events in Reactor Licensing

Reactor vendors have used the avoidance of DNB as a design criterion for many years. Furthermore, the present licensing calculations conservatively assume that clad failure and fission gas release from the gap occurs if DNB is predicted. For these reasons, information on multiple DNB events is not likely to have a significant influence on reactor licensing in the short term. However, a study of multiple DNB events is necessary for a number of reasons:

1) The occurence of multiple DNB events on the same rod and the axial extent of DNB could significantly influence post-DNB behavior such as the ability to quench the fuel rods. Information on multiple DNB events on the same rod is important for the prediction of the fuel rod behavior.

2) Some reactor vendors have accident criteria on clad temperatures. For example, Westinghouse has a 2700°F criteria for the locked-rotor accident. The calculated clad temperature could be somewhat affected by the occurrence of DNB at more than one location on the fuel rod. As more information on post-DNB fuel behavior becomes available, it is likely that licensees and license applicants will submit applications in support of a change in this criterion to a more realistic fuel damage criterion based on fuel temperature and perhaps internal pressure. If this occurs, a better understanding of multiple DNB events and post-DNB behavior will be needed by the NRC staff in support of the review of those applications.

3) Multiple DNB events on different fuel rods are of potential safety significance since the calculations of DNB on one fuel rod might imply degraded heat transfer and the potential clad failure of a number of fuel rods.

Based on the above statements, it can be concluded that multiple DNB events can be of importance for the prediction of the fuel rod behavior and, therefore, of potential safety significance in the future licensing of water reactors.

1.4 Scope and Objectives

The objective of this study is to survey the available test data at Columbia University, Heat Transfer Research Facility, for multiple DNB events, determine the probability of these events versus parameter variations, and assess whether these events can be predicted by the DNB correlations presently used in reactor licensing. This study is divided into two Tasks:

Task I: Survey of the Available DNB Data for Multiple DNB Events and Statistical Analysis

This task consists of the following subtasks:

Steady-State DNB Data

1) Survey the available test data at Columbia University, Heat Transfer Research Facility, for multiple DNB events and compile statistics with bundle average conditions.

2) Determine the probability of multiple DNB events versus parameter variations such as bundle average flow, inlet subcooling, pressure, etc.

Transient DNB Data

1) Survey the available flow decay test data at Columbia University, Heat Transfer Research Facility, for multiple DNB events and compile the information needed by a subchannel computer code, such as COBRA-IIIC, for the determination of the rod bundle local conditions.

TASK II: Determination of Local Conditions and Verification of the Existing DNB Correlations in the Prediction of second and third NDB Events

This task consists of the following subtasks:

Steady-State DNB Data

1) Determine local conditions in the rod bundle, using COBRA-IIIC code, when multiple DNB events are observed.

2) Determine the probability of multiple DNB events versus local parameters variations such as flow, quality, heat flux, etc.

3) Compare the second and third DNB events to the appropriate correlation based on the first DNB.

Transient DNB Data

1) Determine local conditions for multiple DNB events during flow decay tests.

2) Determine the probability of multiple DNB events versus local parameter variations during flow decay tests.

3) Compare multiple DNB events during flow decay tests to appropriate correlations based on the first DNB events.

This report contains the results of studies performed under Task I, described above. Studies under Task II have not yet been undertaken at the time of this write up.

2. ANALYSIS OF STEADY STATE MULTIPLE DNB EVENTS

As stated earlier, the prevailing test conditions (i.e., test section heat flux distribution, pressure, bundle inlet temperature and bundle average mass velocity) for the first DNB are the same as the test conditions for the multiple DNB events of higher rank. Thus, the global experimental information available for the multiple DNB events is essentially the same as the information collected for the first DNB. For this reason, the basic philosophy in the present analysis is to apply the procedures used traditionally for the study of the first DNB to the study of the DNB events of higher rank in order to determine similarities, differences or trends among the multiple DNB events.

The steady state DNB tests are analyzed by the following procedures:

1. Parametric Studies

   a) Plots of bundle average mass velocity contours in the plane of the bundle average DNB heat flux versus bundle inlet temperature for individual test sections at specified test pressures.

   b) Plots of constant pressure contours in the plane of the bundle average DNB heat flux versus steam energy flow for a large number of test sections and test conditions.

2. Statistical Analyses

   a) A comparison of the percent number of the multiple DNB events versus pressure, bundle average mass velocity or bundle inlet quality with the overall trend.

   b) A comparison of the relative cumulative frequency distribution of the multiple DNB events at constant pressure, bundle average mass velocity or bundle inlet quality with the overall trend.

3. Predictive Correlation Studies

a) Plots of the ratio of the calculated to observed multiple DNB heat flux versus observed DNB heat flux, bundle average mass velocity, bundle inlet quality or pressure.

b) Statistical data on the above predictive coorelation studies.

Details of the above studies are presented in the following sections.

2.1 Parametric Studies

Parametric studies are performed by the examination of the following characteristics:

2.1.1 Bundle average mass velocity contours

For a specified test section geometry, axial and radial heat flux distribution and pressure, the bundle average heat flux at DNB is plotted versus bundle inlet temperature with bundle average mass velocity as a parameter. Multiple DNB points are labeled on this plot by using the following notation. The first DNB is designated by an asterisk (*). A multiple DNB point of the nth rank is labeled by a word having n-1 characters representing second, third, -- and nth DNB from left to right respectively following the asterisk. Each character may be A, B or C, depending on the type of DNB as described in the previous section. For example, a DNB point labeled *CCA means that the point plotted represents a multiple DNB point in which the second DNB occurred on a rod different from the first DNB rod, the third DNB also occurred on a rod different from the first, and the fourth DNB occurred on the same rod as the first and at the same elevation. Reasons for the application of this notation are as follows:

a) All multiple DNB events are related to the first DNB which is logically the most important phenomenon.

b) The order of occurrence of DNB is shown on the plot with a simple and compact notation occupying the least amount of space.

c) All single DNB points are plotted with a simple asterisk and no accompanying label.

It should be noted that for axially uniform heat flux, all DNB detecting thermocouples are placed on the rods near the channel exit. For this reason, only multiple DNB events of categories A and C are observed. For axially nonuniform heat flux, the DNB detecting thermocouples are distributed vertically on the rods. For this reason, only multiple DNB events of categories B and C are observed.

Typical plots are shown in Figures 6a to 6e for Combustion Engineering test section number 37 with uniform axial and non-uniform radial heat flux distribution and operating pressures of 900, 1400, 1800, 2000 and 2300 psia respectively. Since all DNB events occur at the end of the rod, the plotted DNB events are of the A and C categories. A complete specification for this test section is given in Figure 1.

An examination of these typical bundle average mass velocity contours in the plane of the bundle average DNB heat flux versus bundle inlet temperature indicates that:

1) The mass velocity contours are essentially linear.

2) The number of multiple DNB events of higher rank are significant as compared to the first DNB.

3) The bundle pressure, inlet temperature and average mass velocity affect the location, rank and the frequency of occurrence of multiple DNB events. To determine the effect of each parameter, it is necessary to re-examine the data by changing one parameter at a time while keeping the remaining variables constant. This study is undertaken later in this report.

FIGURE 6a TYPICAL AVERAGE BUNDLE HEAT FLUY AT DNB VERSUS INLET TEMPERATURE AT 900 PSIA

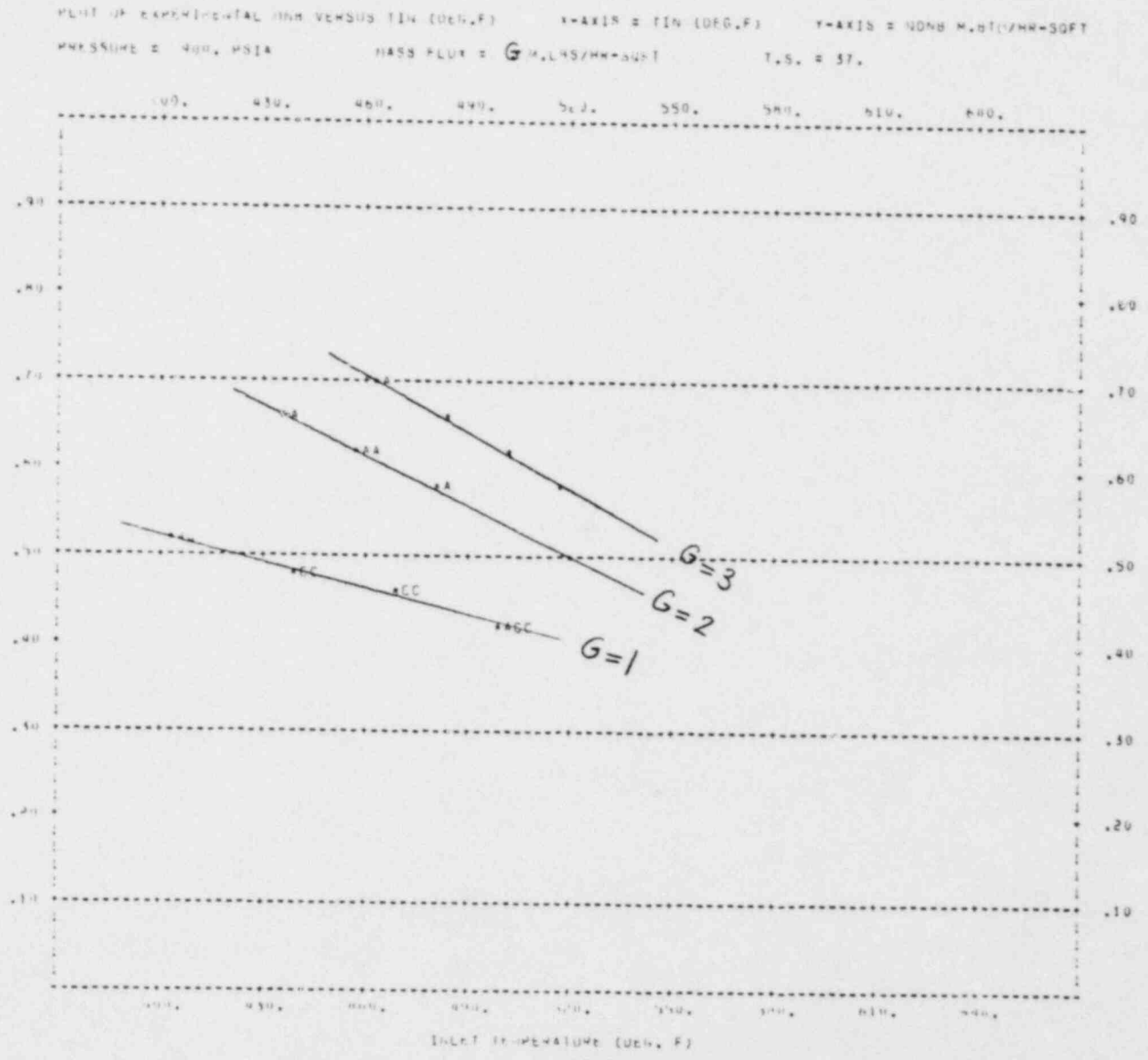

FIGURE 6b TYPICAL AVERAGE BUNDLE HEAT FLUX AT DNB VERSUS INLET TEMPERATURE AT 1400 PSIA

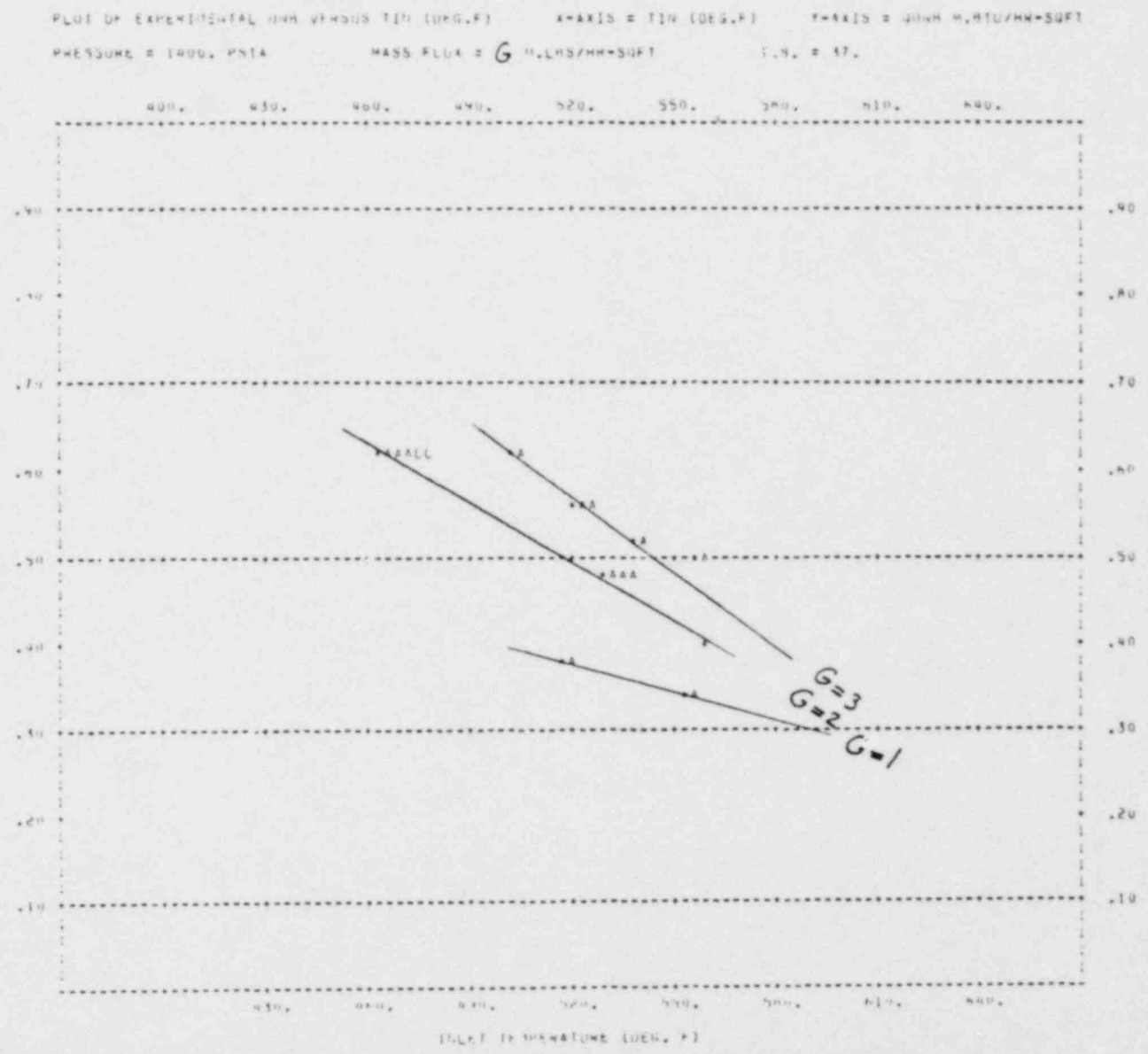

FIGURE 6c TYPICAL AVERAGE BUNDLE HEAT FLUX AT DNB VERSUS INLET TEMPERATURE AT 1800 PSIA

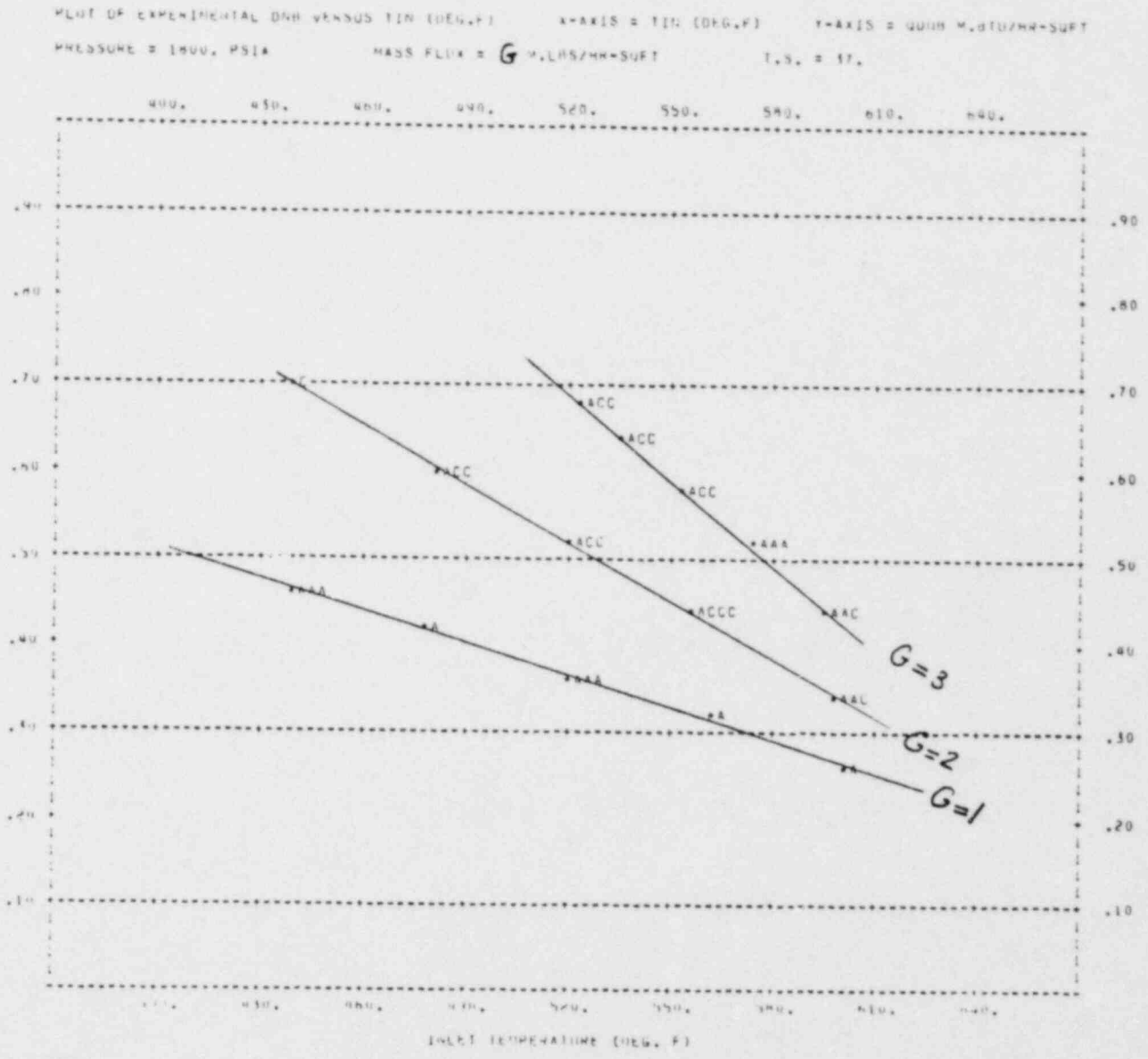

FIGURE 6d TYPICAL AVERAGE BUNDLE HEAT FLUX AT DNB VERSUS INLET TEMPERATURE AT 2000 PSIA

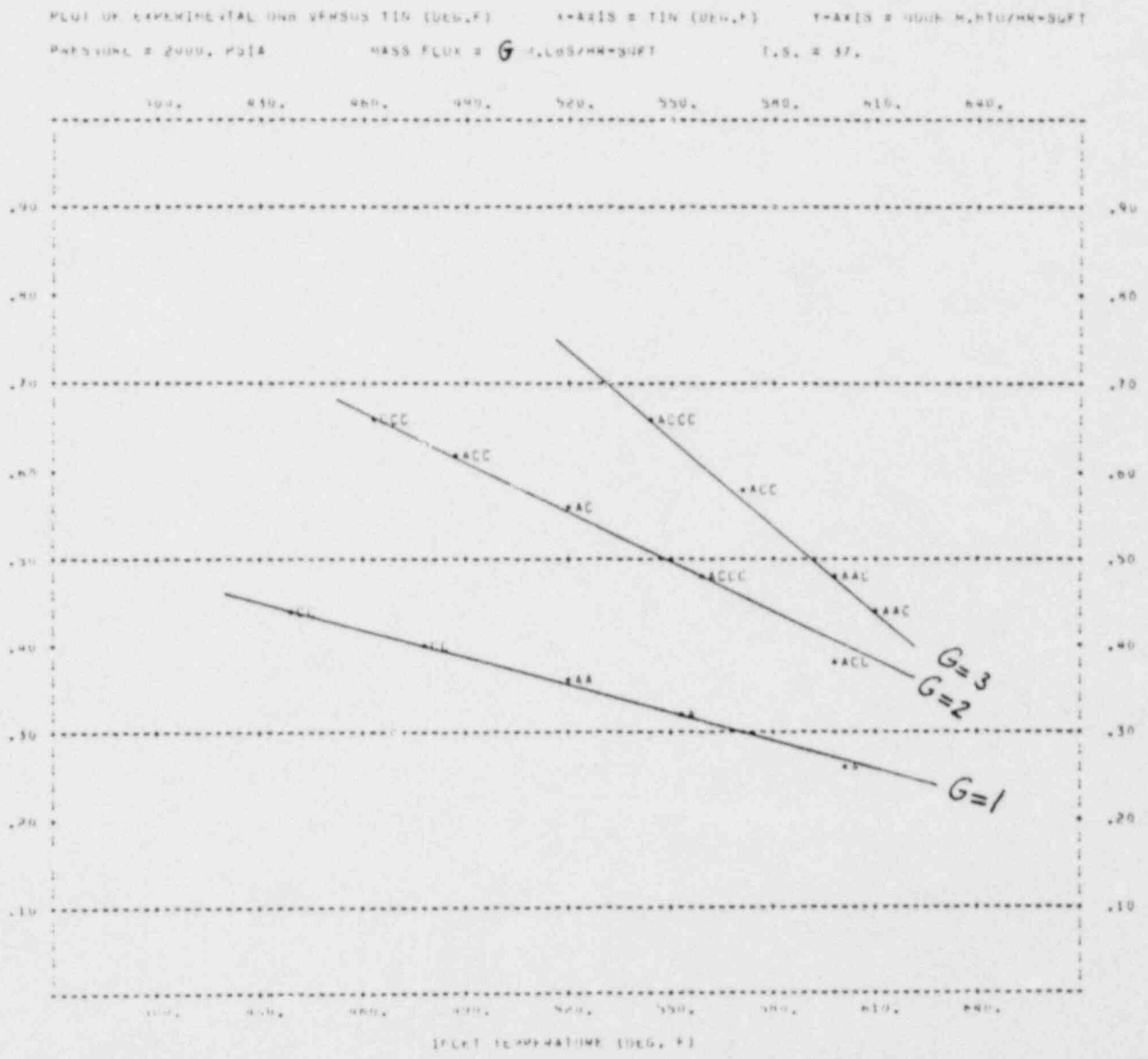

FIGURE 6e TYPICAL AVERAGE BUNDLE HEAT FLUX AT DNB VERSUS INLET TEMPERATURE AT 2300 PSIA

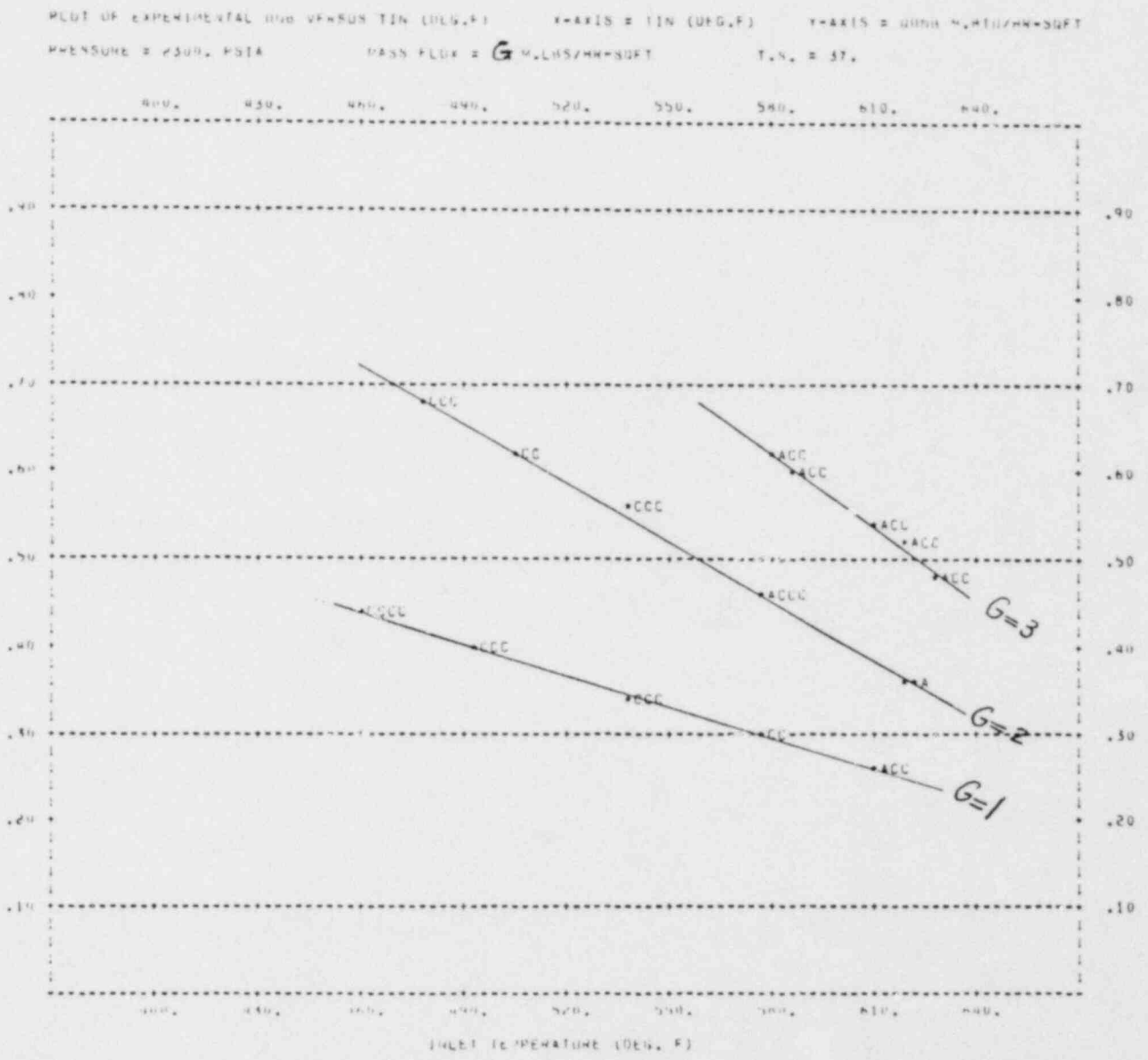

2.1.2 Constant pressure contours

The utility of the characteristics, described above, are limited to the test section geometry under consideration. To correlate data from multiple DNB tests with different test section geometry, the DNB heat flux is plotted against the steam energy flow (SEF). The steam energy flow at any point along the channel is defined as the departure of the total flow enthalpy from that of the saturated liquid. Considering the saturated liquid flow enthalpy as the datum, the steam energy flow for any point along the channel is given by

$$SEF = G(h - h_f) \tag{1}$$

where

G = average mass velocity, M lbs/hr-ft^2

h = coolant enthalpy, Btu/lb

h_f = saturated liquid enthalpy, Btu/lb

On the basis of this equation, the steam energy flow for the channel inlet and DNB point are

$$\begin{aligned} (SEF)_{in} &= G(h_{in} - h_f) \\ (SEF)_{DNB} &= GX_{DNB}\, h_{fg} \end{aligned} \tag{2}$$

where

h_{in} = inlet enthalpy, Btu/lb

h_{fg} = latent heat of vaporization, Btu/lb

X_{DNB} = steam quality at DNB point

It should be noted that since the calculation of local conditions is beyond the scope of the present study, the steam energy flow at DNB is based on the bundle global conditions, i.e., the bundle average mass velocity and the bundle average steam quality at DNB point.

The DNB heat flux is plotted versus the steam energy flow, as defined above, with the test section pressure used as a parameter for a large number of test section geometries. The data points corresponding to a narrow band around several operating pressures are curve fitted by straight lines using a least square error regression analysis.

Typical plots are shown in Figures 7a to 7d for 2000 test data obtained from 60 Combustion Engineering test sections with uniform axial and non-uniform radial heat flux distribution at operating pressures above 1700 psia. Since all DNB events occur at the end of the rod, the plotted DNB events are of the A and C categories. Furthermore, among the DNB events occurring at the same elevation, only the first indication is considered in the analysis and the remaining indications are ignored. Figure 7a to 7d show the DNB heat flux versus the steam energy flow for the first, second, third and fourth DNB events respectively. These figures also show the following pressure contours:

Pressure contour	Linear least square fit to data points in the following range
1800 psia	1775 to 1825 psia
2000 psia	1975 to 2025 psia
2300 psia	2275 to 2325 psia

An examination of the constant pressure contours in the bundle average heat flux at DNB versus steam energy flow plane indicates that:

1) The slope and the intercept of the pressure contours for DNB events of higher ranks are essentially close to those of the pressure contours for the first DNB. This suggests that the presently available DNB correlations, for the first DNB based on the bundle average conditions, may be useful in the prediction of the DNB events of higher rank. This finding will be verified later in this report.

FIGURE 7a DNB HEAT FLUX VERSUS STEAM ENERGY FLOW FOR FIRST DNB

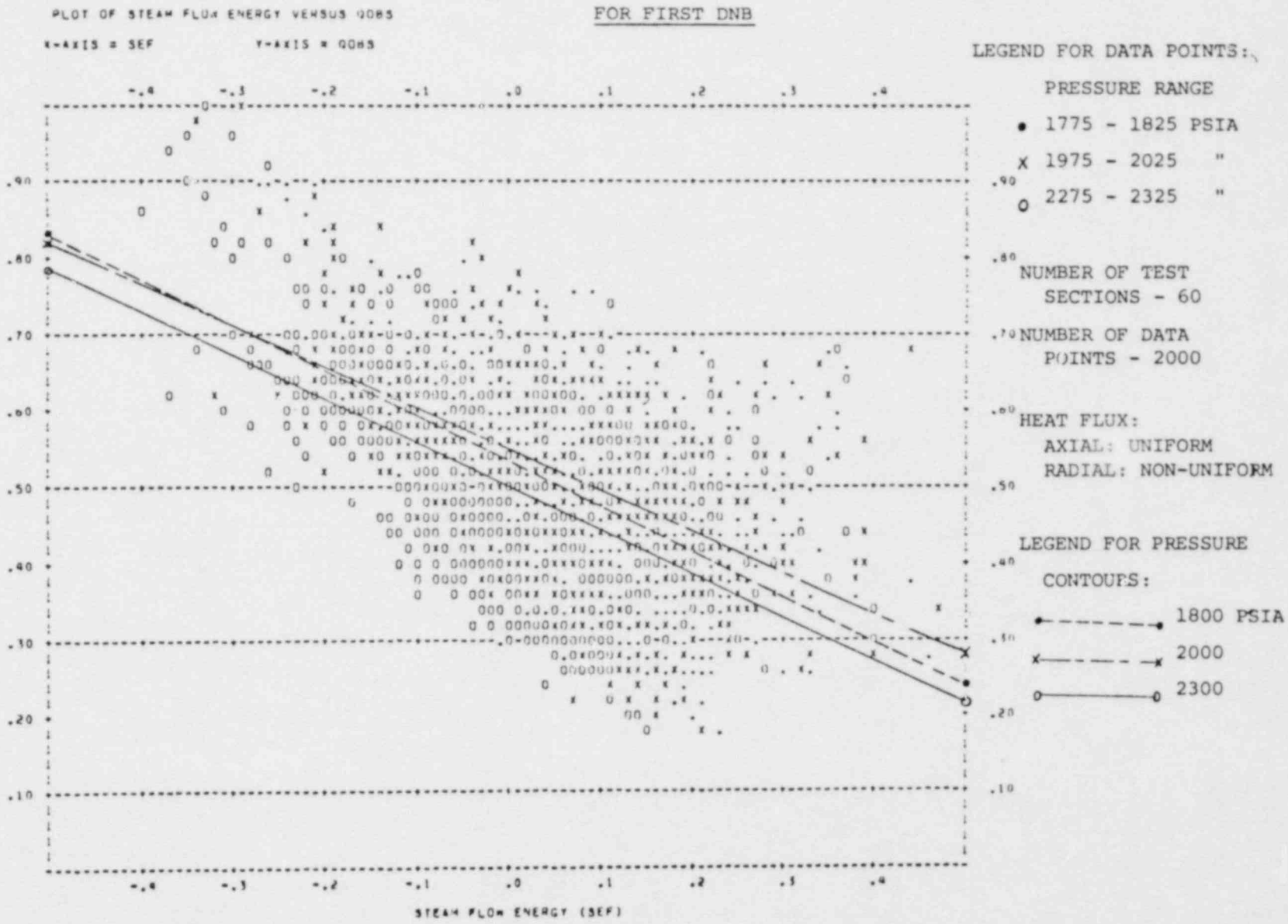

FIGURE 7b DNB HEAT FLUX VERSUS STEAM ENERGY FLOW FOR SECOND DNB

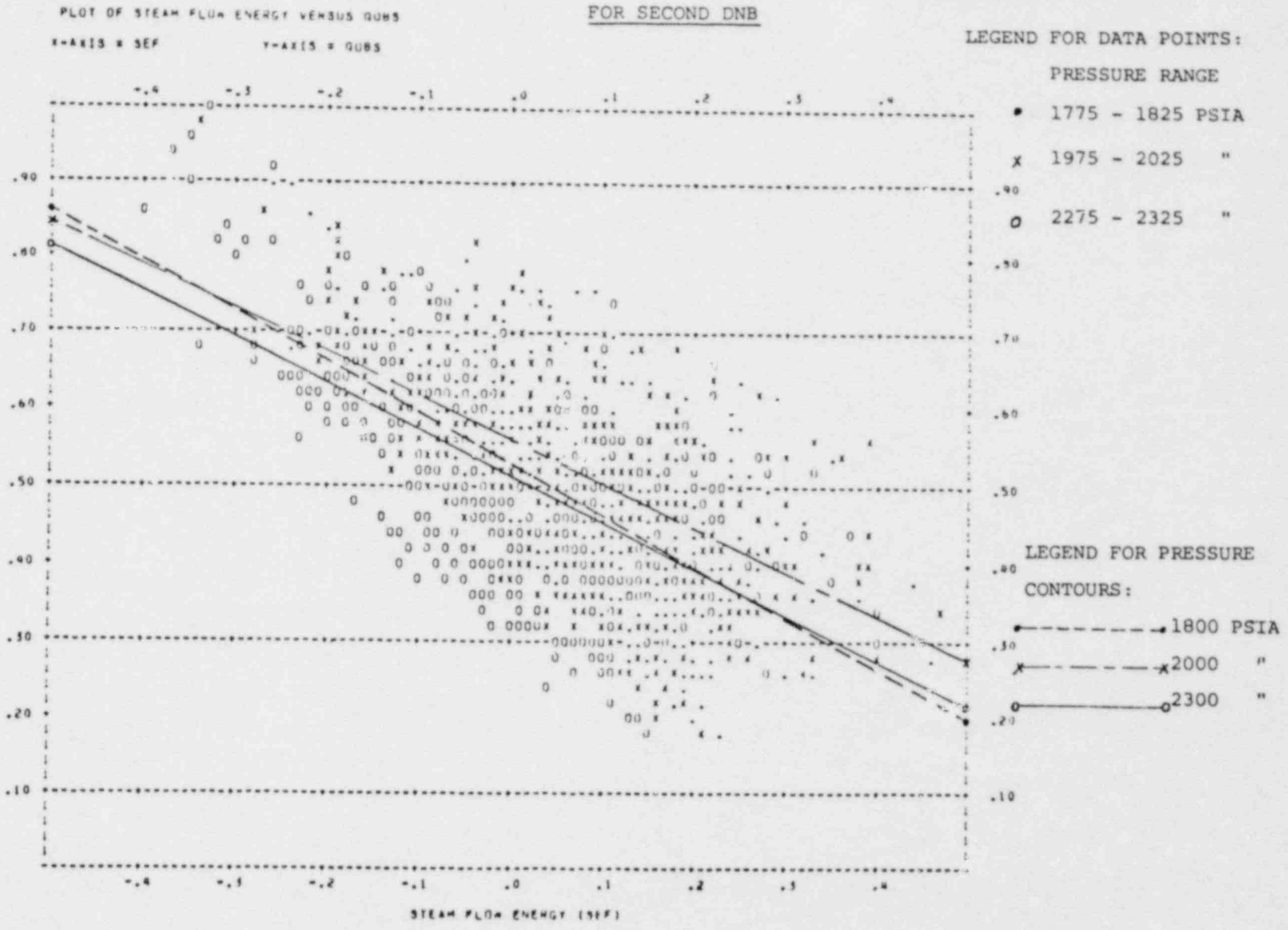

FIGURE 7c DNB HEAT FLUX VERSUS STEAM ENERGY FLOW FOR THIRD DNB

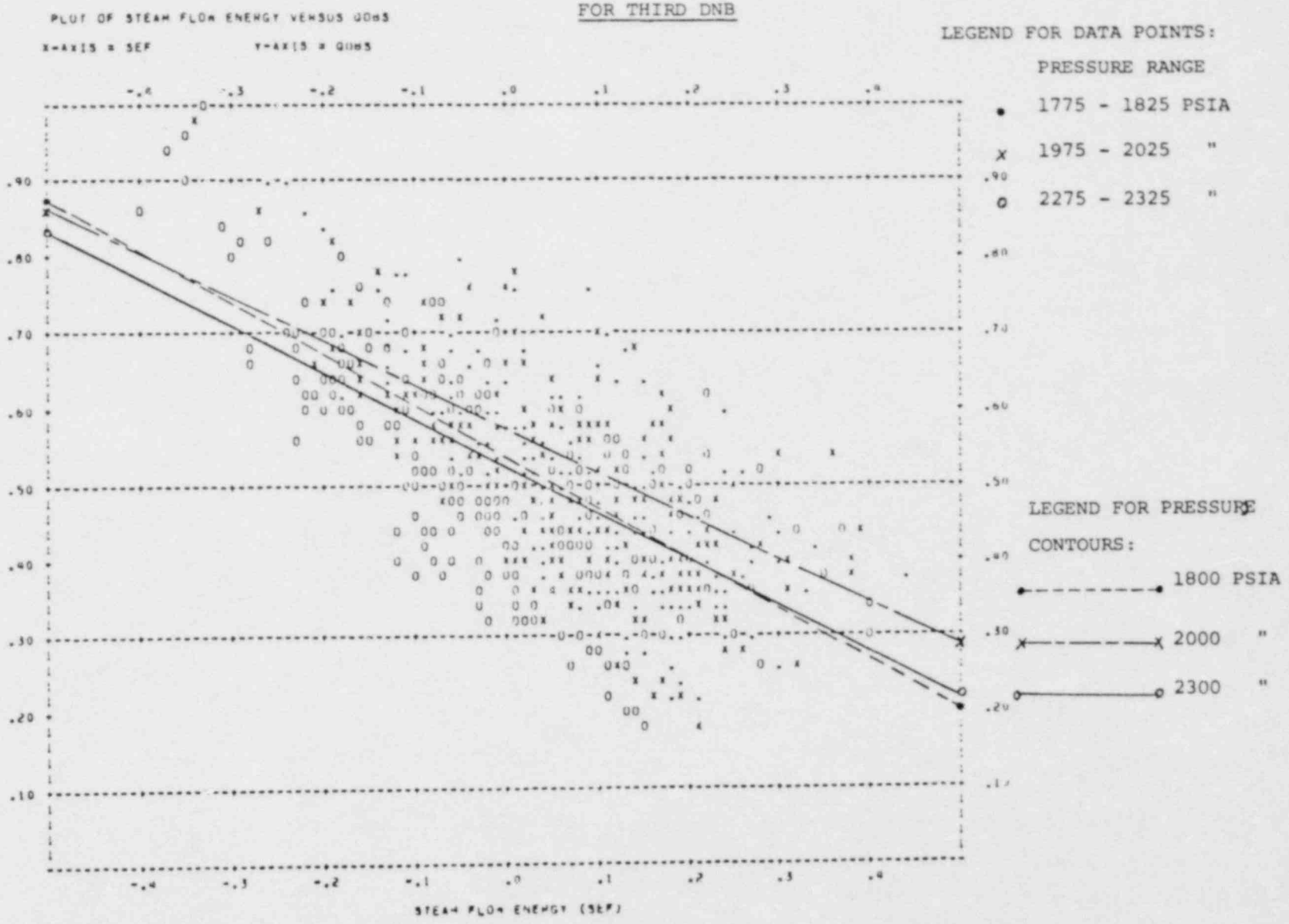

FIGURE 7d DNB HEAT FLUX VERSUS STEAM ENERGY FLOW FOR FOURTH DNB

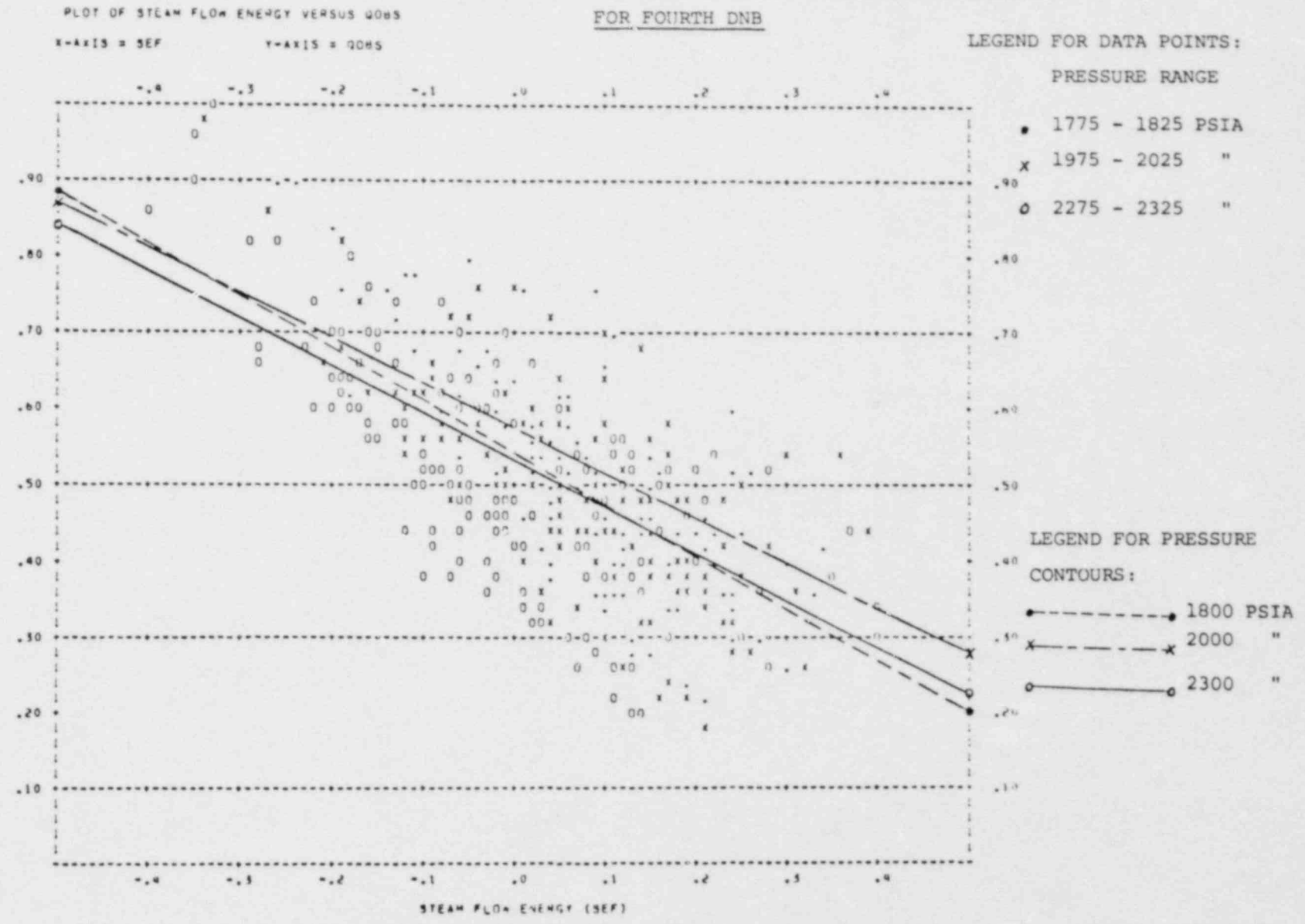

2) The significant amount of scatter of data points about the pressure contours suggests that the predictive correlations for multiple DNB events of higher rank should be based on the bundle local conditions as in the case of the first DNB and not on the bundle average conditions as employed here.

It should be noted that the 2000 psia pressure contour is located above the 2300 psia pressure contour. As will be shown later, in Figure 8b, the frequency of occurrence of multiple DNB events is lower at 2000 psia as compared to 2300 psia This means that DNB heat fluxes corresponding to 2000 psia would be generally higher than those at 2300 psia, under otherwise similar test conditions. Based on this line of reasoning, the 1800 psia pressure contour should have been above the 2000 psia pressure contour, which is not obviously the case in Figure 7a to 7d. The reasons for this apparent inconsistency are as follows:

a) As will be shown later, in Figure 8b, the slope of the frequency of occurrence of multiple DNB events versus pressure is smaller in the 1800 to 2000 psia region as compared to the 2000 to 2300 psia region.

b) As indicated in References 3 and 4, a portion of data points in the DNB heat flux versus steam energy flow plot located on the right hand side are premature DNB events and should not be used in the linear curve fitting procedures. The relatively large scatter of data on the right hand side of the plot, gives credibility to this argument. However, since our objective here was a comparison of pressure contours for multiple DNB events, no attempt was made to separate the data corresponding to premature DNB events from the rest of the data.

2.2 Statistical Analyses

Statistical analyses are performed on 3800 test data obtained from 60 Combustion Engineering test sections with uniform axial and non-uniform radial heat flux distribution. In

these studies, all DNB events occur at the end of the rod and, therefore, the multiple DNB events are of the A and C categories. Furthermore, consistent with the parametric studies for constant pressure contours, among the DNB events occurring on the same rod at the same elevation, only the first indication is considered in the analysis and the remaining indications are ignored. Two types of statistical analyses are undertaken.

2.2.1 Frequency of occurrence of DNB events

In the first analysis, the percent number of the multiple DNB events (i.e., the number of second, third, fourth and fifth DNB events in 100 first DNB events) are calculated and used as an overall norm to determine the effect of the variation of such parameters as, pressure, bundle average mass velocity or bundle inlet quality, on the frequency of occurrence of multiple DNB events. This purpose is achieved by calculating the percent number of the multiple DNB events at the following values of the test conditions and by comparing these results with the overall norm.

Pressure, psia: 900, 1400, 1800, 2000, 2300, 2400

Inlet quality: -0.90, -0.70, -0.50, -0.30, -0.10

Average mass velocity, M lb/ft^2-hr: 1, 2, 3

The results of this study are plotted in Figures 8a to 8c. A study of these results leads to the following conclusions:

1) The percent numbers of the multiple DNB events in the overall norm are:

First	DNB	100
Second	DNB	34
Third	DNB	16
Fourth	DNB	7
Fifth	DNB	3

2) As shown on Figure 8a, the percent numbers of the

FIGURE 8a EFFECT OF MASS VELOCITY ON PERCENT NUMBER OF DNB EVENTS

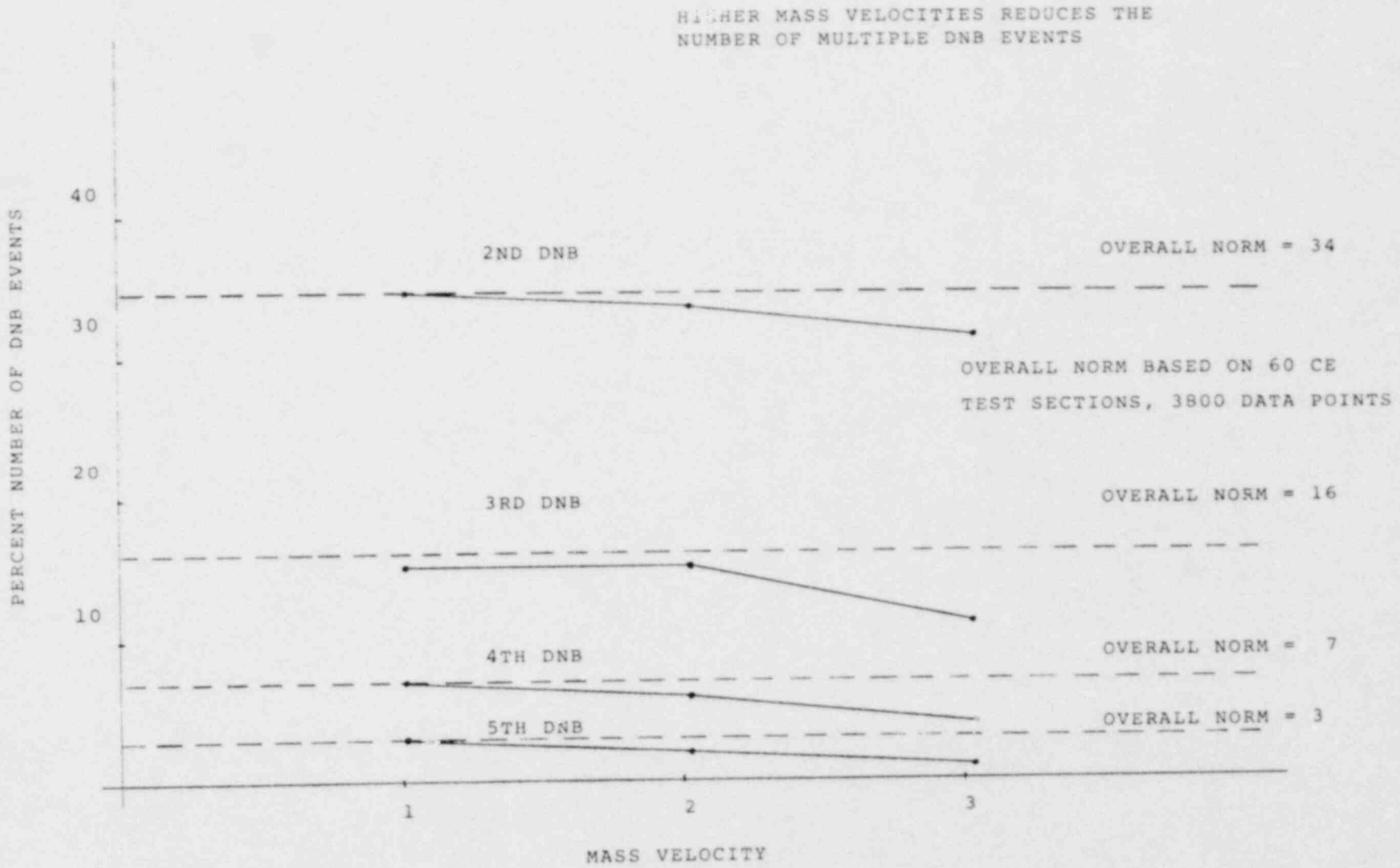

FIGURE 8b EFFECT OF PRESSURE ON PERCENT NUMBER OF DNB EVENTS

HIGHER PRESSURE INCREASES THE NUMBER OF MULTIPLE DNB
MEDIUM PRESSURE DECREASES THE NUMBER OF MULTIPLE DNB

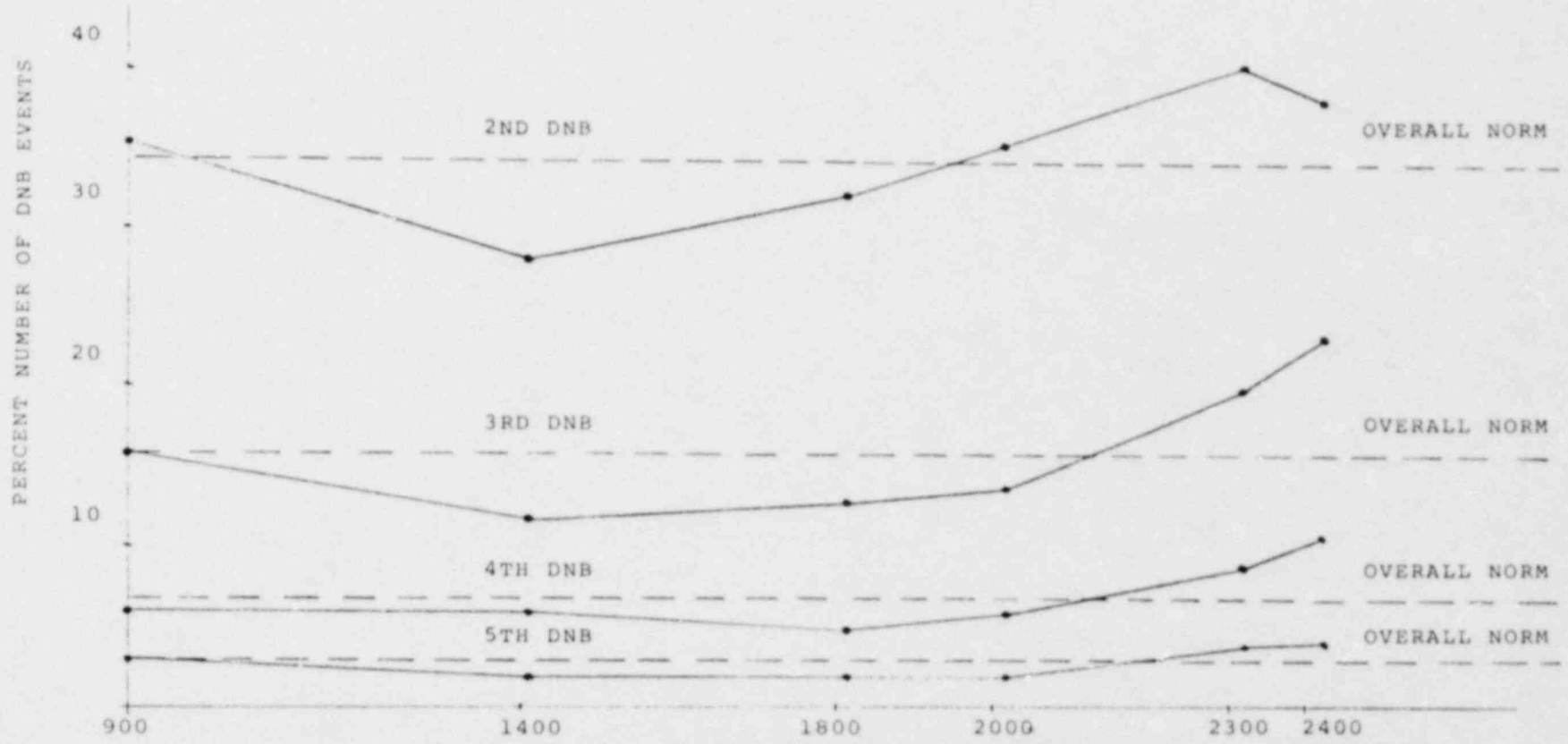

FIGURE 8c EFFECT OF INLET SUBCOOLING (INLET QUALITY) ON PERCENT NUMBER OF DNB EVENTS

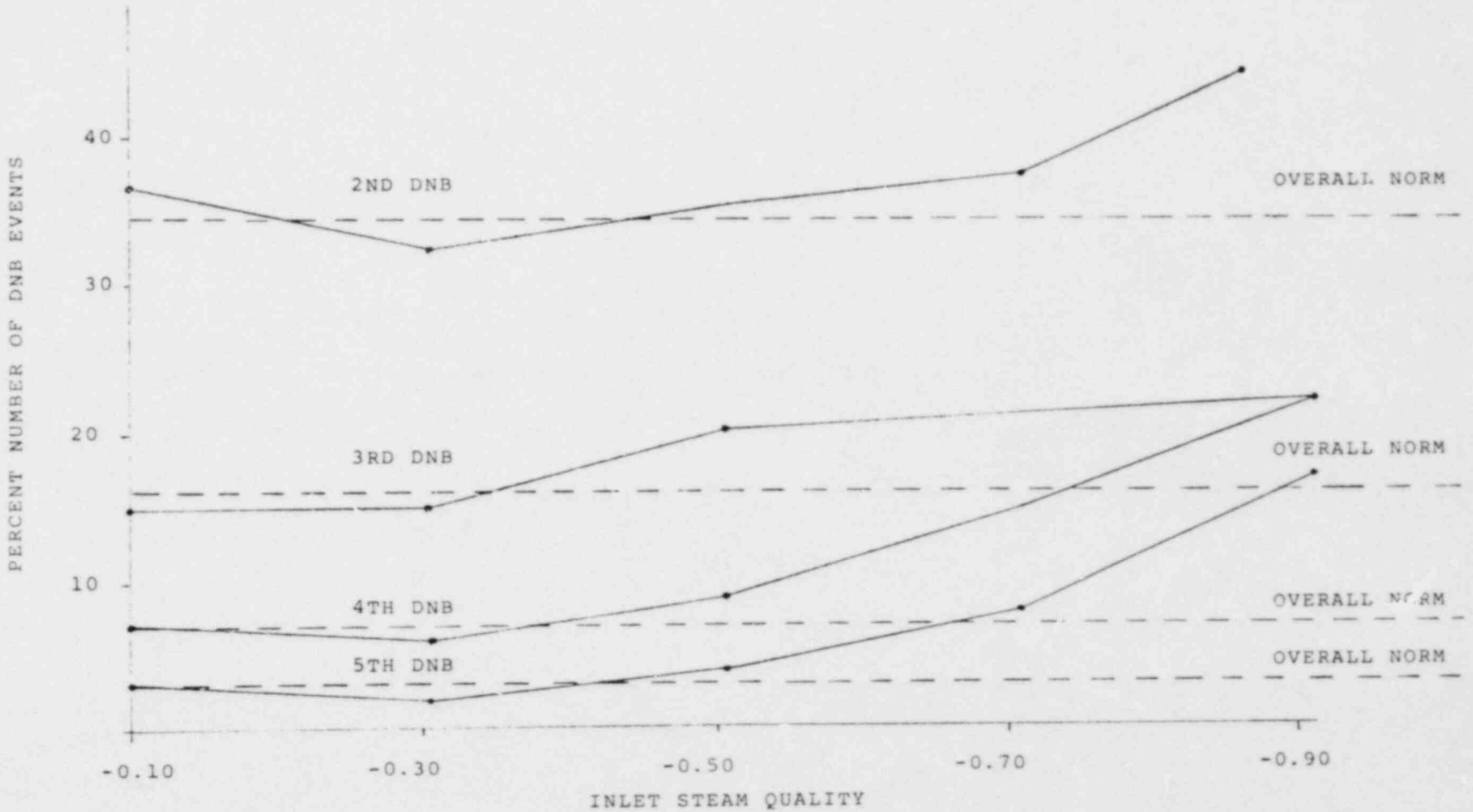

multiple DNB events decrease as the mass velocities increase. In this respect, the behavior of the DNB events of higher rank than first is similar to that of the first DNB. Higher mass velocities tend to disperse the steam bubbles formed near the heated rod and cause a retardation in steam blanketing phenomenon and the subsequent DNB events.

3) As shown in Figure 8b, the percent numbers of the multiple DNB events first decrease as the operating pressure increases and then increase at higher operating pressures.

4) As shown in Figure 8c, the percent numbers of the multiple DNB events increase dramatically as the inlet subcooling increases.

It is interesting to note that the above conclusions agree quite well with the results of analytical studies and experimental observations performed on boiling loop hydrodynamic instabilities and the attendant premature DNB phenomenon. These studies have demonstrated that the boiling loop instabilities and the attendant probability of the occurrence of premature DNB events will increase by:

a) Lower circulation;

b) Lower operating pressure; and

c) Higher inlet subcooling

2.2.2 Relative cumulative frequency distribution

In the second statistical analysis, the frequency distribution of the occurrence of multiple DNB events is considered. In these studies, for every test section, the number of first, second, third, and fourth DNB events are recorded. For example:

	DNB		Ranks	
Test Section #	1	2	3	4
36	167	65	30	6

Based on the above data for all test sections, the number of

second, third and fourth DNB events for 100 first DNB events are calculated. For example,

	DNB Ranks			
Test Section #	1	2	3	4
36	100	38.92	17.96	3.59

The relative number of DNB events for all test sections are then compiled in tabular form. Table 1 shows a typical compilation of the relative number of DNB events for all test sections for the first and second DNB events. Similarly, DNB events of ranks higher than two are also compiled.

The relative cumulative frequency distribution is then obtained by sorting the percent number of second, third and fourth DNB events in ascending order to provide the x coordinates and arranging the percent cumulative number of test sections in ascending order to provide the y coordinates. Table 2 shows a typical compilation of the relative frequency distribution for all test sections for the first and second DNB events. Similarly, DNB events of ranks higher than second are also compiled.

Values of percent cumulative number of test sections are then plotted versus the percent number of second, third and fourth DNB events. Figure 9a shows the relative cumulative frequency distribution for all test data.

The relative cumulative frequency distribution curves are useful in estimating the probabilities of occurrence (or non-occurrence) of the multiple DNB events as described hereunder.

1) The y-intercepts of the frequency distribution curves indicate the percent number of test sections with no multiple DNB events. Referring to Figure 9a and the computer results one concludes that:

TABLE 1 TYPICAL CALCULATION OF RELATIVE NUMBER OF DNB EVENTS

TEST SECTION NUMBER	NUMBER OF DNB EVENTS		RELATIVE NUMBER OF DNB EVENTS	
	FIRST DNB	SECOND DNB	FIRST DNB	SECOND DNB
1	29	5	100	17.24
2	44	3	100	6.81
3	13	6	100	46.15
4	30	9	100	30.00
5	70	9	100	12.85
6	27	4	100	14.81
7	43	10	100	23.25
8	77	12	100	15.58
9	108	36	100	33.33
10	60	25	100	41.66
11	54	9	100	16.66
12	51	7	100	13.72
13	111	68	100	61.26
14	50	16	100	32.00
15	39	15	100	38.46
16	56	14	100	25.00
17	57	12	100	21.05
18	72	17	100	23.61
19	53	11	100	20.75
20	68	20	100	29.41
21	64	22	100	34.37
22	61	10	100	16.39
23	53	13	100	24.52
24	62	14	100	22.58
25	65	13	100	20.00
26	54	15	100	27.77
27	55	29	100	52.72
28	55	19	100	34.54
29	59	10	100	16.94
30	84	26	100	30.95

TABLE 1 TYPICAL CALCULATION OF RELATIVE NUMBER OF DNB EVENTS (Cont'd)

TEST SECTION NUMBER	NUMBER OF DNB EVENTS		RELATIVE NUMBER OF DNB EVENTS	
	FIRST DNB	SECOND DNB	FIRST DNB	SECOND DNB
31	61	7	100	11.47
32	62	23	100	37.09
33	65	25	100	38.46
34	59	31	100	52.54
35	30	5	100	16.66
36	167	65	100	38.92
37	70	39	100	55.71
38	96	55	100	57.29
39	72	39	100	54.16
40	20	0	100	0
41	57	22	100	38.59
42	75	1	100	1.33
43	82	29	100	35.36
44	35	24	100	68.57
45	70	32	100	45.71
46	73	35	100	47.94
47	149	60	100	40.26
48	87	51	100	58.62
49	82	32	100	39.02
50	65	24	100	36.92
51	64	30	100	46.87
52	101	35	100	34.65
53	58	30	100	51.72
54	70	27	100	38.57
55	11	6	100	54.54
56	47	29	100	61.70
57	12	3	100	25.00
58	68	29	100	42.64
59	55	21	100	38.18
60	118	13	100	11.01

TABLE 2 TYPICAL CALCULATION OF RELATIVE CUMULATIVE FREQUENCY DISTRIBUTION FOR SECOND DNB EVENTS

ROW NUMBER	RELATIVE CUMULATIVE NUMBER OF TEST SECTIONS (Y-AXIS)	RELATIVE NUMBER OF DNB EVENTS FIRST DNB	RELATIVE NUMBER OF DNB EVENTS SECOND DNB (X-AXIS)
1	1.67	100	0.0
2	3.33	100	1.33
3	5.00	100	6.81
4	6.67	100	11.01
5	8.33	100	11.47
6	10.00	100	12.85
7	11.67	100	13.72
8	13.33	100	14.81
9	15.00	100	15.58
10	16.67	100	16.39
11	18.33	100	16.66
12	20.00	100	16.66
13	21.67	100	16.94
14	23.33	100	17.24
15	25.00	100	20.00
16	26.67	100	20.75
17	28.33	100	21.05
18	30.00	100	22.58
19	31.67	100	23.25
20	33.33	100	23.61
21	35.00	100	24.52
22	36.67	100	25.00
23	38.33	100	25.00
24	40.00	100	27.77
25	41.67	100	29.41
26	43.33	100	30.00
27	45.00	100	30.95
28	46.67	100	32.00
29	48.33	100	33.33
30	50.00	100	34.37

TABLE 2 TYPICAL CALCULATION OF RELATIVE CUMULATIVE FREQUENCY DISTRIBUTION FOR SECOND DNB EVENTS (Cont'd)

ROW NUMBER	RELATIVE CUMULATIVE NUMBER OF TEST SECTIONS (Y-AXIS)	RELATIVE NUMBER OF DNB EVENTS	
		FIRST DNB	SECOND DNB (X-AXIS)
31	51.67	100	34.54
32	53.33	100	34.65
33	55.00	100	35.36
34	56.67	100	36.92
35	58.33	100	37.09
36	60.00	100	38.18
37	61.67	100	38.46
38	63.33	100	38.46
39	65.00	100	38.57
40	66.67	100	38,59
41	68.33	100	38.92
42	70.00	100	39.02
43	71.67	100	40.26
44	73.33	100	41.66
45	75.00	100	42.64
46	76.67	100	45.71
47	78.33	100	46.15
48	80.00	100	46.87
49	81.67	100	47.94
50	83.33	100	51.72
51	85.00	100	52.54
52	86.67	100	52.72
53	88.33	100	54.16
54	90.00	100	54.54
55	91.67	100	55.71
56	93.33	100	57.29
57	95.00	100	58.62
58	96.67	100	61.26
59	98.33	100	61.70
60	100.00	100	68.57

FIGURE 9a RELATIVE CUMULATIVE FREQUENCY DISTRIBUTION FOR ALL TEST DATA

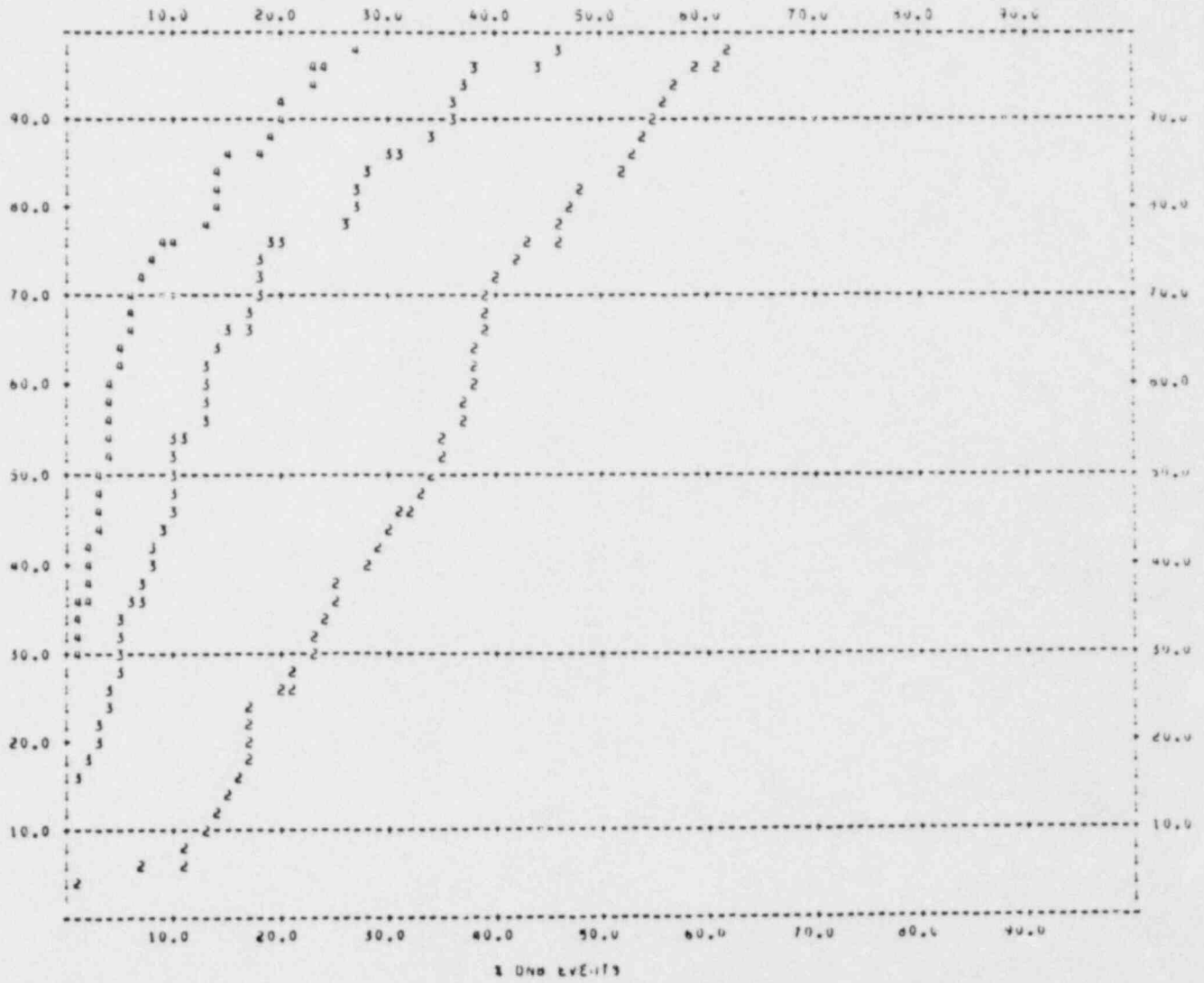

DATA CONSISTS OF 3800 POINTS FROM 60 CE TEST SECTIONS WITH UNIFORM AXIAL HEAT FLUX

DNB rank	Percent number of test sections with no DNB events
1	0
2	1.67
3	13.33
4	28.33

2) The intersection of a vertical line at x = c with the frequency distribution curves indicates the percent numbers of test sections with DNB events less than c in 100 first DNB. For example, the intersection of a vertical line at x = 30 provides the following information:

DNB rank	Percent number of test sections with DNB events less than 30 in 100 first DNB
1	0.00
2	43.33
3	85.00
4	99.00

3) The intersection of a horizontal line at y = c with the frequency distribution curves indicates the percent number of DNB events in c test sections. For example, the intersection of a horizontal line at y = 50 provides the following information:

DNB rank	Percent number of DNB events in 50 test sections (in 100 test sections)
1	100.00
2	34.37
3	10.17
4	3.39

4) The area between the frequency distribution curve and the y-axis provides the probability of the occurrence of DNB events for 100 test sections experiencing 100 first DNB events. This value divided by 100 (the total number of test sections)

gives the mean value of the number of multiple DNB events in 100 first DNB events. For Figure 9a, the calculation of the area between the frequency distribution curve and the y-axis provides the following information:

DNB rank	Area	Probability of the occurrence of DNB events	Mean Value
1	10,000.00	1.	100
2	3,306.86	0.330	33.0
3	1,432.32	0.143	14.3
4	665.50	0.066	6.6

5) The area between the frequency distribution curve and the x-axis provide the probability of non-occurrence of DNB events for 100 test sections experiencing 100 first DNB events.

The relative cumulative frequency distribution curves (Figure 9a) are based on 3800 data points from 60 CE test sections with uniform axial heat flux distribution. These curves can be used as an overall norm for the determination of the effect of the variation of such parameters as, pressure, bundle average mass velocity and bundle inlet subcooling, on the probability of occurrence of multiple DNB events. This purpose is achieved by plotting the relative cumulative frequency distribution curves at the following test conditions and by comparing these results with the overall norm:

Pressure, psia: 900, 1400, 1800, 2000, 2300, 2400

Inlet quality: -0.90, -0.70, -0.50, -0.30, -0.10

Average mass velocity, M lbs/ft^2-hr: 1, 2, 3

The results of this study are plotted in Figures 9b to 9o. A study of these results leads to the following conclusions:

1) The relative cumulative frequency distribution curves provide a useful tool for estimating the probabilities of

FIGURE 9b RELATIVE CUMULATIVE FREQUENCY DISTRIBUTION FOR INLET QUALITY = -0.1

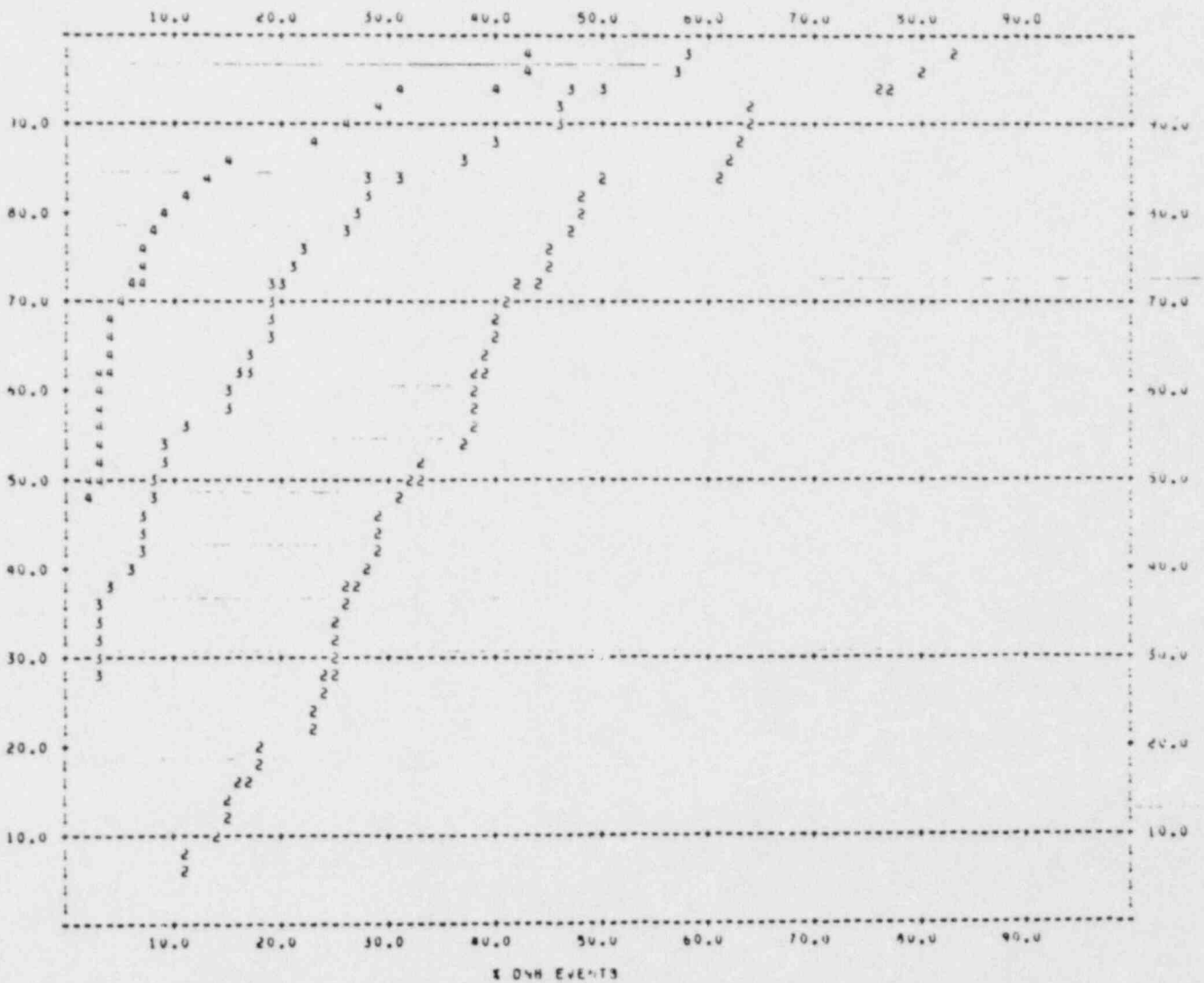

DATA IS A SUBSET OF 3800 POINTS FROM 60 CE TEST SECTIONS WITH UNIFORM AXIAL HEAT FLUX

FIGURE 9c RELATIVE CUMULATIVE FREQUENCY DISTRIBUTION FOR INLET QUALITY = -0.3

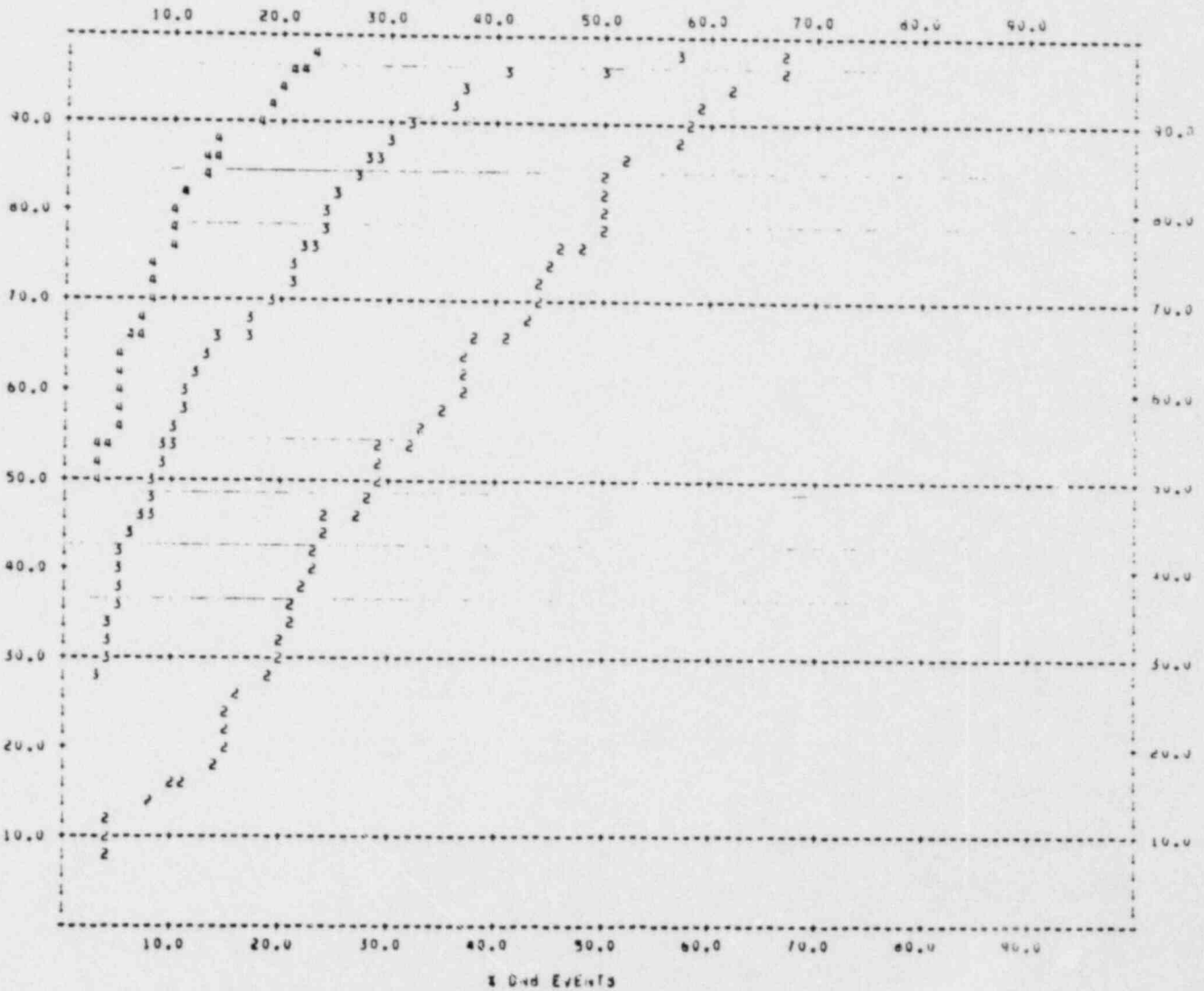

DATA IS A SUBSET OF 3800 POINTS FROM 60 CE TEST SECTIONS WITH UNIFORM AXIAL HEAT FLUX

FIGURE 9d RELATIVE CUMULATIVE FREQUENCY DISTRIBUTION FOR INLET QUALITY = -0.5

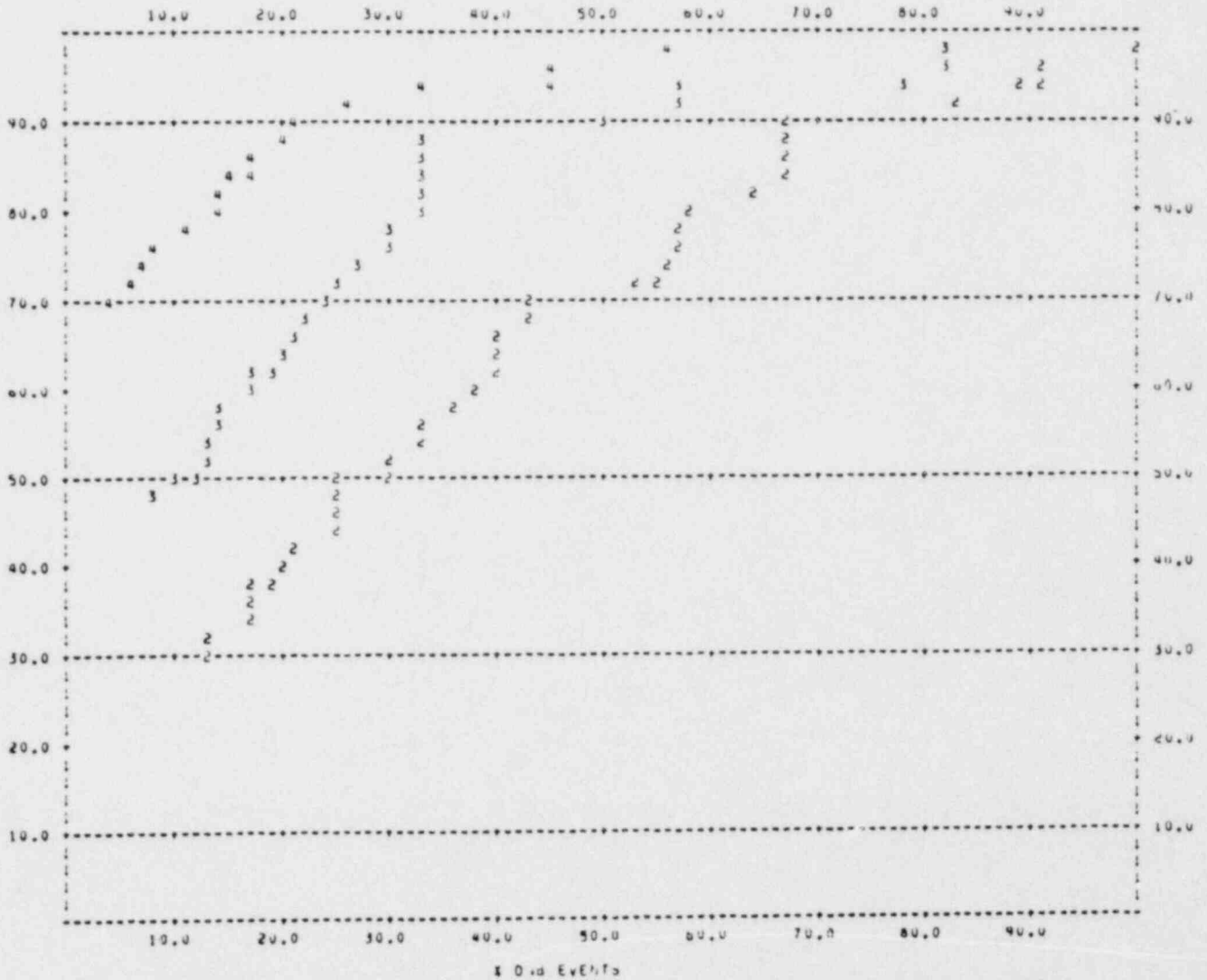

DATA IS A SUBSET OF 3800 POINTS FROM 60 CE TEST SECTIONS WITH UNIFORM AXIAL HEAT FLUX

FIGURE 9e RELATIVE CUMULATIVE FREQUENCY DISTRIBUTION FOR INLET QUALITY = -0.7

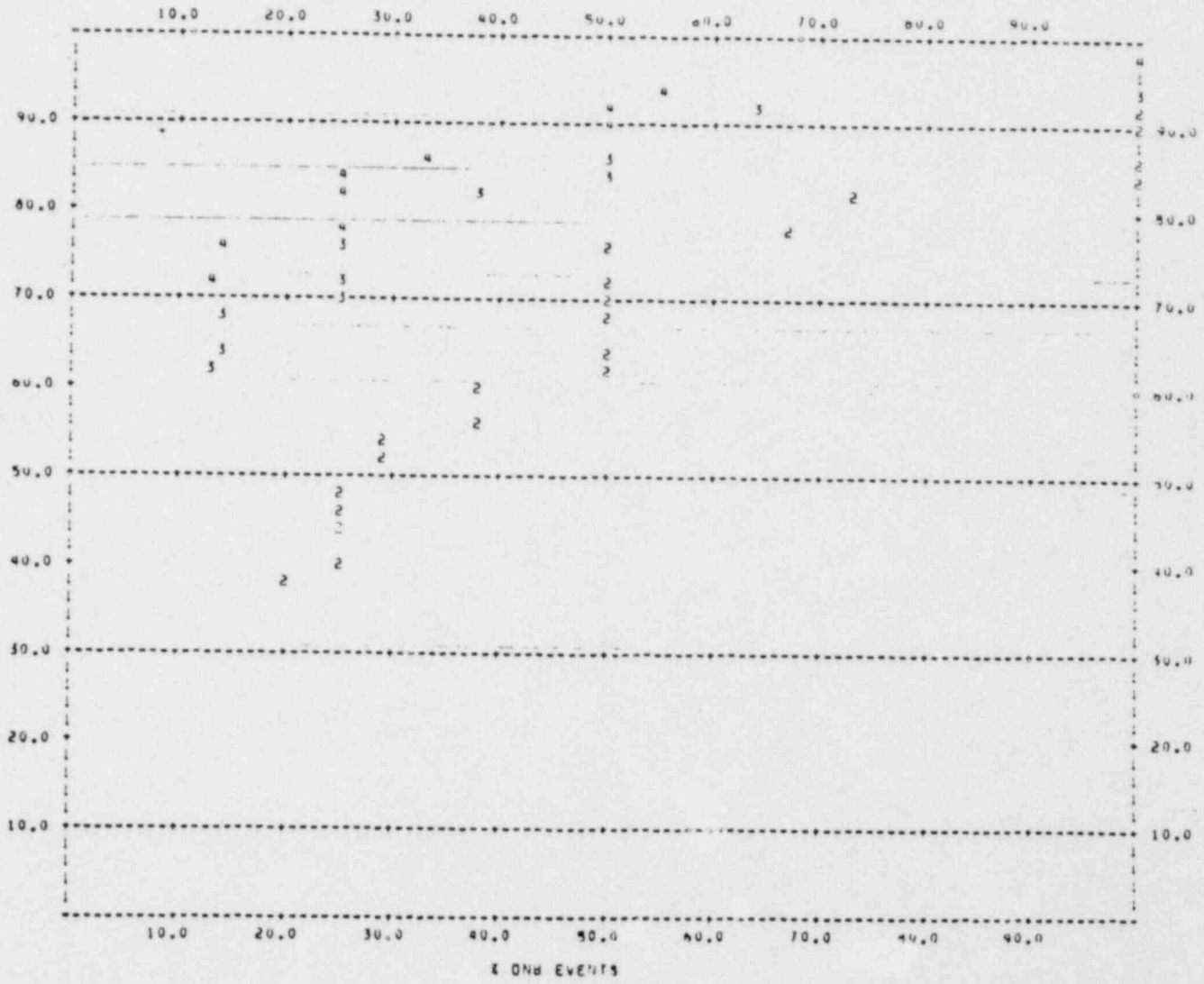

DATA IS A SUBSET OF 3800 POINTS FROM 60 CE TEST SECTIONS WITH UNIFORM AXIAL HEAT FLUX

FIGURE 9f RELATIVE CUMULATIVE FREQUENCY DISTRIBUTION FOR INLET QUALITY = -0.9

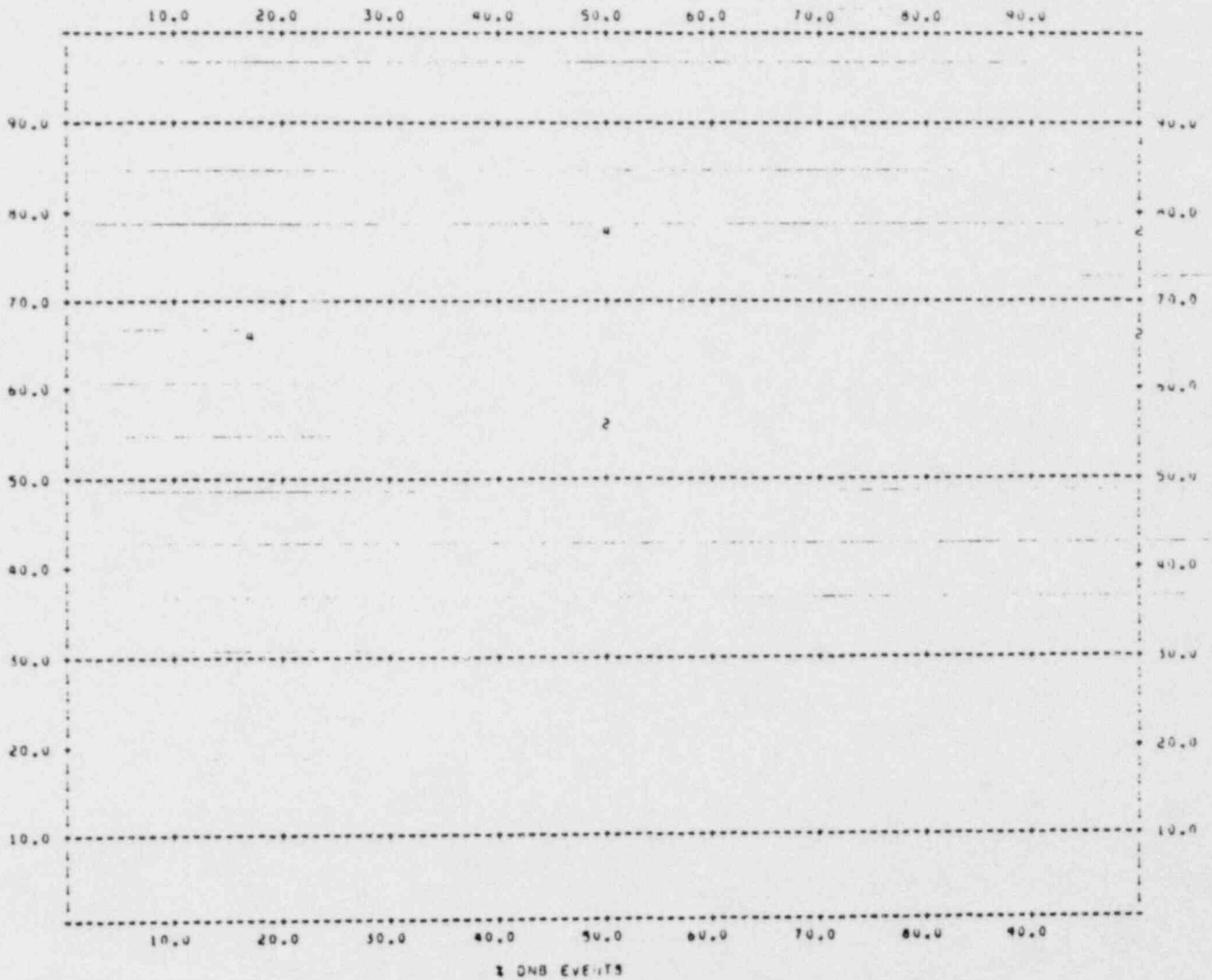

DATA IS A SUBSET OF 3800 POINTS FROM 60 CE TEST SECTIONS WITH UNIFORM AXIAL HEAT FLUX

FIGURE 9g RELATIVE CUMULATIVE FREQUENCY DISTRIBUTION FOR MASS VELOCITY = 1 MLBS/HR-SQFT

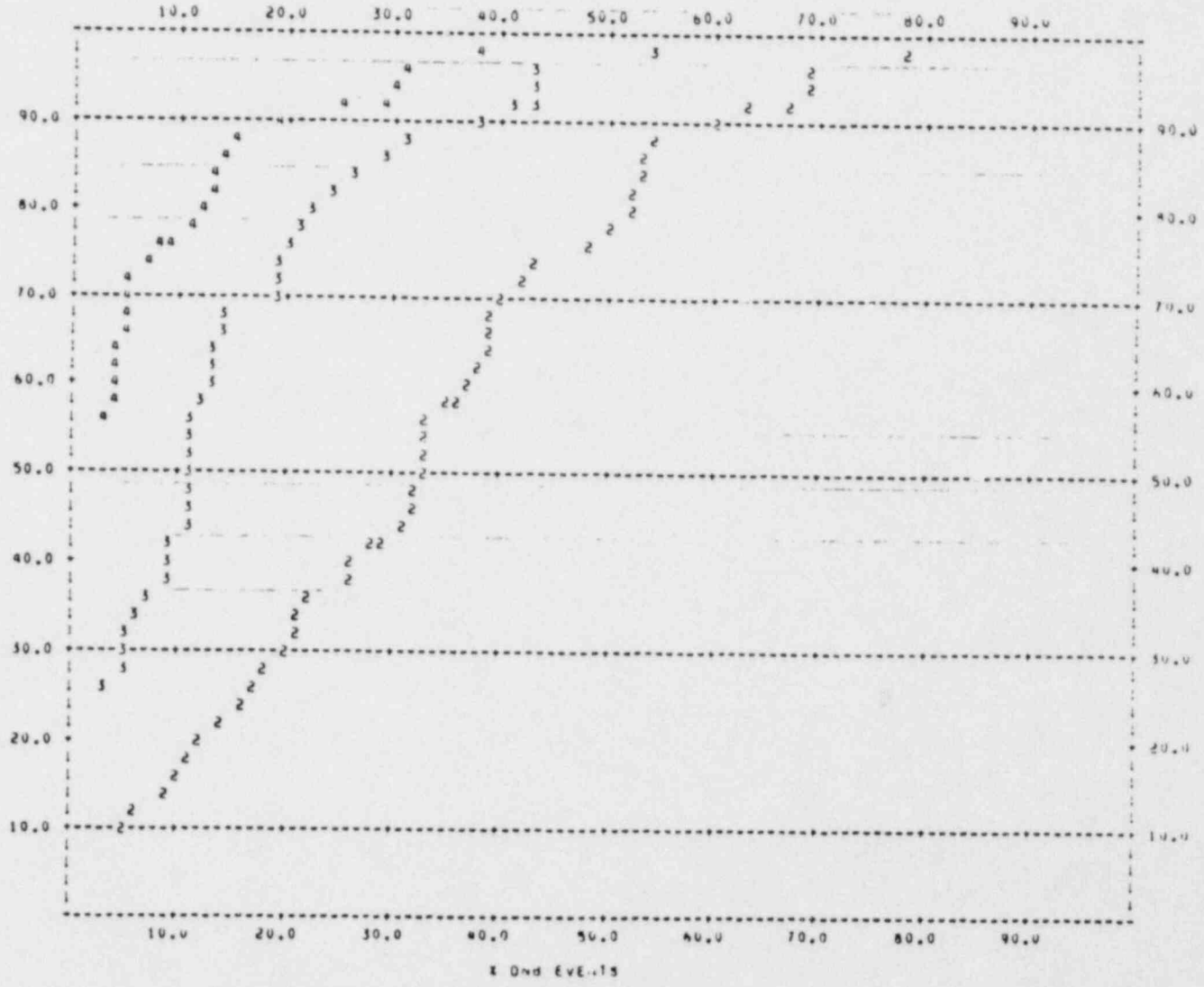

DATA IS A SUBSET OF 3800 POINTS FROM 60 CE TEST SECTIONS WITH UNIFORM AXIAL HEAT FLUX

FIGURE 9h RELATIVE CUMULATIVE FREQUENCY DISTRIBUTION FOR MASS VELOCITY = 2 MLBS/HR-SQFT

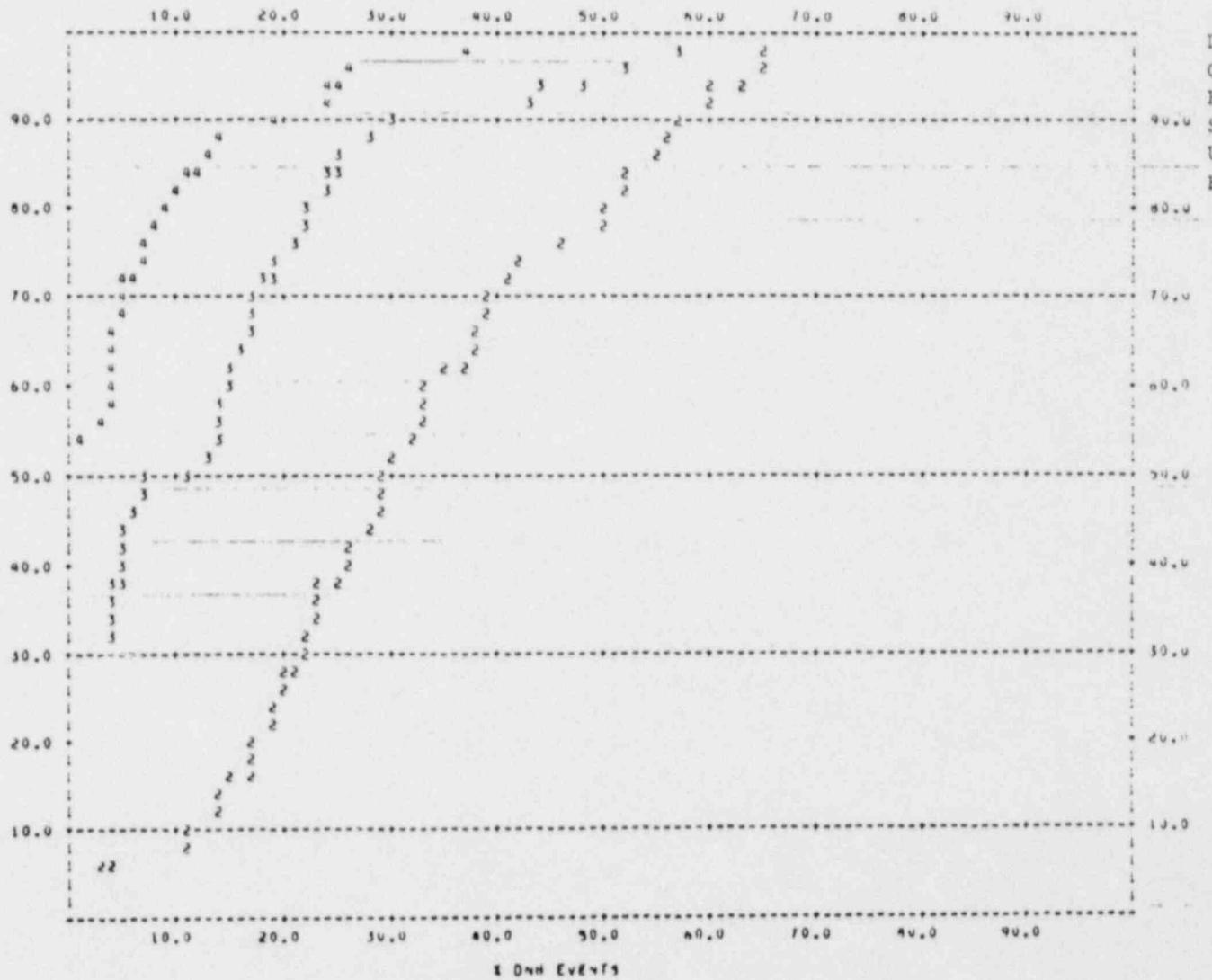

DATA IS A SUBSET OF 3800 POINTS FROM 60 CE TEST SECTIONS WITH UNIFORM AXIAL HEAT FLUX

FIGURE 9i RELATIVE CUMULATIVE FREQUENCY DISTRIBUTION FOR MASS VELOCITY = 3 MLBS/HR-SQFT

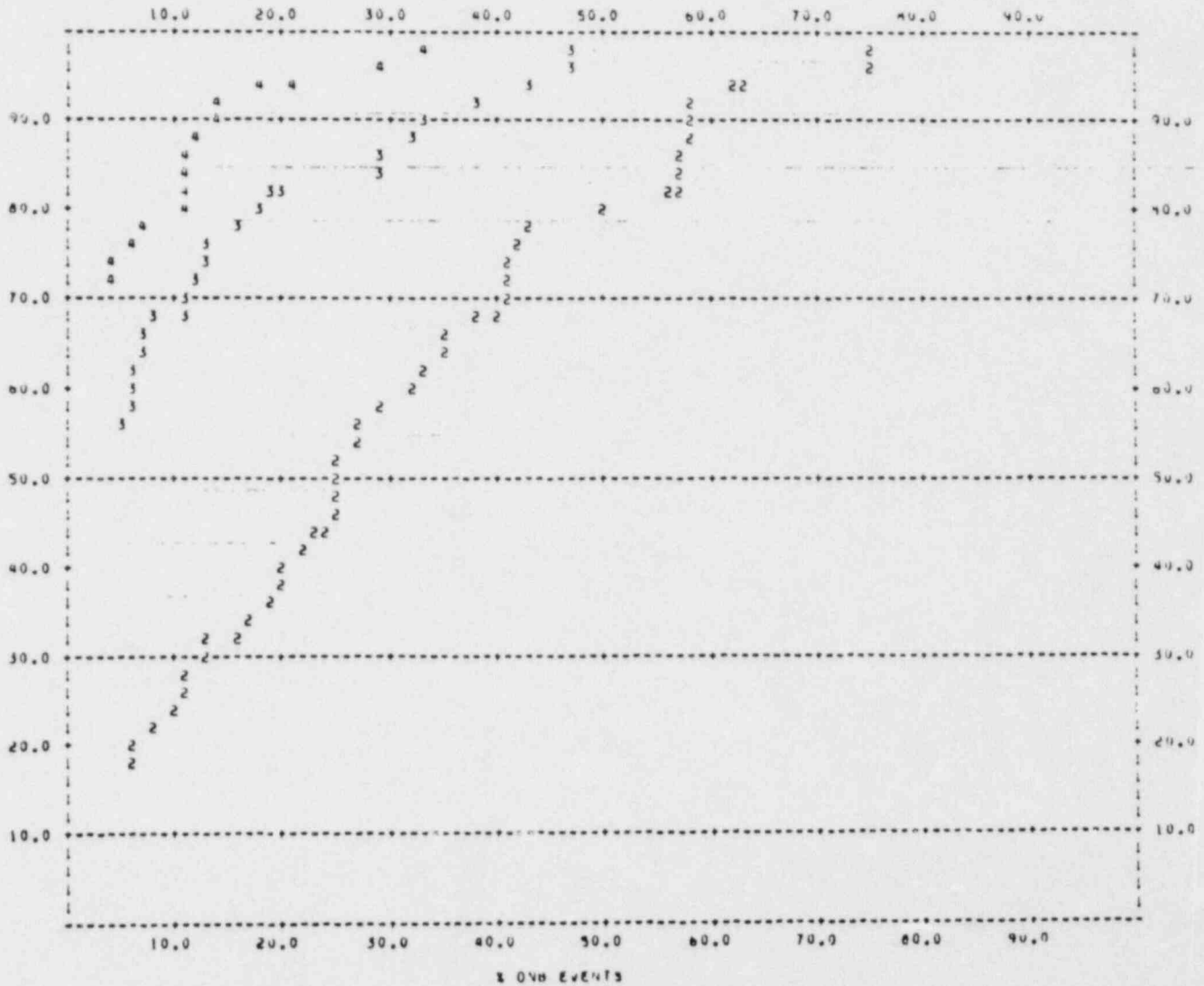

DATA IS A SUBSET OF 3800 POINTS FROM 60 CE TEST SECTIONS WITH UNIFORM AXIAL HEAT FLUX

FIGURE 9j RELATIVE CUMULATIVE FREQUENCY DISTRIBUTION FOR PRESSURE = 2400 PSIA

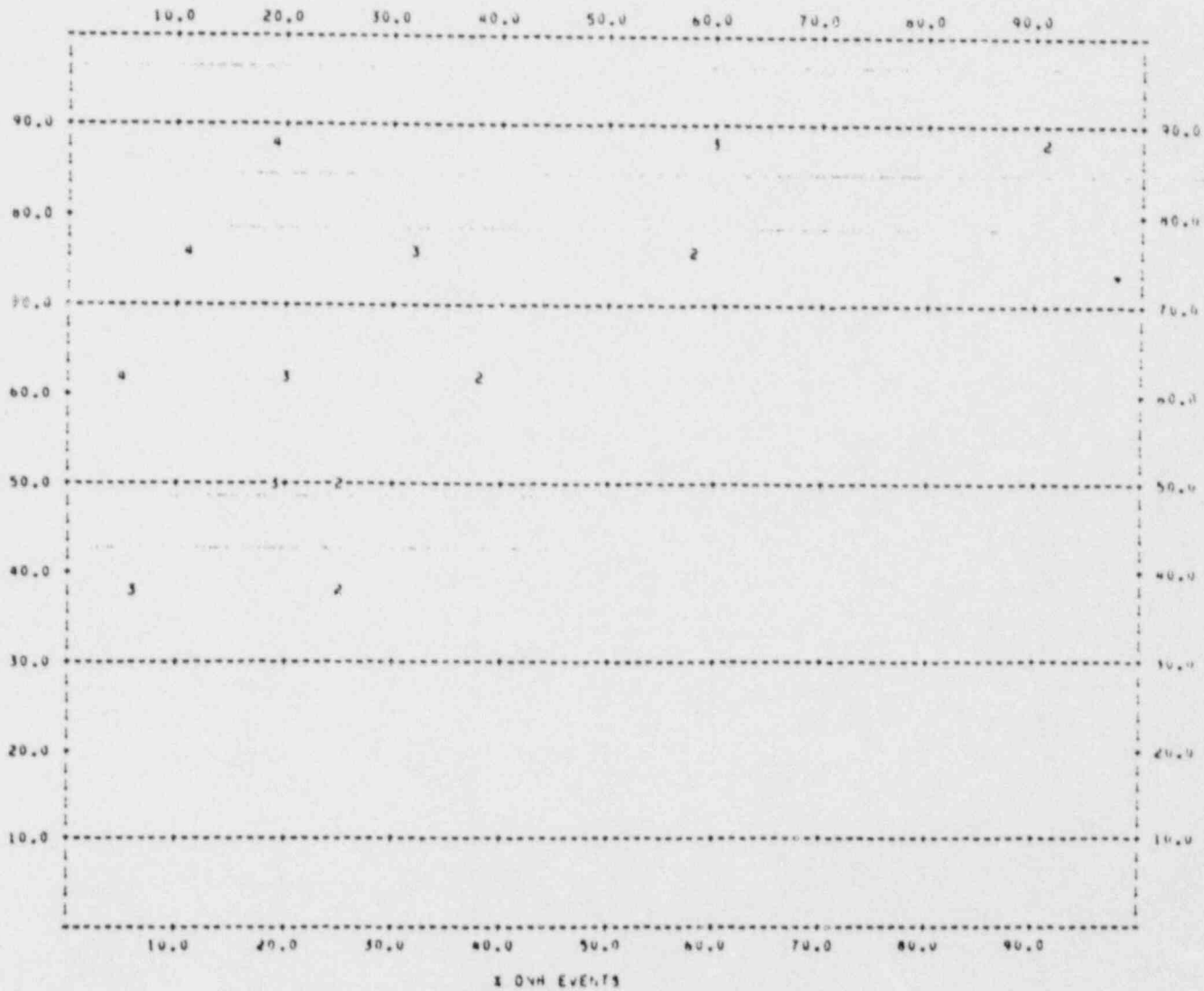

DATA IS A SUBSET OF 3800 POINTS FROM 60 CE TEST SECTIONS WITH UNIFORM AXIAL HEAT FLUX

FIGURE 9k RELATIVE CUMULATIVE FREQUENCY DISTRIBUTION FOR PRESSURE = 2300 PSIA

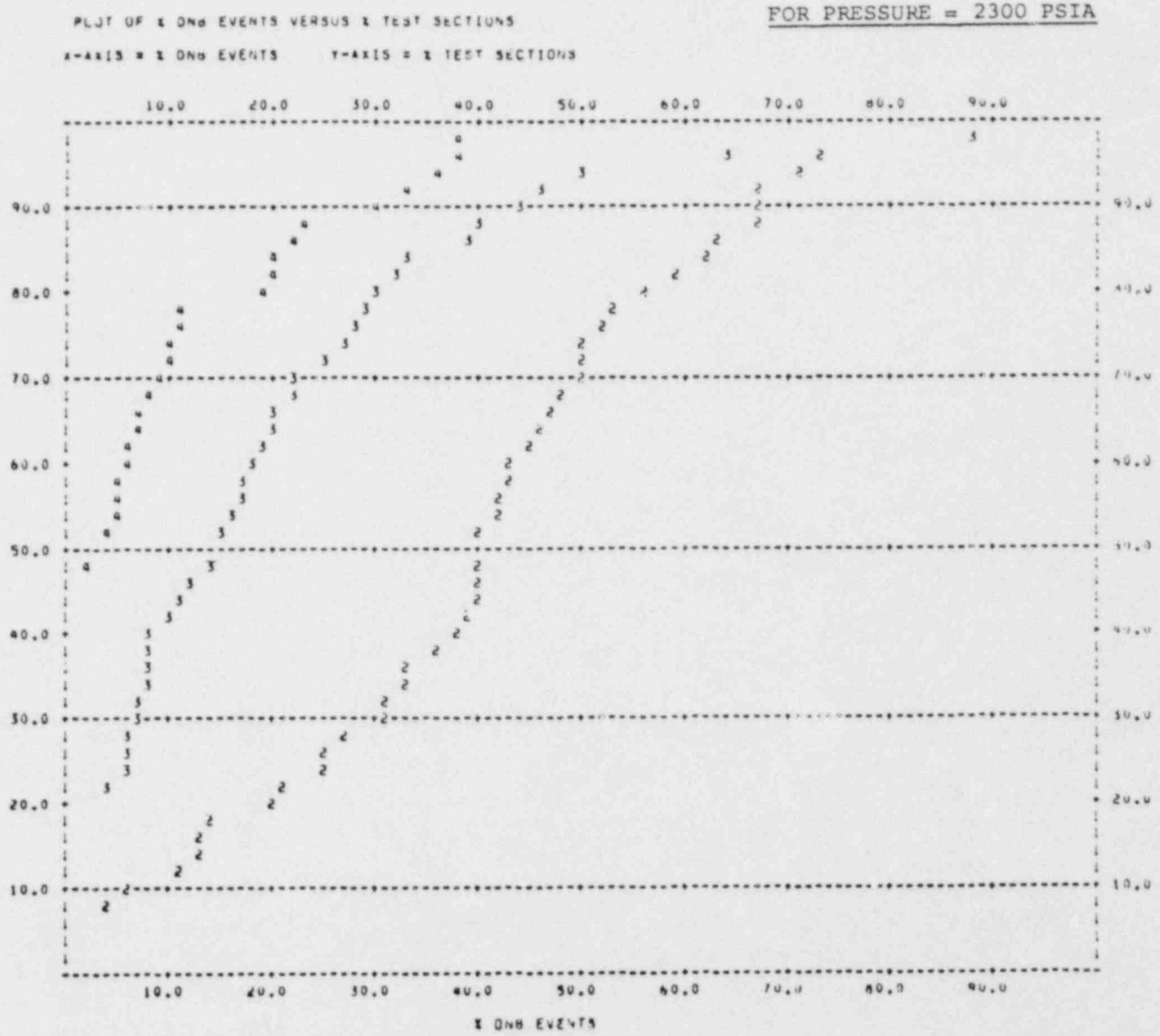

DATA IS A SUBSET OF 3800 POINTS FROM 60 CE TEST SECTIONS WITH UNIFORM AXIAL HEAT FLUX

FIGURE 9ℓ RELATIVE CUMULATIVE FREQUENCY DISTRIBUTION FOR PRESSURE = 2000 PSIA

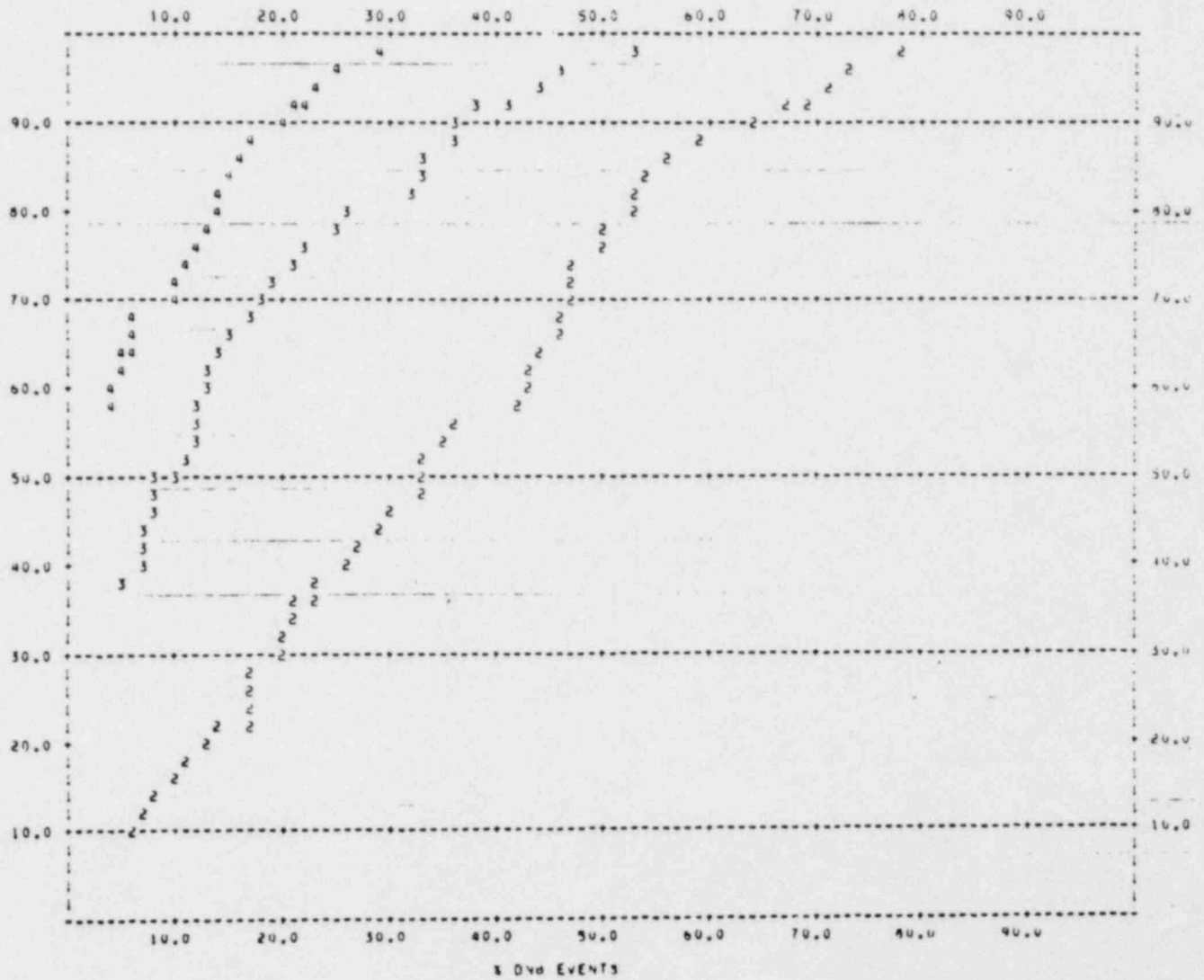

DATA IS A SUBSET OF 3800 POINTS FROM 60 CE TEST SECTIONS WITH UNIFORM AXIAL HEAT FLUX

FIGURE 9m RELATIVE CUMULATIVE FREQUENCY DISTRIBUTION FOR PRESSURE = 1800 PSIA

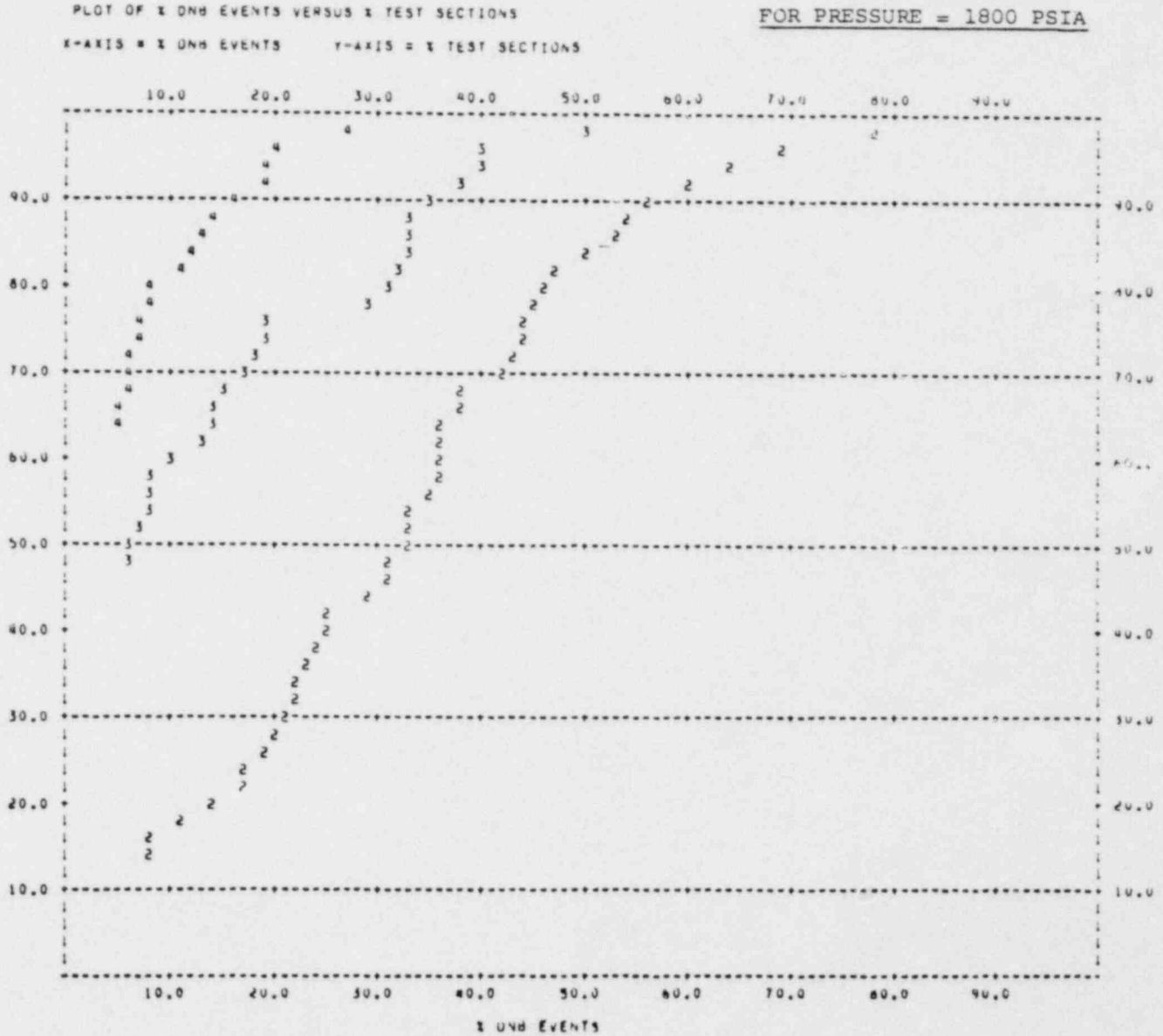

DATA IS A SUBSET OF 3800 POINTS FROM 60 CE TEST SECTIONS WITH UNIFORM AXIAL HEAT FLUX

FIGURE 9n RELATIVE CUMULATIVE FREQUENCY DISTRIBUTION FOR PRESSURE = 1400 PSIA

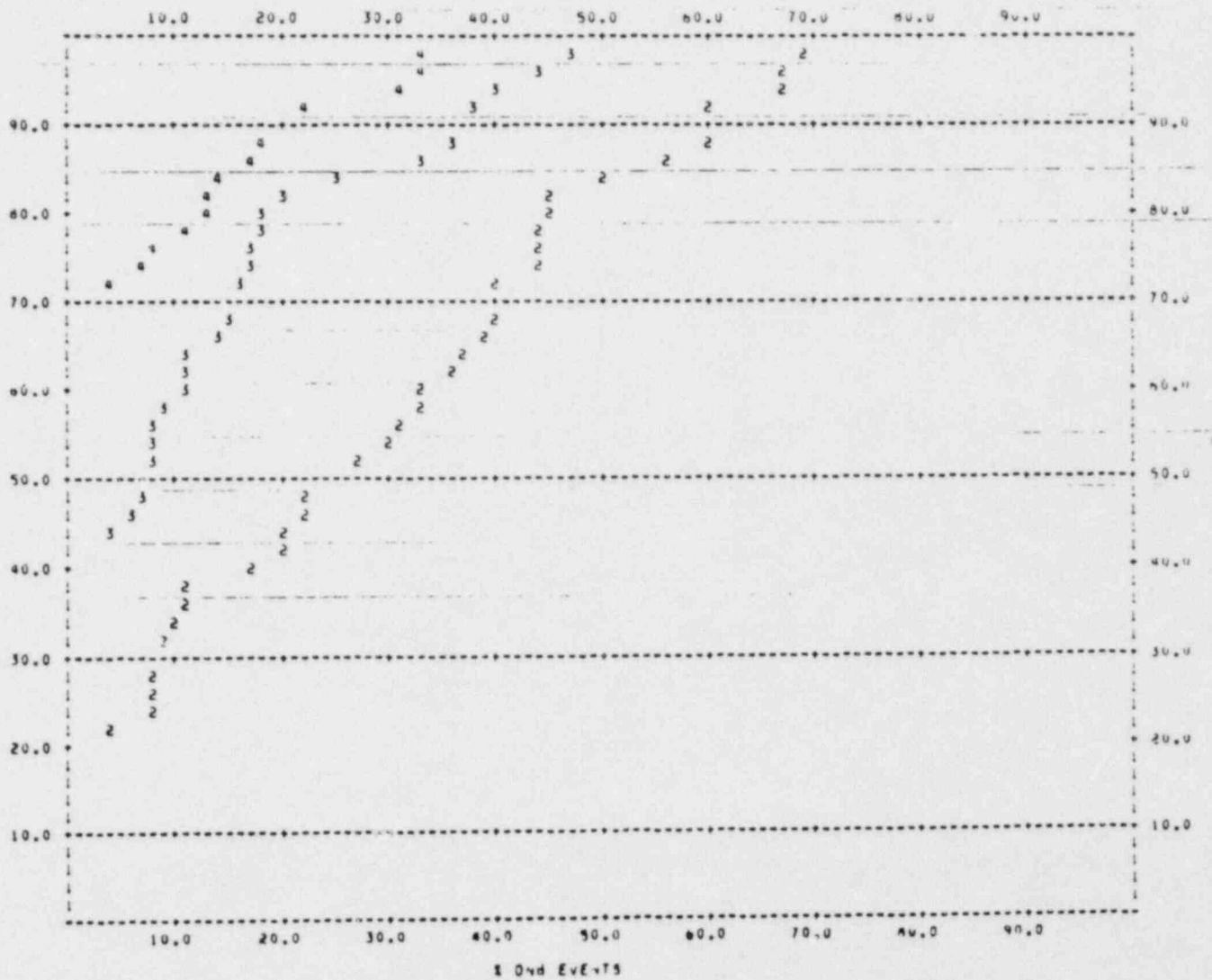

DATA IS A SUBSET OF 3800 POINTS FROM 60 CE TEST SECTIONS WITH UNIFORM AXIAL HEAT FLUX

FIGURE 9o RELATIVE CUMULATIVE FREQUENCY DISTRIBUTION FOR PRESSURE = 900 PSIA

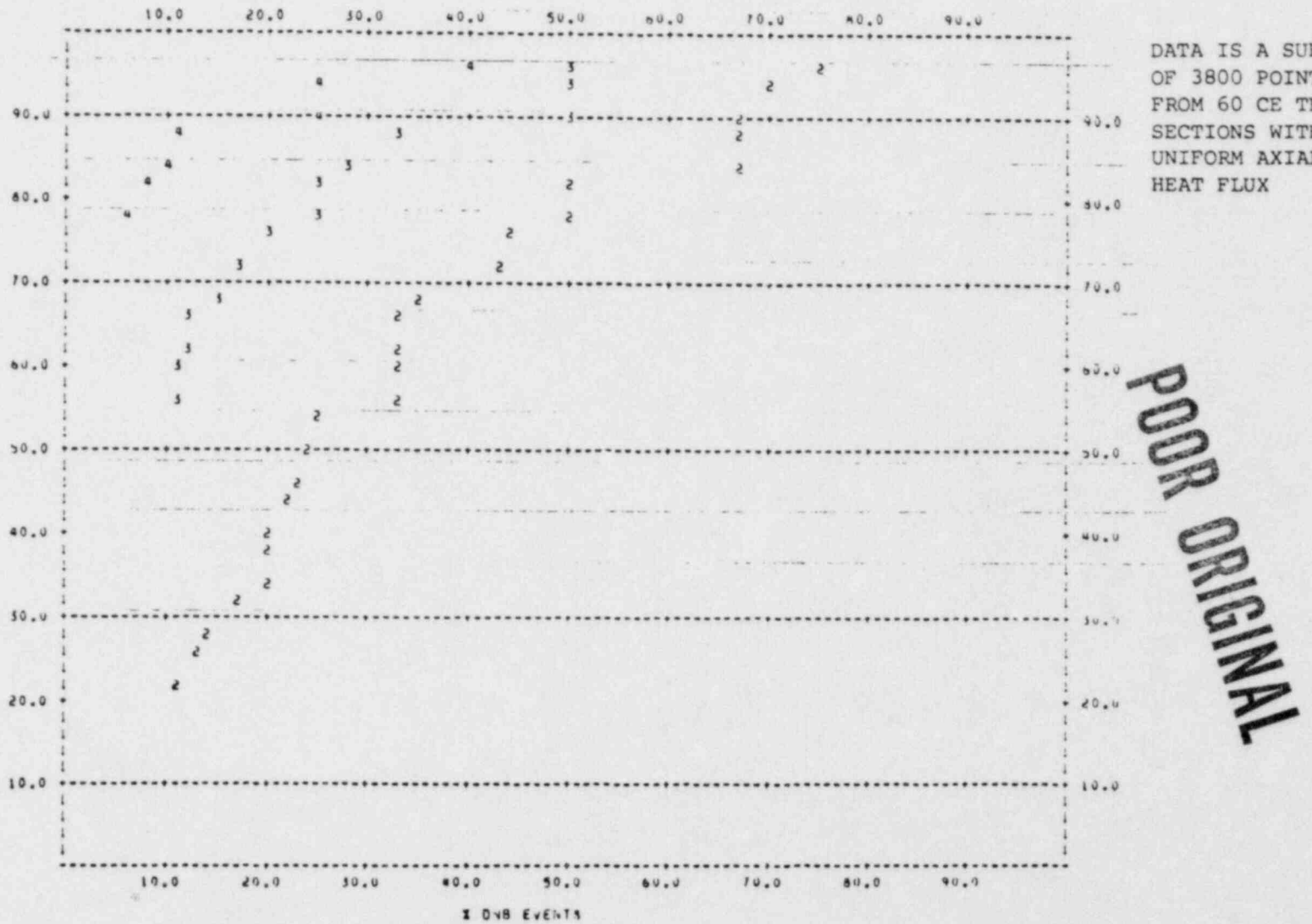

DATA IS A SUBSET OF 3800 POINTS FROM 60 CE TEST SECTIONS WITH UNIFORM AXIAL HEAT FLUX

occurrence (or non-occurrence) of the multiple DNB events for various test conditions.

2) The effect of the variation of test conditions, such as pressure, bundle average mass velocity and bundle inlet subcooling, can be determined by plotting the mean values (obtained from the frequency distribution curves) versus pressure, mass velocity or inlet subcooling and comparing the results with the overall mean value. This comparison is performed in Figures 9p to 9r and confirms the general conclusions arrived at, in the previous statistical analysis.

2.3 Predictive Correlation Studies

Earlier parametric studies on the bundle average DNB heat flux versus steam energy flow (with pressure as a parameter) for a large number of test sections and test conditions indicated that the presently available DNB correlations, for the first DNB, may be useful in the prediction of the DNB events of higher rank. In this section, the capability of an available DNB correlation, in the prediction of multiple DNB events will be tested. However, since the scope of the present study is limited to the bundle average test conditions, a DNB correlation based on global parameters will be chosen for this purpose.

Among the available DNB correlation (such as Barnett, Macbeth and Bowring correlations) the Bowring correlation, described in the appendix (2), has an RMS error of 11% over the whole pressure range, as compared to 18% and 21% for the Macbeth and Barnett correlations respectively. For this reason, the Bowring correlation was chosen for the prediction of DNB heat flux for multiple DNB events. The data employed in this study are the same as the data used earlier for parametric studies involving the bundle average DNB heat flux versus steam energy flow. This data consists of 2000 test points obtained from 60 Combustion Engineering test sections with uniform axial and non-uniform radial heat flux distribution at operating pressures above 1700 psia. Employing this data set, the DNB heat flux for the first,

FIGURE 9p EFFECT OF MASS VELOCITY ON PERCENT NUMBER OF DNB EVENTS BASED ON THE MEAN VALUE OF RELATIVE CUMULATIVE FREQUENCY DISTRIBUTION

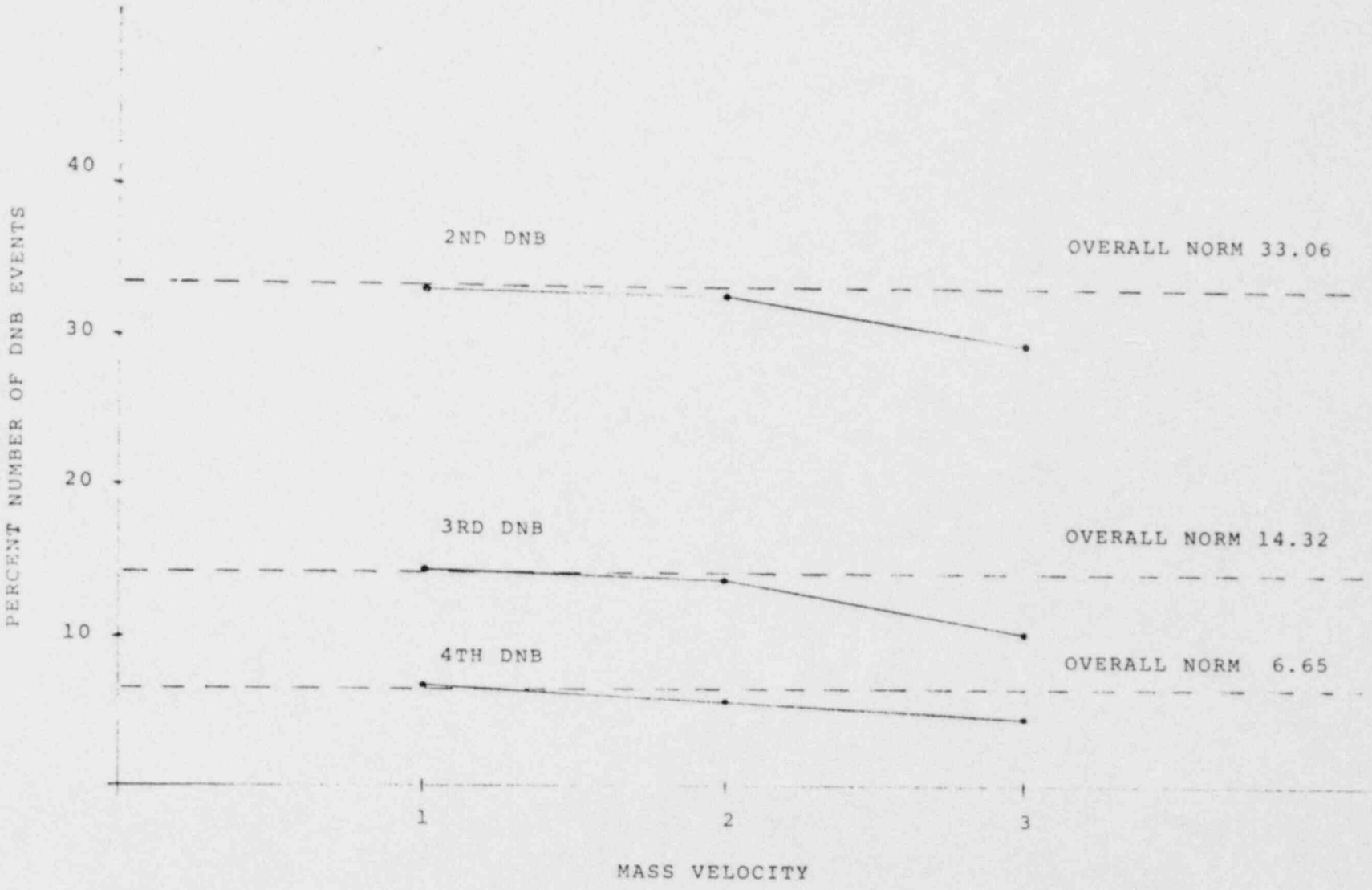

FIGURE 9q EFFECT OF PRESSURE ON PERCENT NUMBER OF DNB EVENTS BASED ON THE MEAN VALUE OF RELATIVE CUMULATIVE FREQUENCY DISTRIBUTION

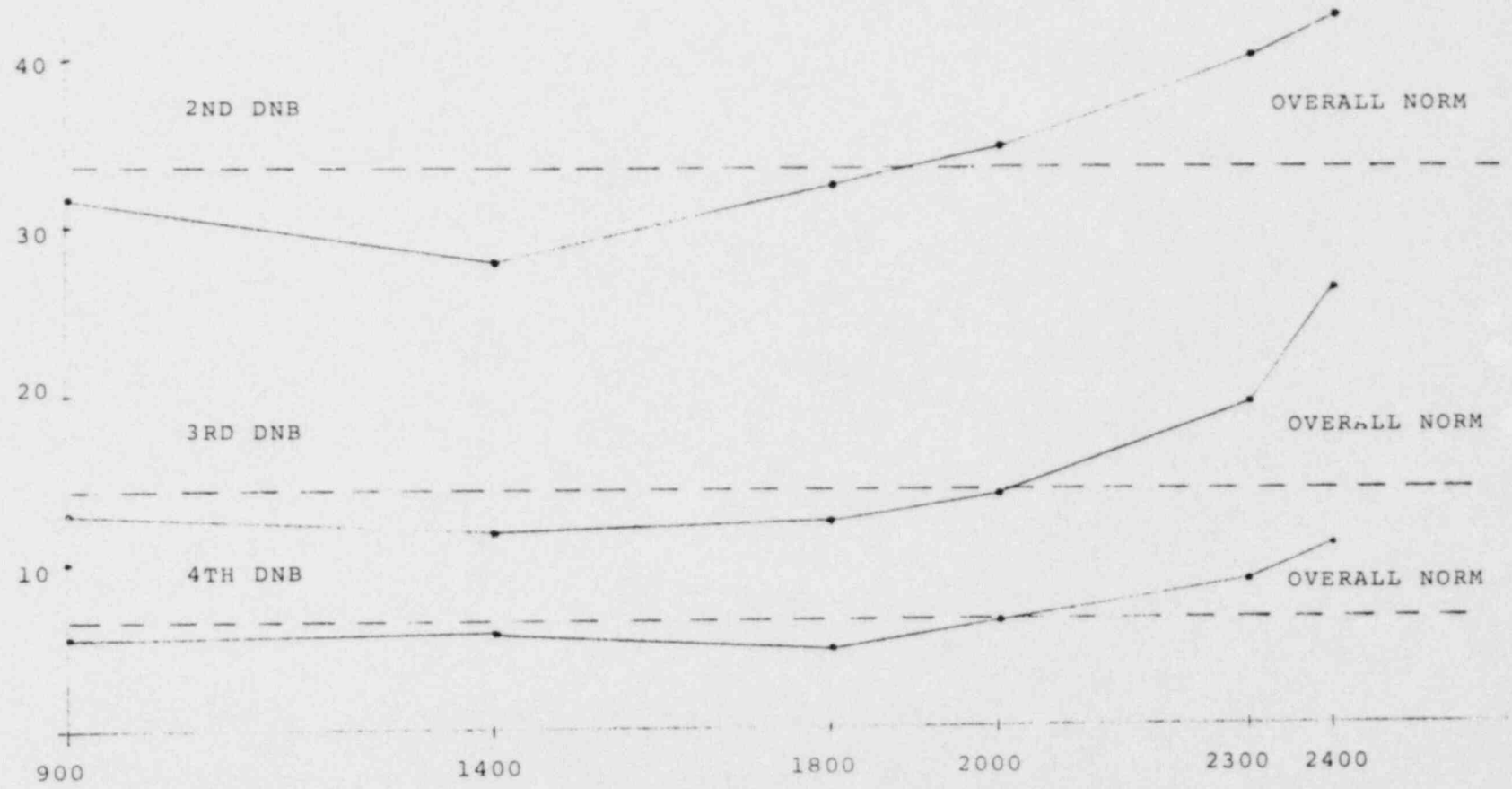

FIGURE 9r EFFECT OF INLET SUBCOOLING (INLET QUALITY) ON PERCENT NUMBER OF DNB EVENTS BASED ON THE MEAN VALUE OF RELATIVE CUMULATIVE FREQUENCY DISTRIBUTION

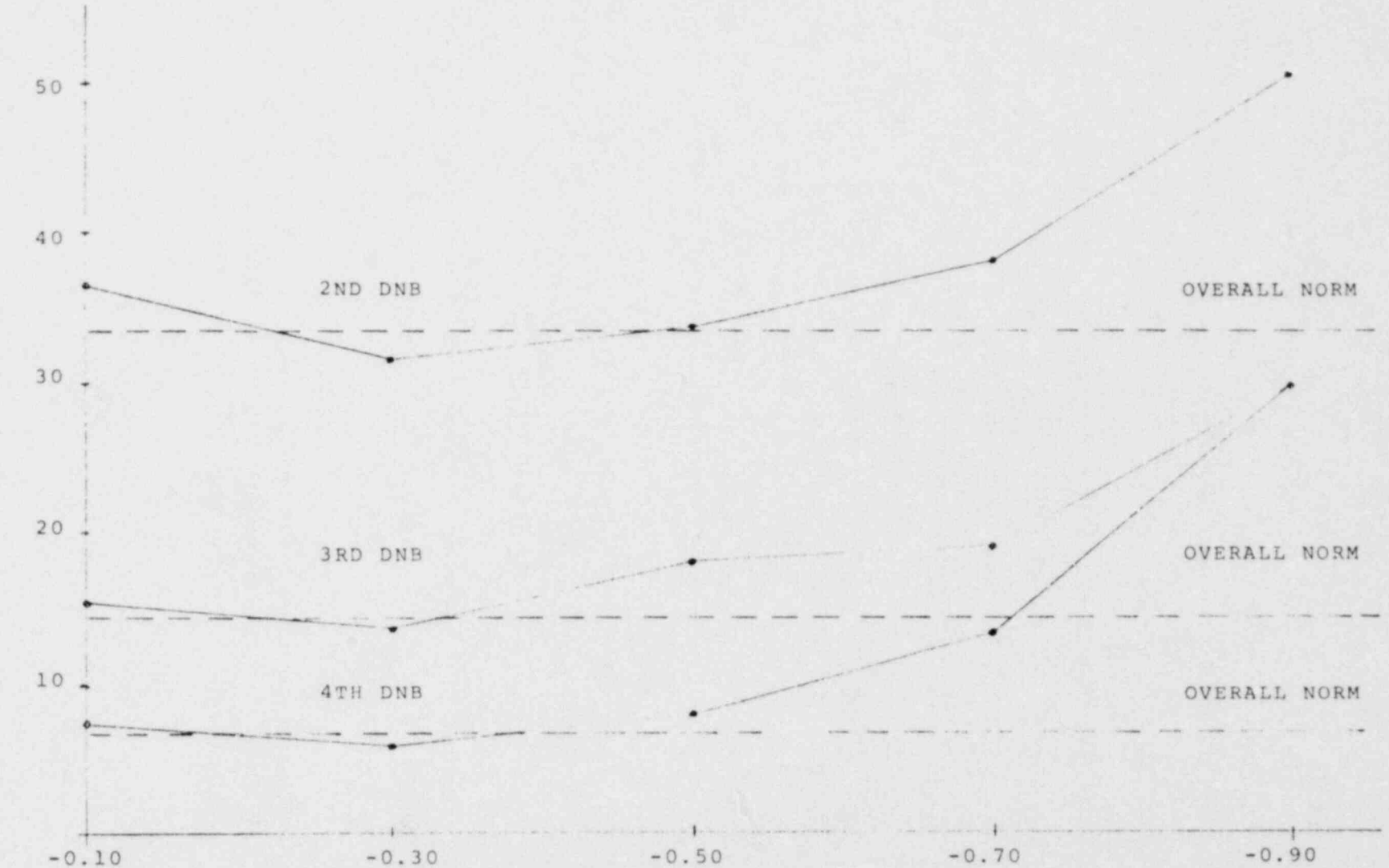

second, third and fourth DNB events are calculated using the Bowring correlation. The ratio of the calculated to the observed DNB heat flux for the first, second, third and fourth DNB events are then plotted versus the following variables in Figures 10a to 10p:

1) The observed DNB heat flux

2) The bundle average mass velocity

3) The bundle inlet quality

4) The operating pressure

Based on these characteristics, the statistical results consisting of the average values and standard deviations of the calculated to the observed DNB heat flux for first, second, third and fourth DNB events are computed and compiled in Table 3.

A study of the above characteristics and the associated statistics leads to the following conclusions:

1) The trends in DNB events of higher rank, as evidenced by the overall patterns of the above characteristics and the statistical results, generally follow those of the first DNB.

2) The DNB correlations for the first DNB, based on the bundle average conditions, are useful in the prediction of DNB events of higher rank. These correlations could predict the DNB events of high rank with the same degree of accuracy as the first DNB.

3) To ascertain the adequacy of the predictive correlations based on local conditions at the first DNB, for the prediction of DNB events of high rank, the following studies are required:

a) Computation of local conditions at DNB points of higher rank, using a subchannel analysis code such as COBRA-IIIC

b) Verification of the predictive correlations for the

FIGURE 10a RATIO OF CALCULATED TO OBSERVED DNB HEAT FLUX VERSUS OBSERVED DNB HEAT FLUX FOR FIRST DNB

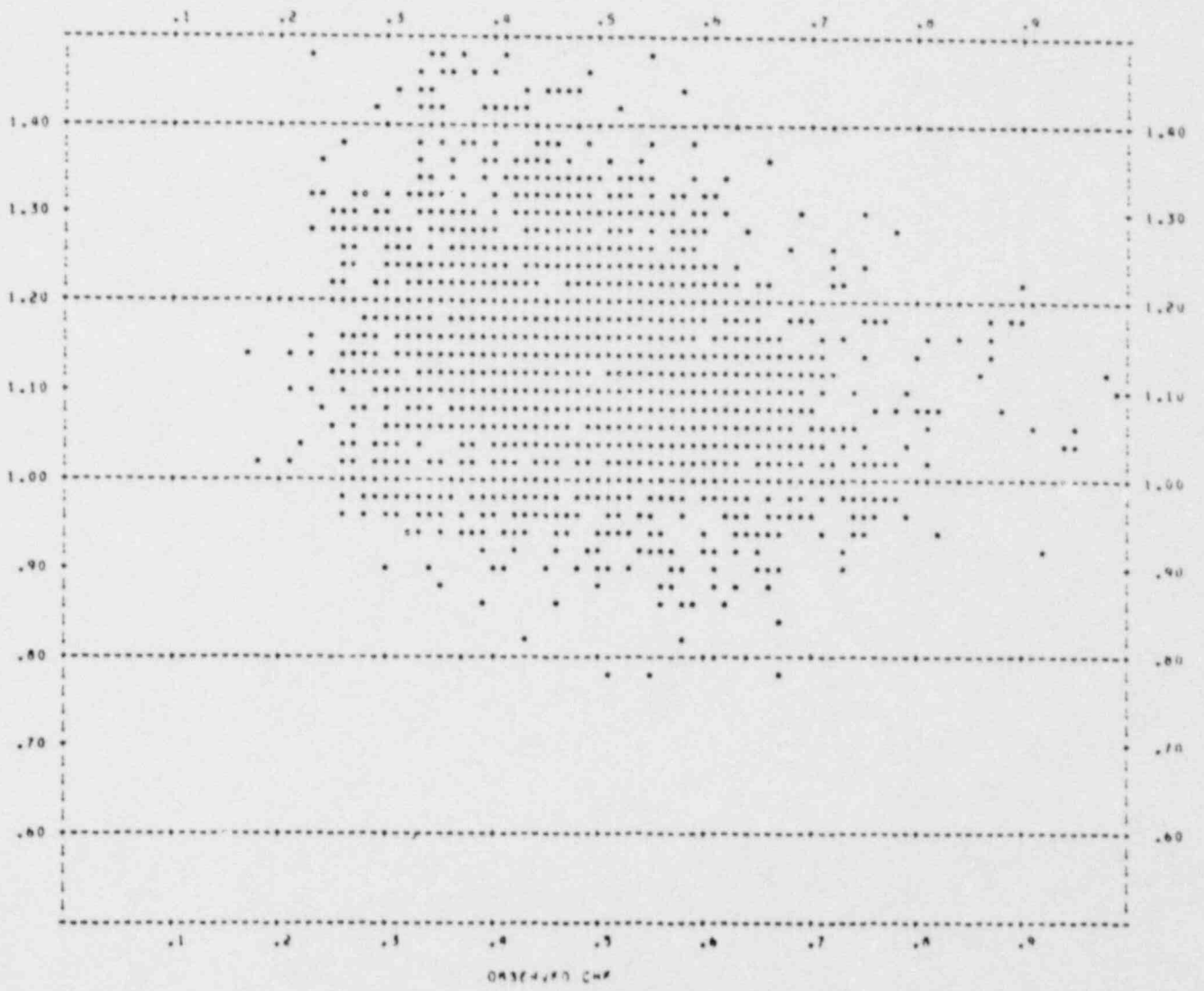

FIGURE 10 b RATIO OF CALCULATED TO OBSERVED DNB HEAT FLUX VERSUS MASS FLUX FOR FIRST DNB

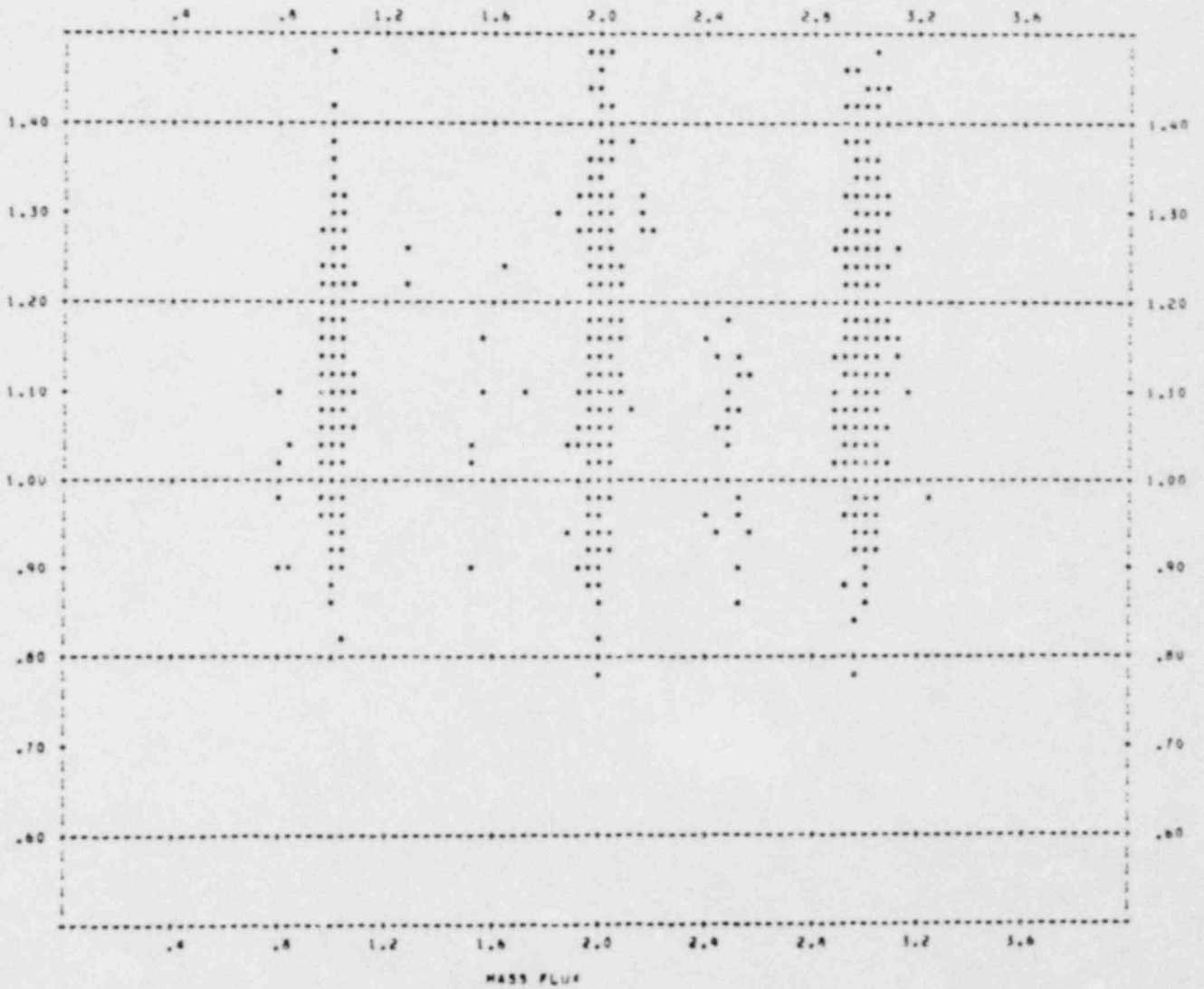

FIGURE 10c RATIO OF CALCULATED TO OBSERVED DNB HEAT FLUX VERSUS QUALITY FOR FIRST DNB

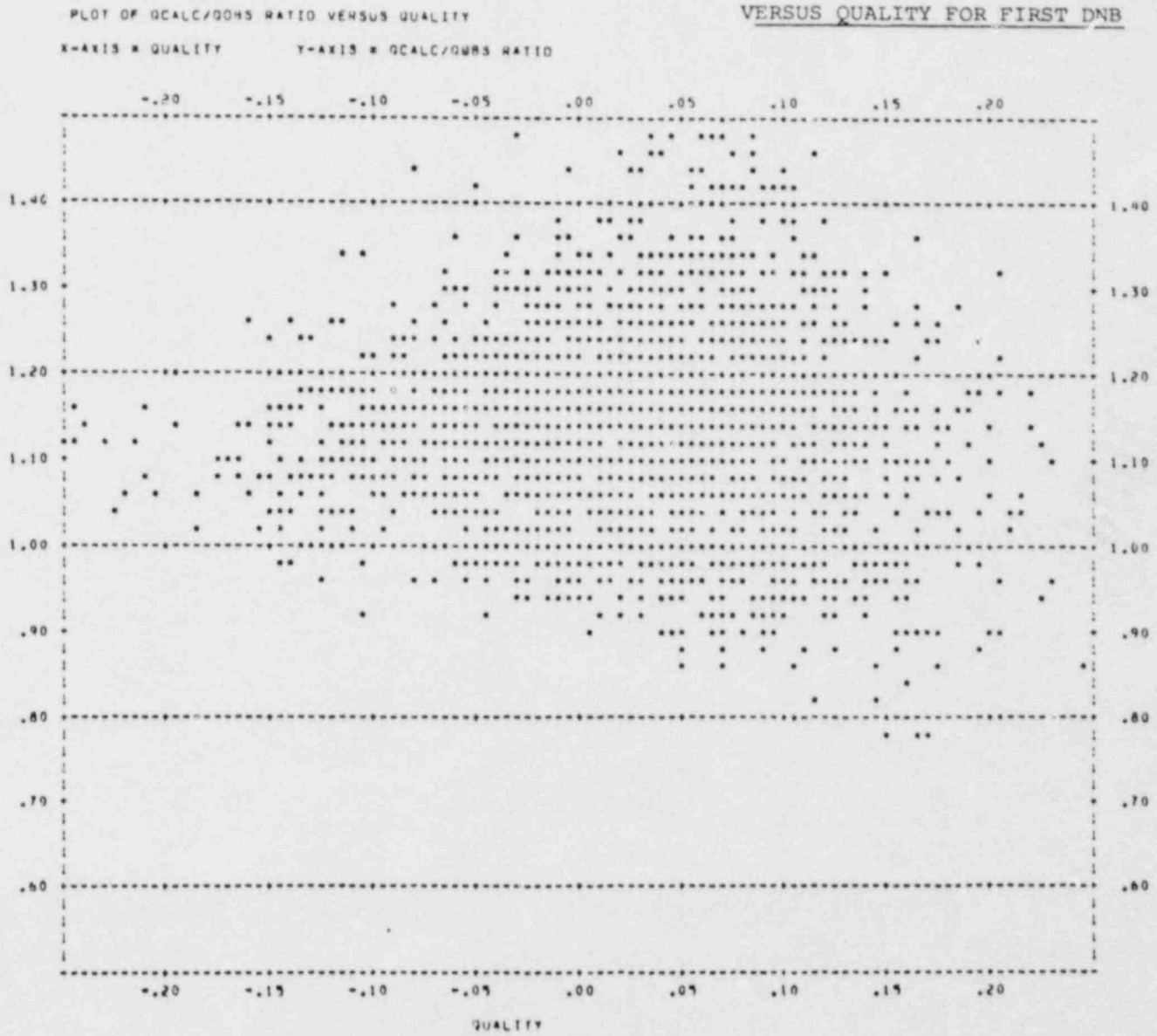

FIGURE 10d RATIO OF CALCULATED TO OBSERVED DNB HEAT FLUX VERSUS PRESSURE FOR FIRST DNB

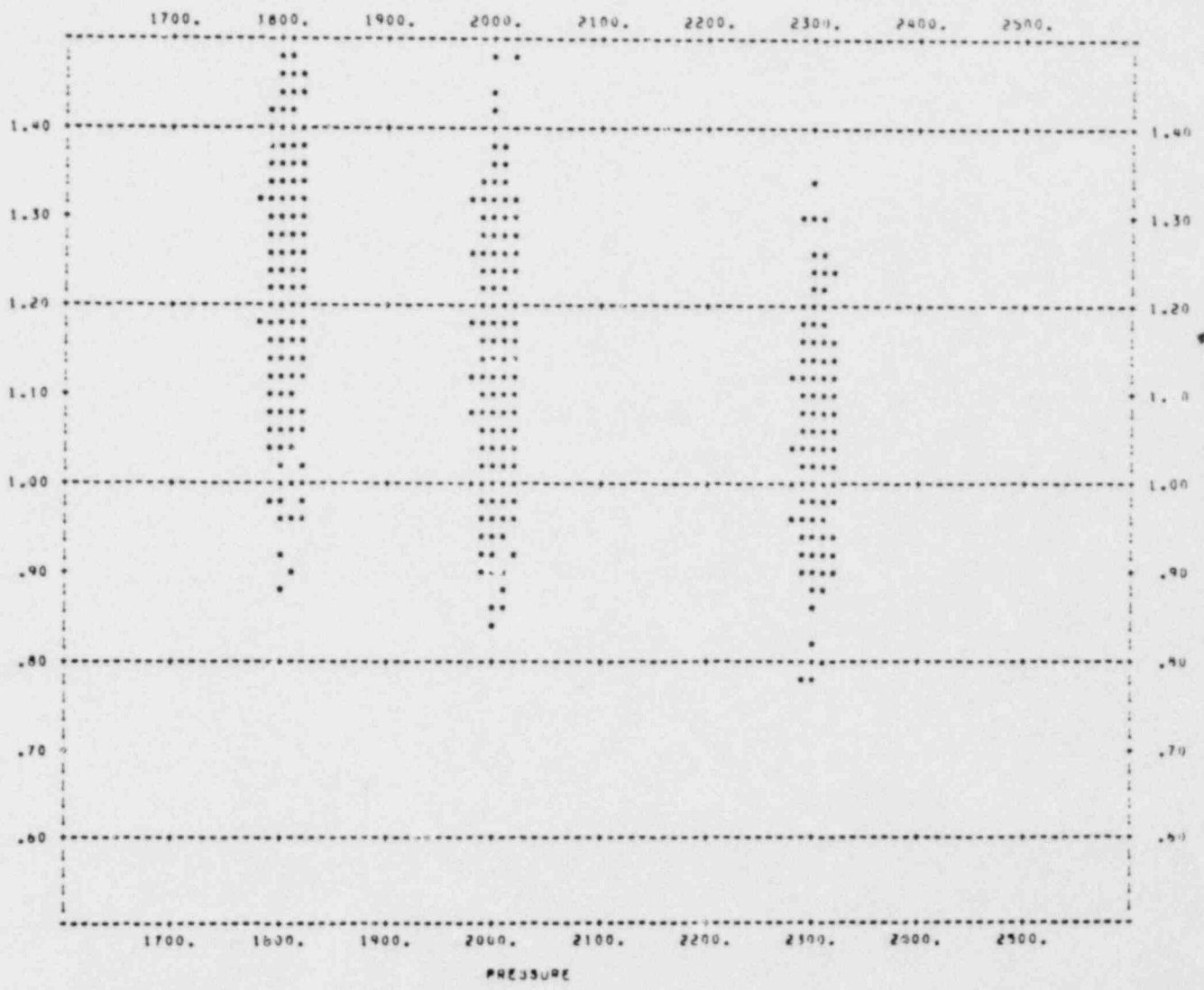

FIGURE 10e RATIO OF CALCULATED TO OBSERVED DNB HEAT FLUX VERSUS OBSERVED DNB HEAT FLUX FOR SECOND DNB

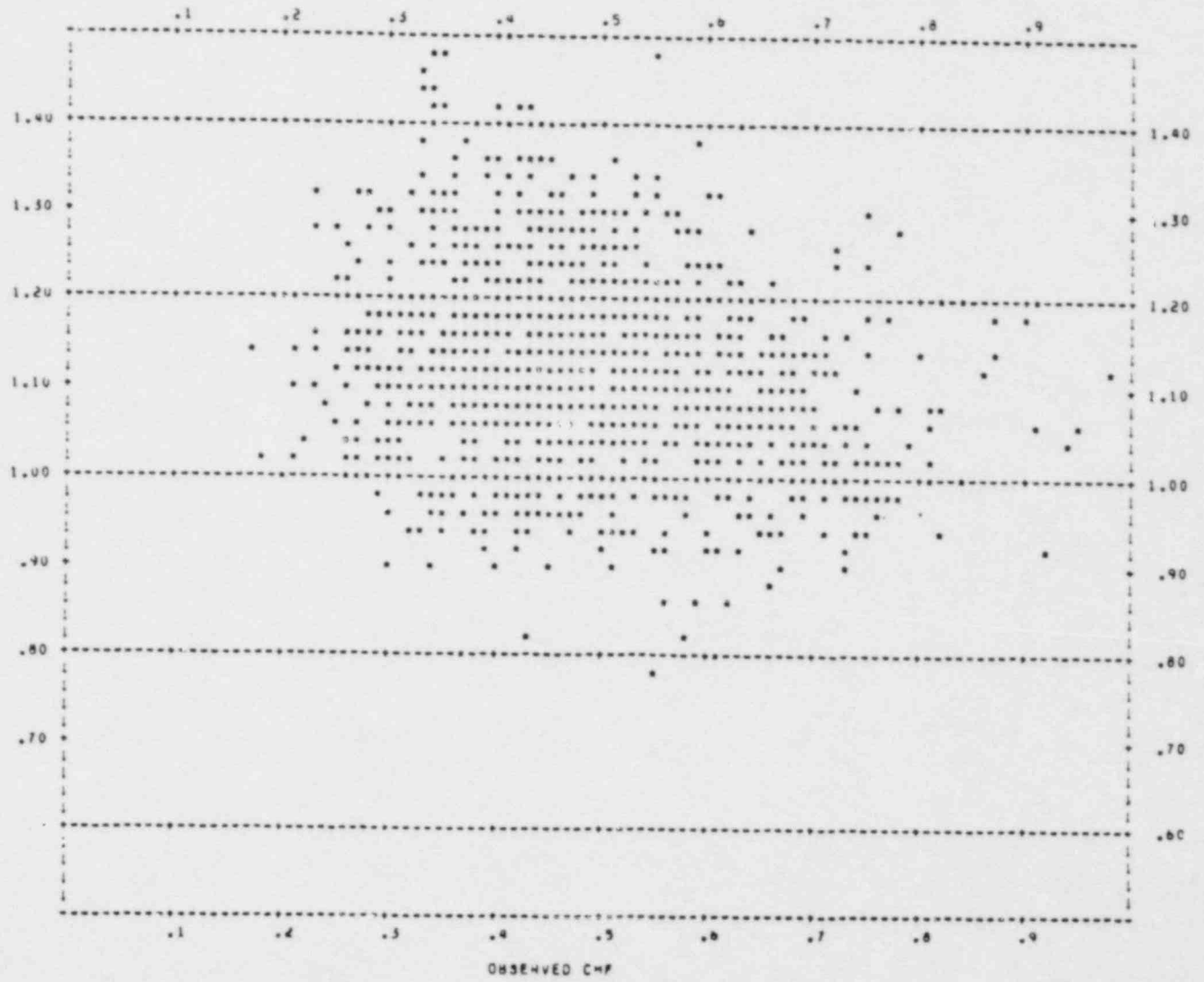

FIGURE 10f RATIO OF CALCULATED TO OBSERVED DNB HEAT FLUX VERSUS MASS FLUX FOR SECOND DNB

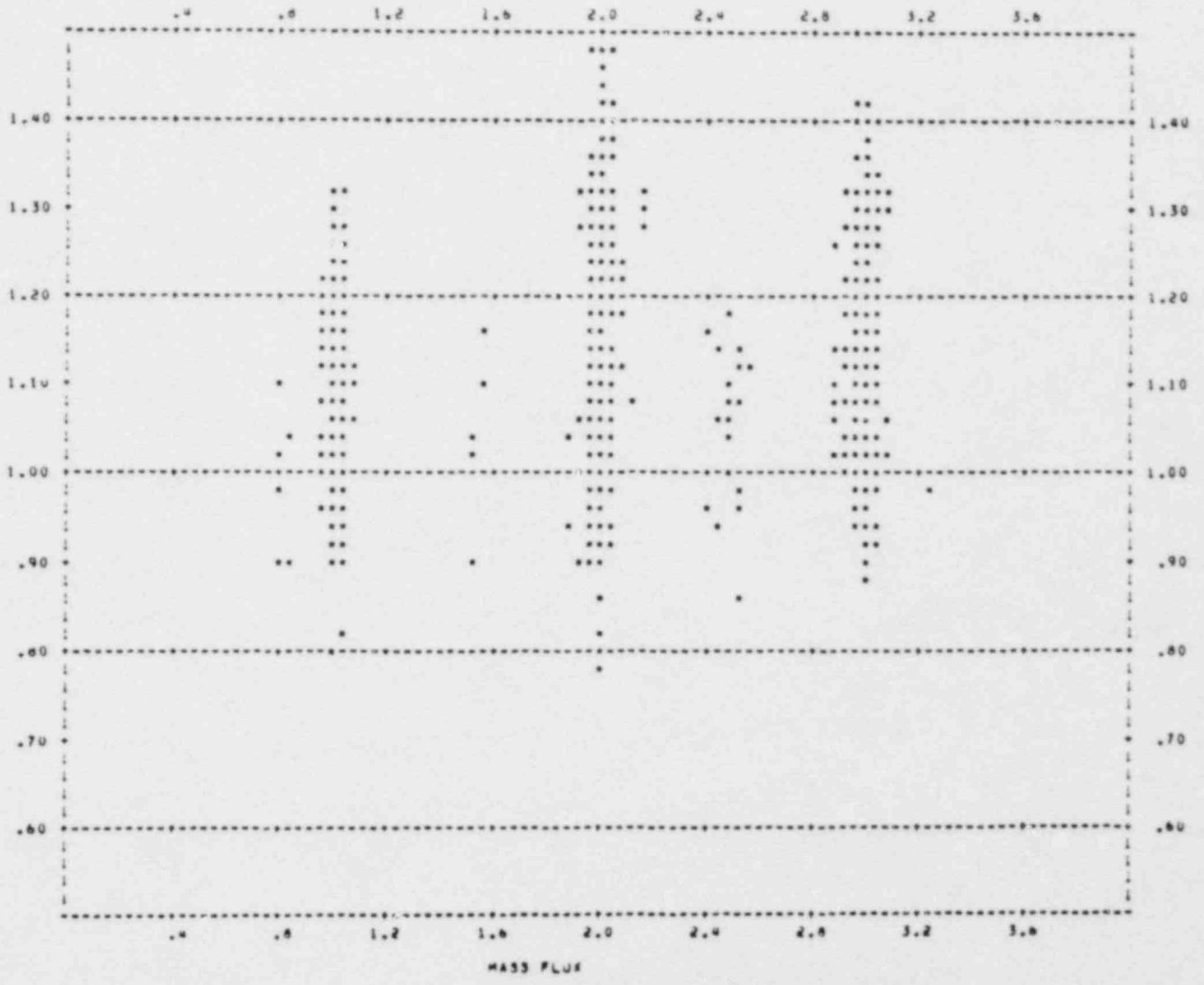

FIGURE 10g RATIO OF CALCULATED TO OBSERVED DNB HEAT FLUX VERSUS QUALITY FOR SECOND DNB

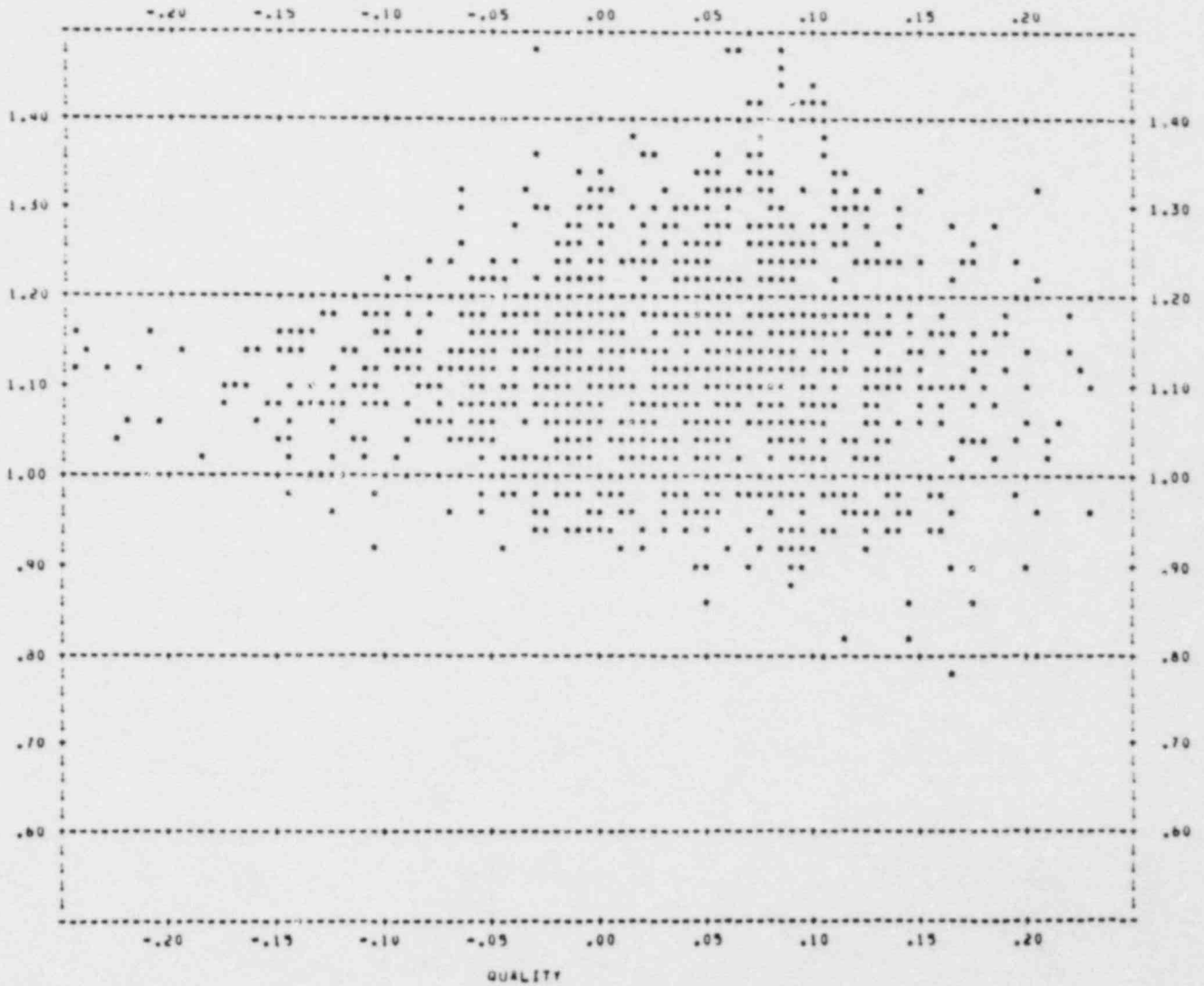

FIGURE 10h RATIO OF CALCULATED TO OBSERVED DNB HEAT FLUX VERSUS PRESSURE FOR SECOND DNB

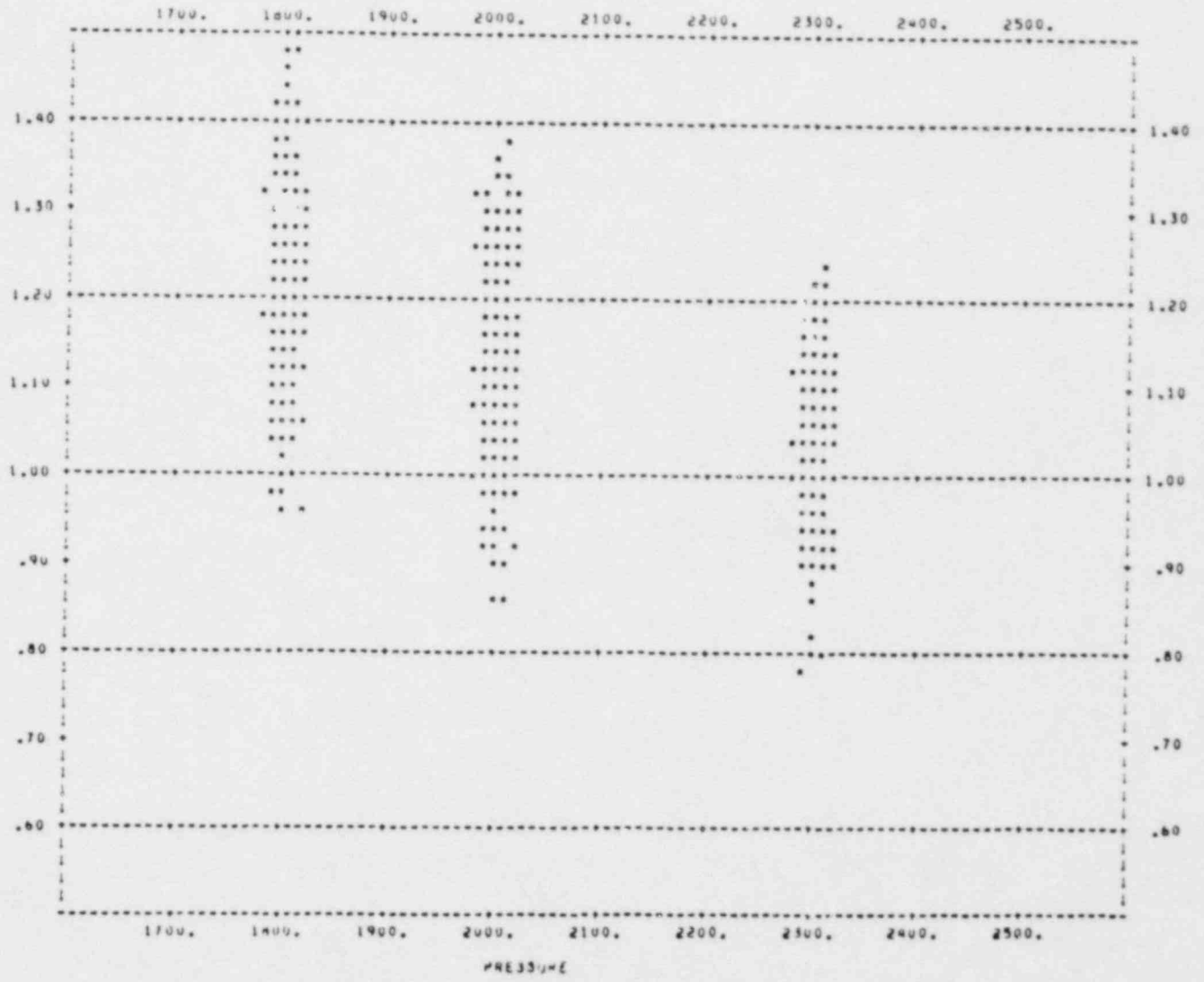

FIGURE 10i RATIO OF CALCULATED TO OBSERVED DNB HEAT FLUX VERSUS OBSERVED DNB HEAT FLUX FOR THIRD DNB

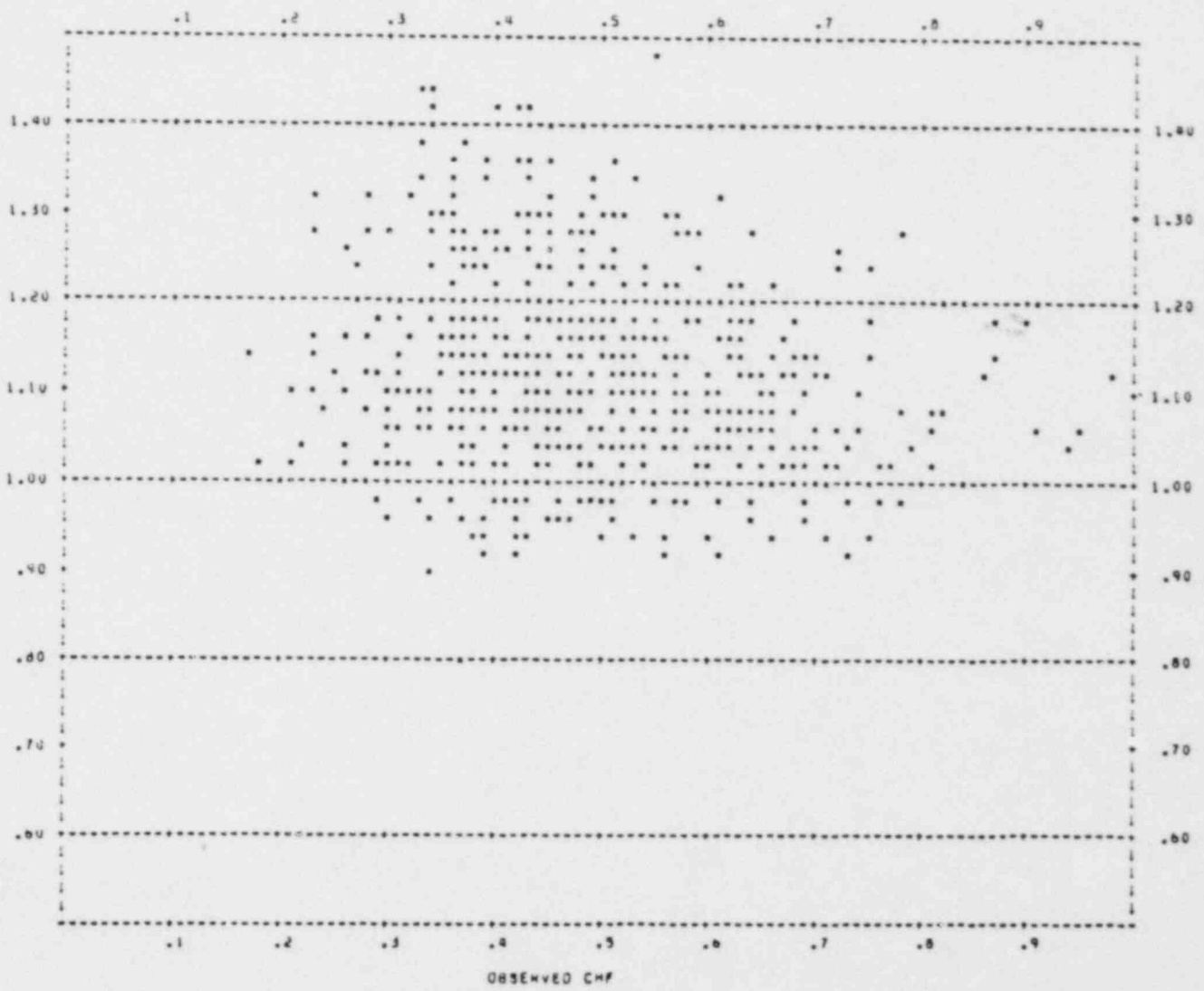

FIGURE 10j RATIO OF CALCULATED TO OBSERVED DNB HEAT FLUX VERSUS MASS FLUX FOR THIRD DNB

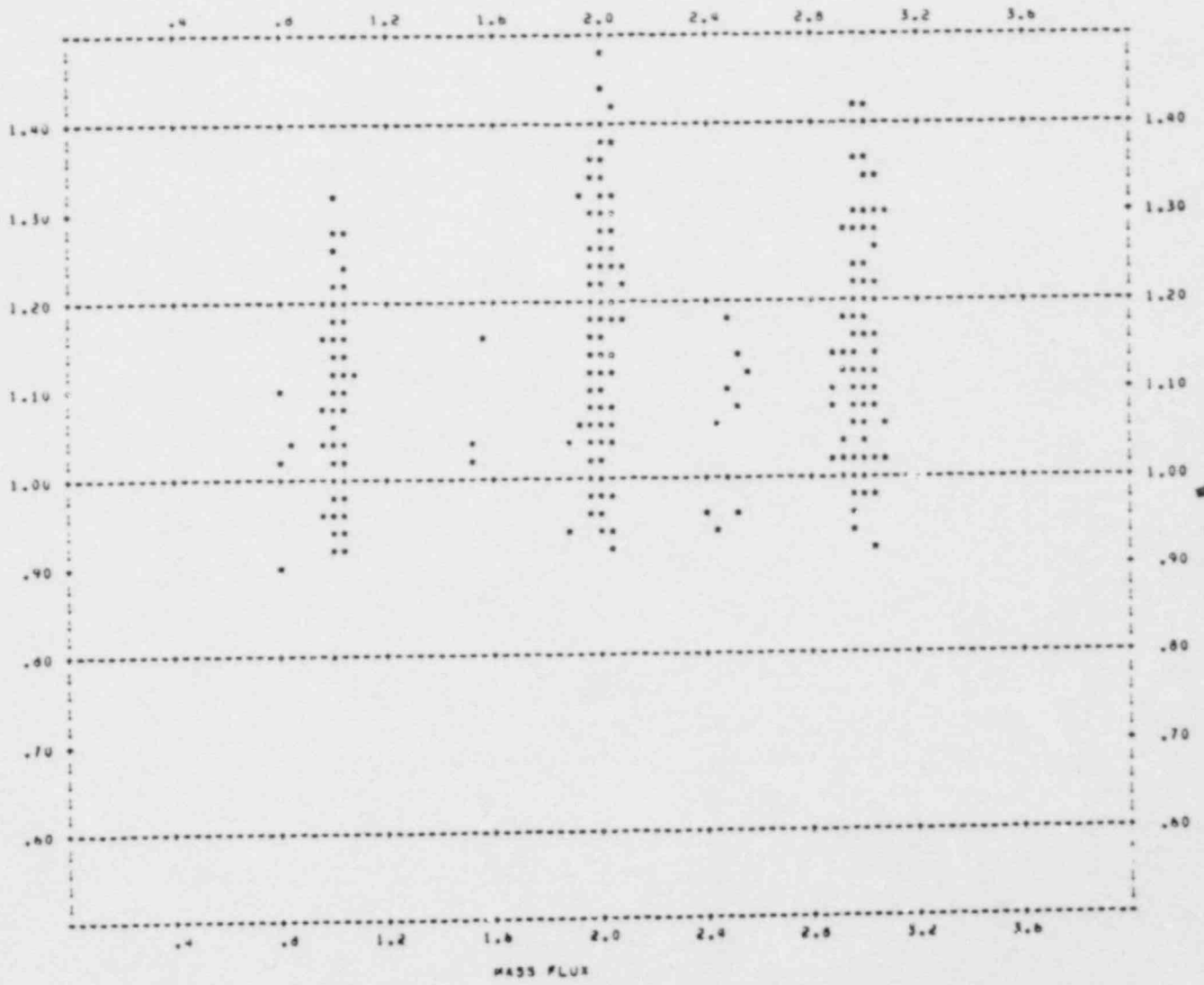

FIGURE 10k RATIO OF CALCULATED TO OBSERVED DNB HEAT FLUX VERSUS QUALITY FOR THIRD DNB

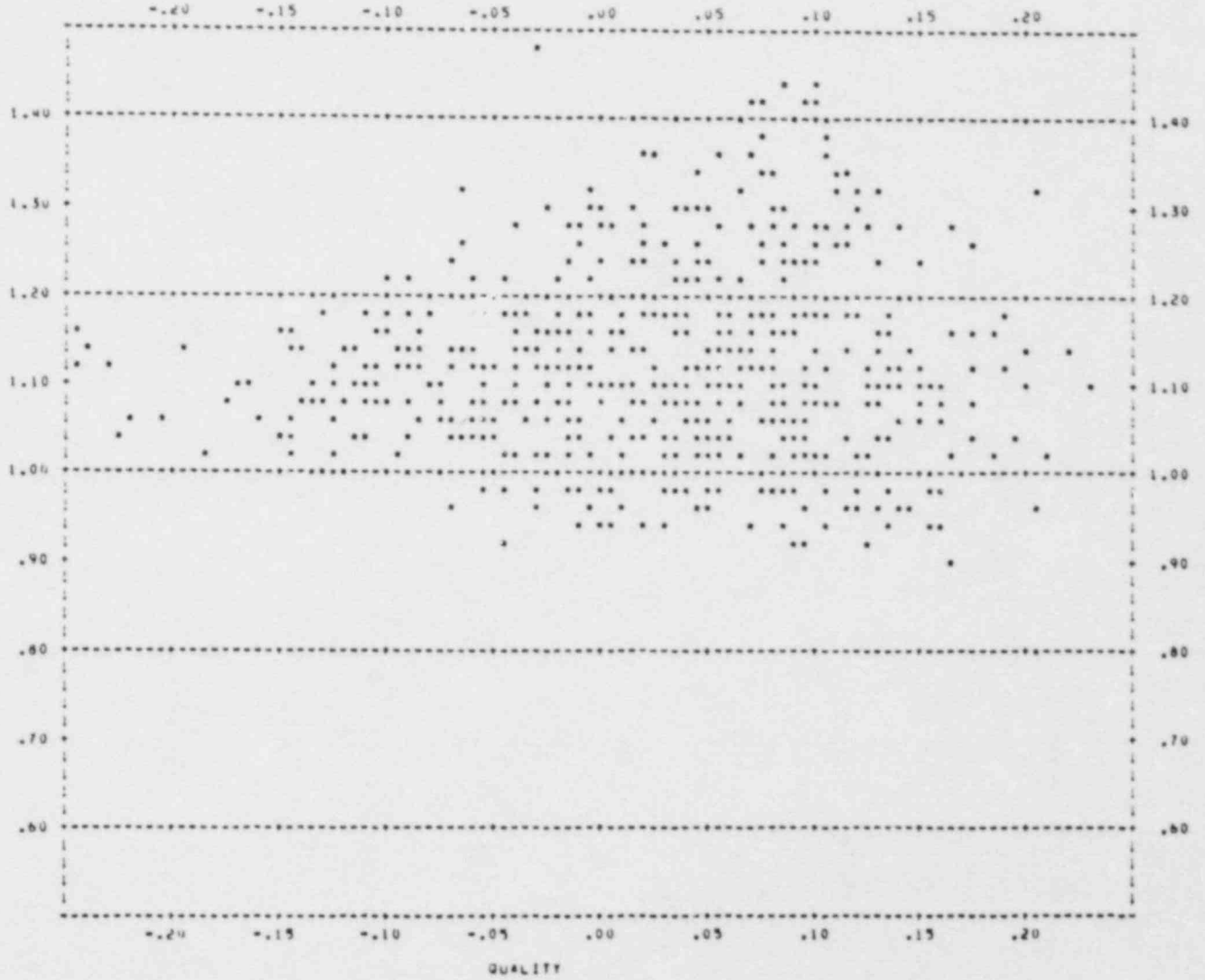

FIGURE 10ℓ RATIO OF CALCULATED TO OBSERVED DNB HEAT FLUX VERSUS PRESSURE FOR THIRD DNB

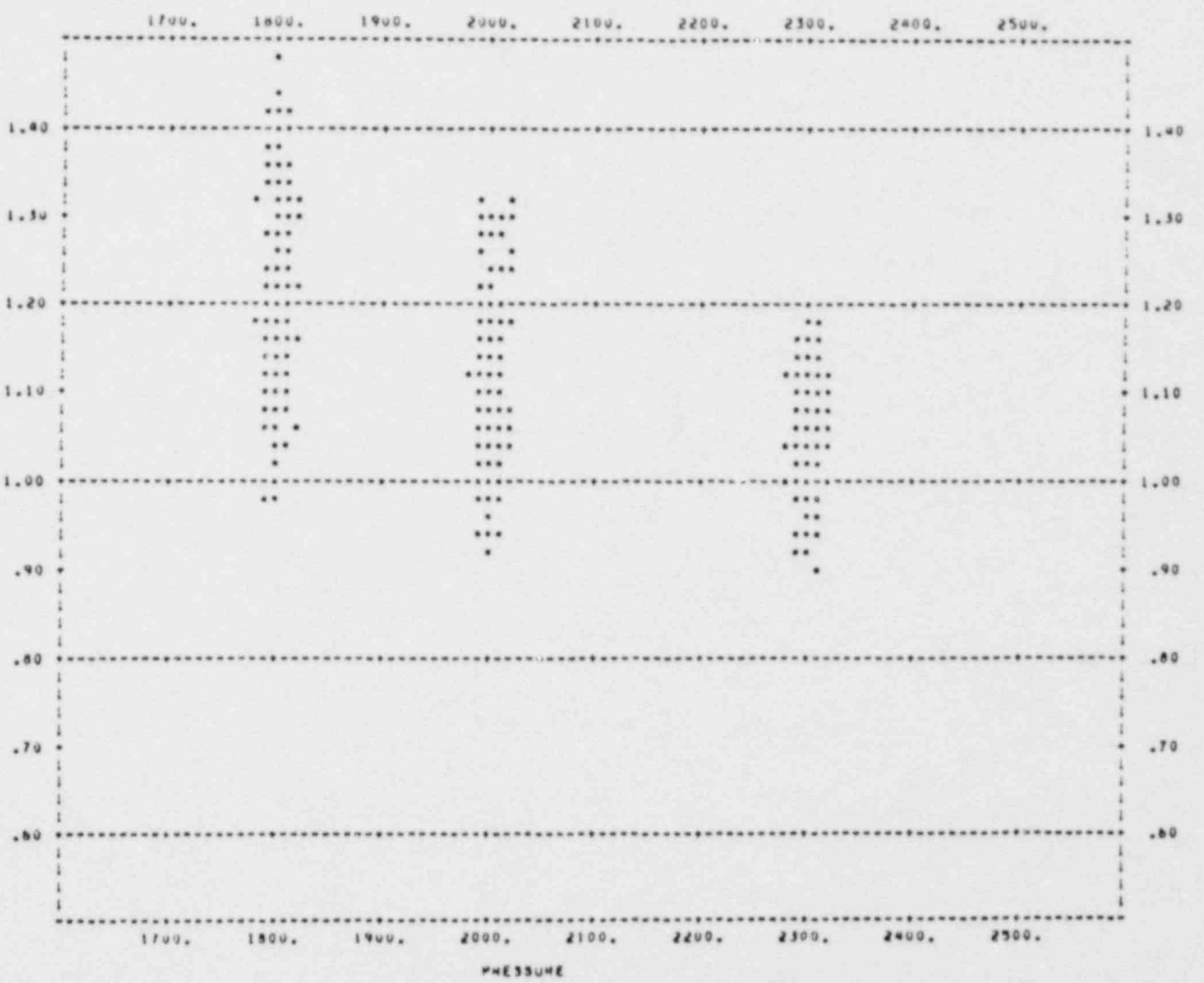

FIGURE 10m RATIO OF CALCULATED TO OBSERVED DNB HEAT FLUX VERSUS OBSERVED DNB HEAT FLUX FOR FOURTH DNB

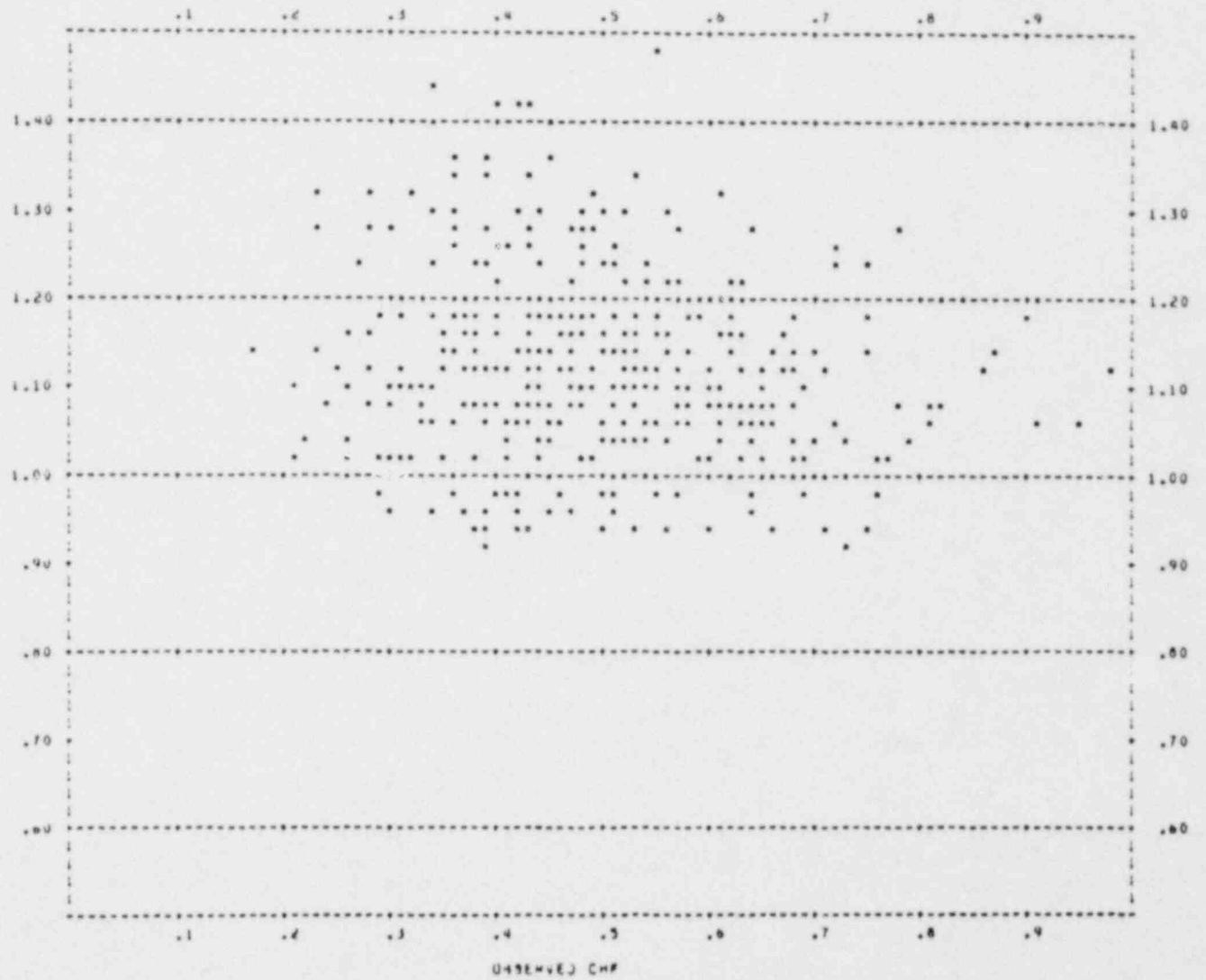

FIGURE 10n RATIO OF CALCULATED TO OBSERVED DNB HEAT F
VERSUS MASS FLUX FOR FOURTH DNB

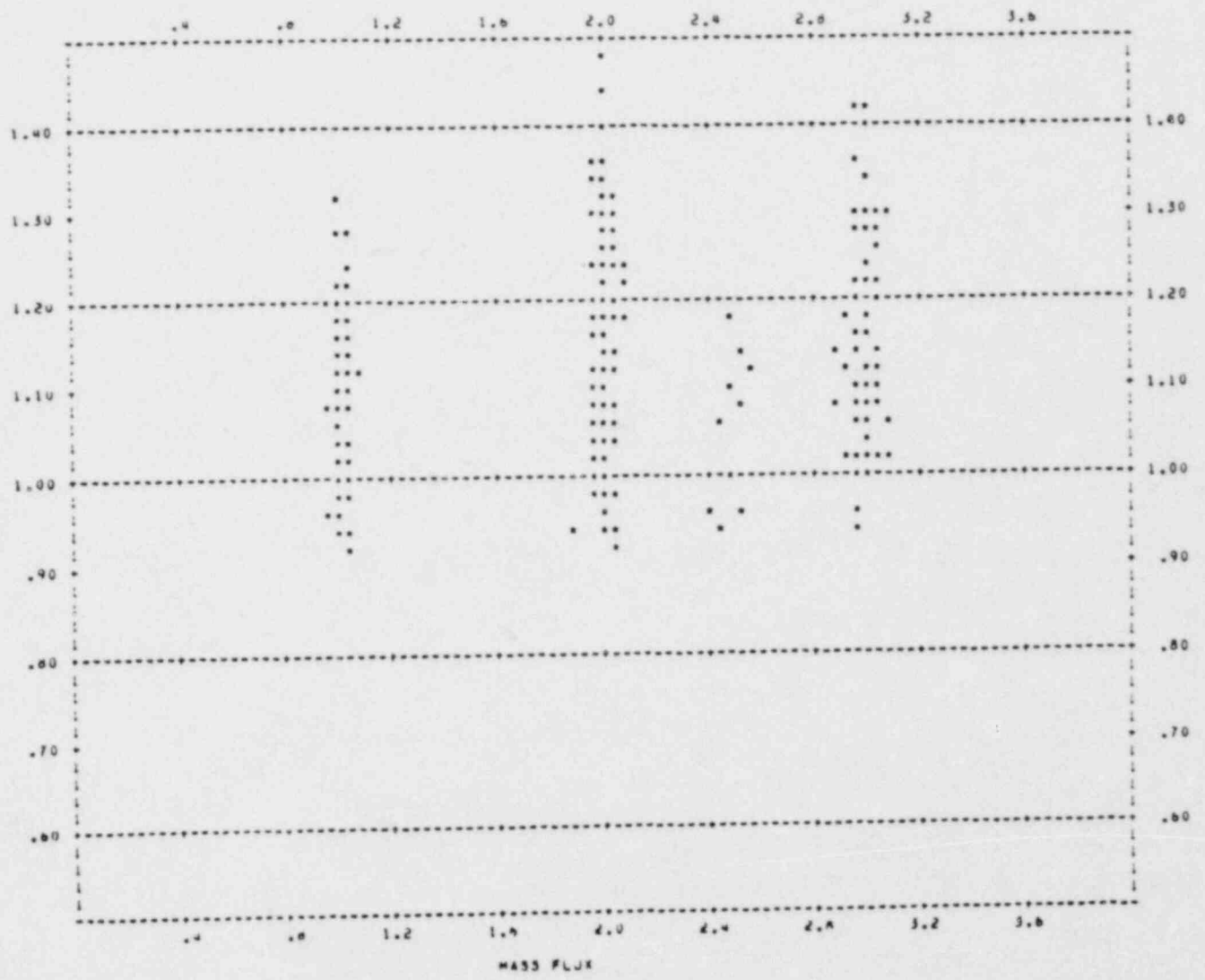

FIGURE 10o RATIO OF CALCULATED TO OBSERVED DNB HEAT FLUX VERSUS QUALITY FOR FOURTH DNB

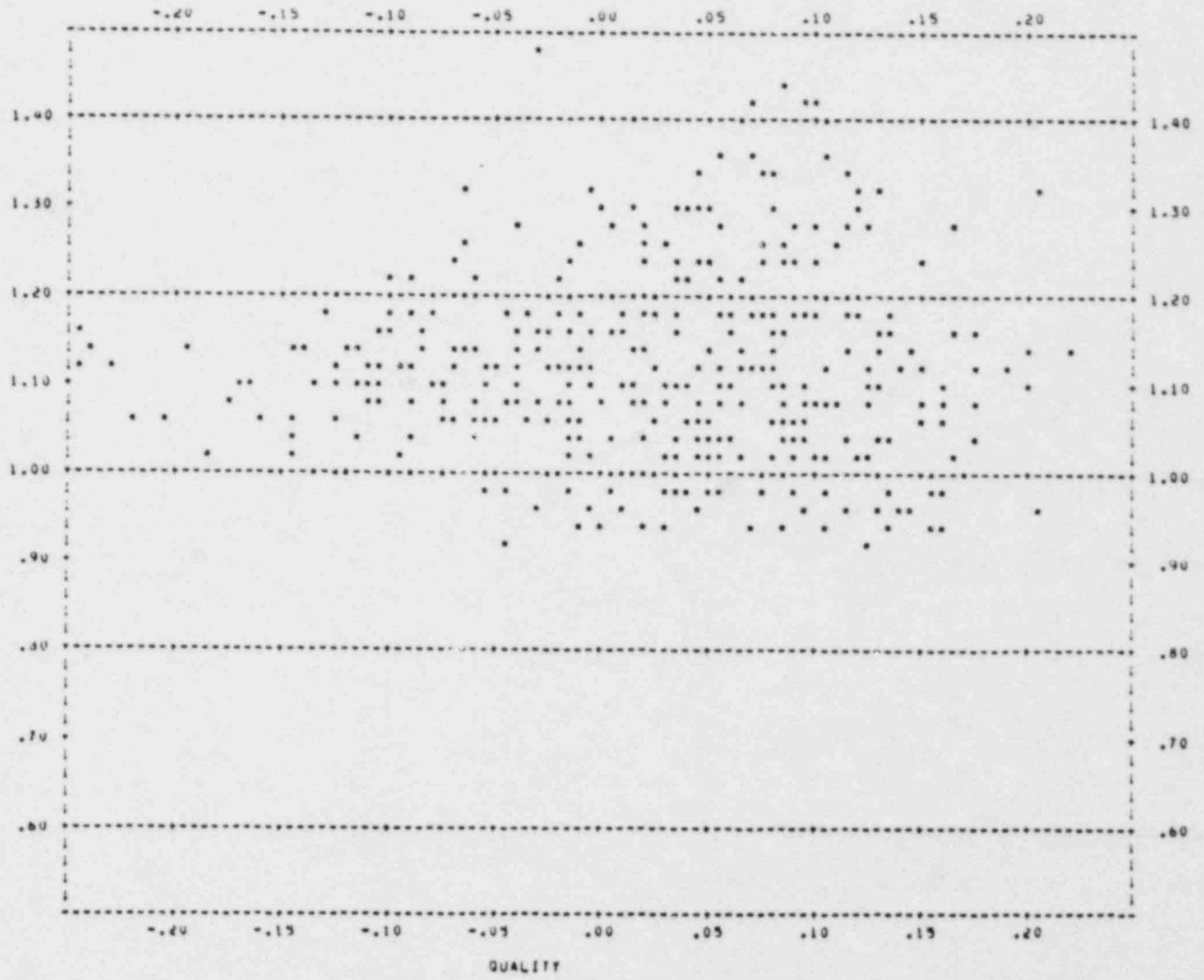

FIGURE 10p RATIO OF CALCULATED TO OBSERVED DNB HEAT FLUX VERSUS PRESSURE FOR FOURTH DNB

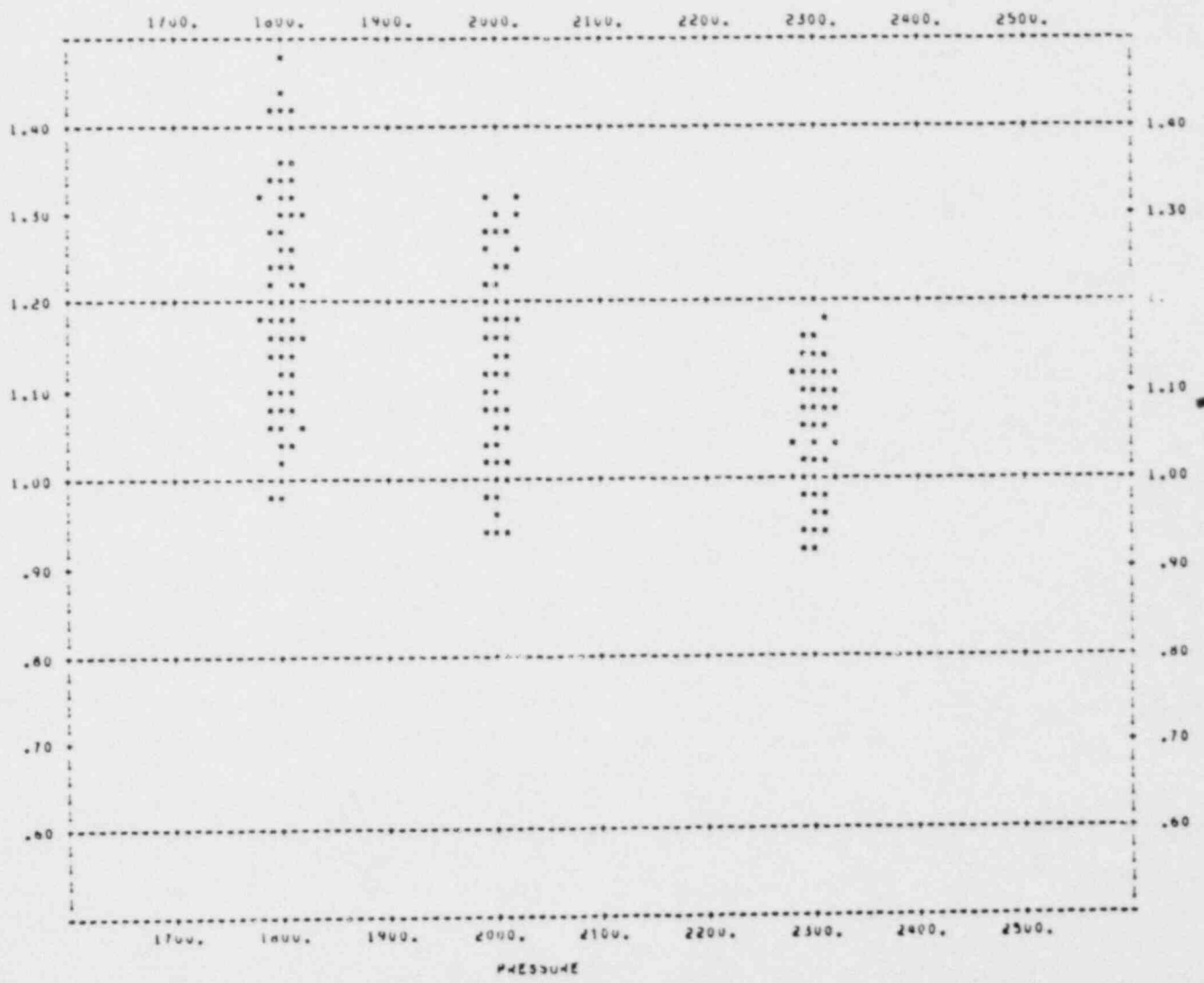

TABLE 3 STATISTICAL DATA ON DNB PREDICTIVE CORRELATION STUDIES

	Average Ratio of Calculated To Observed DNB Heat Flux				Standard Deviation			
	DNB Rank				DNB Rank			
	1	2	3	4	1	2	3	4
MASS FLUX								
1.00	1.122	1.102	1.095	1.101	.106	.094	.092	.091
2.00	1.135	1.131	1.133	1.129	.125	.122	.113	.110
3.00	1.152	1.140	1.140	1.144	.134	.116	.114	.110
PRESSURE								
1800	1.219	1.207	1.206	1.200	.115	.108	.106	.105
2000	1.146	1.132	1.130	1.133	.107	.097	.093	.092
2300	1.059	1.054	1.055	1.058	.084	.076	.063	.061
QUALITY								
-.15	1.114	1.098	1.098	1.108	.071	.061	.063	.063
-.10	1.123	1.104	1.107	1.112	.076	.064	.060	.063
-.05	1.130	1.110	1.109	1.120	.095	.091	.091	.100
.00	1.145	1.119	1.123	1.122	.120	.103	.104	.097
+.05	1.151	1.145	1.131	1.129	.132	.122	.113	.113
+.10	1.139	1.141	1.150	1.154	.137	.132	.132	.123
+.15	1.087	1.093	1.090	1.076	.131	.118	.105	.099
+.20	1.063	1.076	1.050	1.058	.128	.131	.130	.132
ALL	1.134	1.122	1.121	1.21	.123	.113	.108	.105

first DNB, at these points.

The above studies are within the scope of Task II of this project and will not be conducted as a part of this study.

3. GENERALIZATION OF MULTIPLE DNB ANALYSIS

The analysis of steady state multiple DNB events, presented in the previous section, was demonstrated on 3800 data points from 60 Combustion Engineering test sections with uniform axial and non-uniform radial heat flux distribution at operating pressures of 900, 1400, 1800, 2000 and 2300 psia. The conclusions presented in the previous section are, therefore, valid for this data set. In order to generalize the previous conclusions to test sections used by other vendors, it is necessary to apply the analysis to several other data sets and compare the results obtained.

The existing data base for steady state DNB heat flux tests at Columbia University, Heat Transfer Research Facility, is condensed in Table 4. Among the above data base, the data set numbers 5 and 7 are for refueling purposes; the data set numbers 9 and 10 pertain to rod bundles with triangular pitch; and the data set number 6 refer to the LOFT experiments. In view of their limited scope of application, these data sets will not be studied here. The data set numbers 8 and 4 are very similar to data set numbers 1 and 3 respectively, of which the data set number 1 has been already studied. The remaining data set numbers 2 and 3 will be considered for further analysis in this section and the result obtained will be compared with those of data set number 1. Briefly stated, the data sets used for the generalization of multiple DNB analysis will consist of the following:

Data Set No.	Vendor	Axial Flux Distribution	No.of T/S	No. of Data Pts.	Plant Type
1	Combustion Eng.	Uniform	60	3800	PWR
2	General Electric	Uniform	21	871	BWR
3	Westinghouse	Non-Uniform	23	838	PWR

TABLE 4 CONDENSED DATA BASE FOR STEADY STATE DNB HEAT FLUX TESTS[1] AT COLUMBIA UNIVERSITY HEAT TRANSFER RESEARCH FACILITY

NO.	VENDOR	AXIAL FLUX DISTRIBUTION	NUMBER OF TEST SECTIONS	NUMBER OF DATA POINTS	PLANT TYPE
1	Combustion Eng.	Uniform	60	3800	PWR
2	General Electric	Uniform	21	871	BWR
3	Westinghouse	Non-Uniform[2]	50	1500	PWR
4	Combustion Eng.	Non-Uniform	7	600	PWR
5	Exxon	Uniform	8	527	PWR
6	EG&G	Uniform	9	629	PWR
7	United Nuclear	Uniform	12	423	PWR
8	Babcock & Wilcox	Uniform	9	737	PWR
9	Atomic Energy of Canada, Ltd.	Uniform	13	400	PWR
10	United Kingdom Atomic Energy Authority	Uniform	9	45	PWR

Note 1: The radial flux distribution on all above test sections include both uniform and non-uniform flux distribution.

Note 2: Only 838 data points for 23 test sections are ready for processing at this time.

Typical parametric studies involving the plots of bundle average mass velocity contours, in the plane of the bundle average DNB heat flux versus bundle inlet temperature, for two test sections are shown in Figures 11a and 11b. Figure 11a shows the mass velocity contours for General Electric test section number 301 at 1000 psia from data set number 2. The General Electric test sections involve axially uniform heat flux with single (not quadrant) thermocouples placed on each rod near the channel exit. For this reason, only multiple DNB events of category C are observed. For example, *CCC on this figure indicates that the first DNB is followed by three DNB events of second, third and fourth rank occurring on a different rod from the first DNB. Figure 11b shows the mass velocity contours for Westinghouse test section number 147 at 2100 psia from data set number 3. The Westinghouse test sections involve axially non-uniform heat flux with single (no quadrant) thermocouples distributed vertically on the rods. For this reason, multiple DNB events of categories B and C are observed. For example, *BC on this figure indicates that the first DNB is followed by two DNB events of second and third rank, of which the second one occurred on the same rod at a different elevation from the first DNB and the third one occurred on a different rod from the first DNB. Characteristic features of these two plots are very similar to those of Figures 6a to 6e presented earlier for Combustion Engineering test section number 37 for data set number 1.

Parametric studies involving the plots of the bundle average DNB heat flux versus steam energy flow were also conducted for data set numbers 2 and 3. These studies demonstrate that the overall patterns for DNB events of higher rank are quite similar to those of the first DNB. However, these characteristics differ distinctly from those plotted for data set number 1 (Figures 7a to 7d) in two respects:

1) For General Electric test sections (data set number 2), most of the DNB data points are due to dryout referred to as

FIGURE 11a TYPICAL AVERAGE BUNDLE HEAT FLUX AT DNB VERSUS INLET TEMPERATURE AT 1000 PSIA

(FOR DATA SET # 2, GENERAL ELECTRIC BWR UNIFORM AXIAL HEAT FLUX)

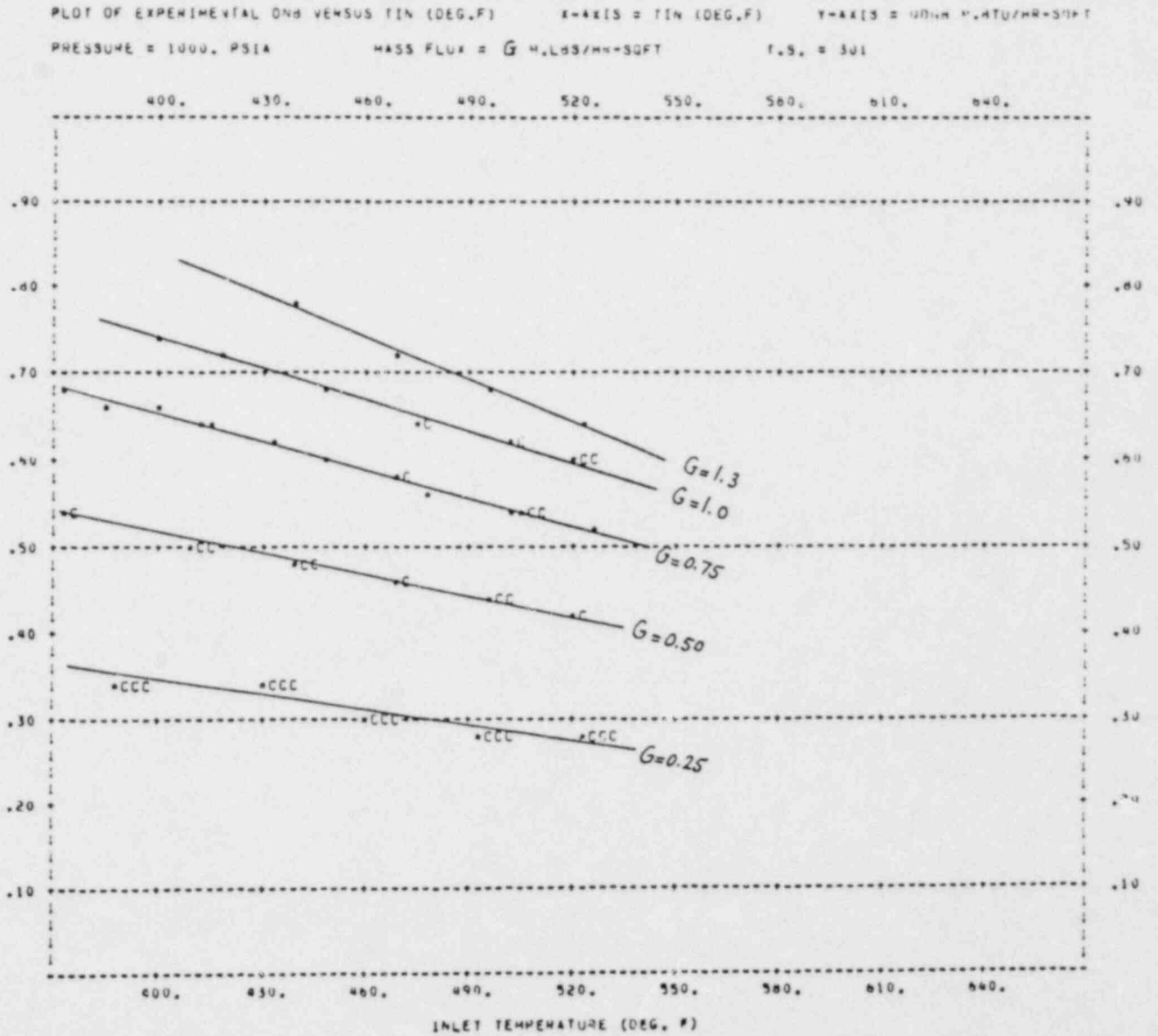

FIGURE 11b TYPICAL AVERAGE BUNDLE HEAT FLUX AT DNB VERSUS INLET TEMPERATURE AT 2100 PSIA

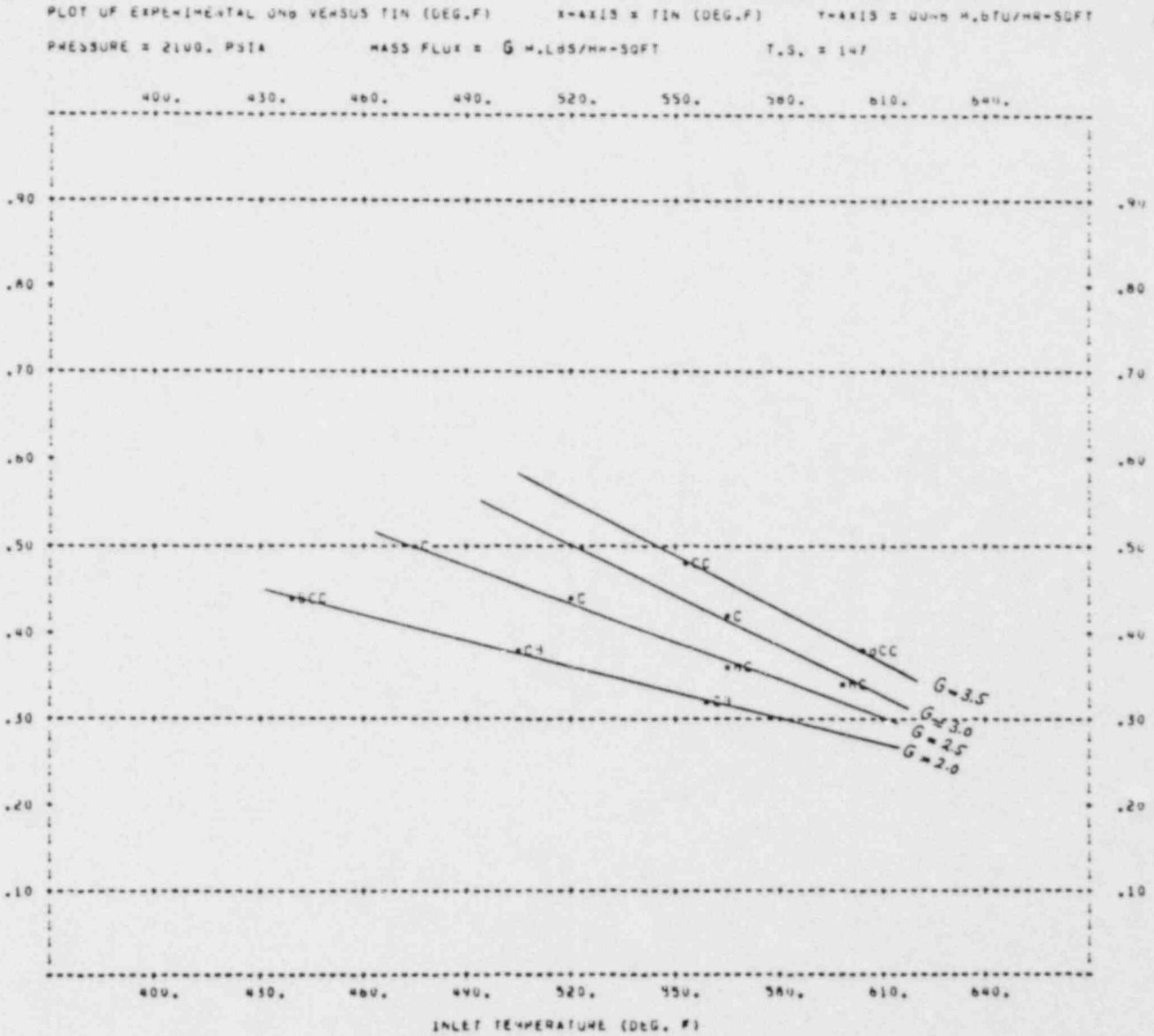

(FOR DATA SET # 3, WESTINGHOUSE PWR NON-UNIFORM AXIAL HEAT FLUX)

DNB-2, as opposed to vapor blanketing and the transition from nucleate boiling to film boiling referred to as DNB-1. The DNB-2 data points characteristically scatter around the line (3, 4):

$$q_{DNB} = k_1 \text{ (SEF)} \tag{3}$$

while the DNB-1 data points characteristically scatter around the lines

$$q_{DNB} = k_2 - k_3 \text{ (SEF)} \tag{4}$$

where k_1 is a positive constant independent of pressure while k_2 and k_3 are positive constants dependent on pressure. In other words, the SEF plots for data set number 1, which is mainly comprised of DNB-1 data points, result in constant pressure contours shown in Figures 7a to 7d characterized by Eq. (4). In contrast, the SEF plots for data set number 2, which is mainly comprised of DNB-2 data, yield points scattered around a line characterized by Eq. (3).

2) For Westinghouse test sections (data set number 3), the SEF plots are similar to those of Combustion Engineering (data set number 1). However, the data points in the former plot, have a larger scatter around the constant pressure contours as compared to the latter. This difference in SEF characteristics can be justified by observing that the data set number 3 involves test sections with non-uniform axial heat flux and as such is not as suitable for SEF plot application as the data set number 1 obtained from test sections with uniform axial heat flux.

Statistical analyses were performed on data set numbers 2 and 3. A comparison of the frequency of occurrence of the multiple DNB events versus pressure, bundle average mass velocity or bundle inlet quality with the overall trend is summarized in Tables 5a and 5b for data set numbers 2 and 3 respectively. The overall norms extracted from these tables, compared with that of data set number 1 in the following table, show a good degree of

TABLE 5a EFFECTS OF MASS FLUX, PRESSURE AND INLET QUALITY ON PERCENT NUMBER OF DNB EVENTS (FOR DATA SET # 2, GENERAL ELECTRIC BWR, UNIFORM AXIAL HEAT FLUX)

	DNB RANKS					
	1	2	3	4	5	Remarks
MASS FLUX:						
0.25	100	52	23	15	2	
0.50	100	45	14	3	–	
0.75	100	33	10	4	–	
1.00	100	29	7	1	–	
1.25	100	33	5	2	–	
PRESSURE:						
1000	100	38	12	5	1	
1200	100	41	10	1	–	
1400	100	35	9	3	–	
QUALITY:						
-0.10	100	42	13	5	–	
-0.30	100	31	9	2	–	
-0.50	100	46	23	11	3	
-0.70	——	—	—	—	–	Insufficient Data
-0.90	100	—	—	—	–	Insufficient Data
ALL	100	37	11	4	–	

TABLE 5b EFFECTS OF MASS FLUX, PRESSURE AND INLET QUALITY ON PERCENT NUMBER OF DNB EVENTS (FOR DATA SET # 3, WESTINGHOUSE PWR, NON-UNIFORM AXIAL HEAT FLUX)

	DNB RANKS					
	1	2	3	4	5	Remarks
MASS FLUX:						
1.00	100	44	44	44	25	
1.50	100	36	30	28	17	
2.00	100	37	16	7	4	
2.50	100	36	14	5	2	
3.00	100	39	18	6	3	
3.50	100	37	14	7	3	
PRESSURE:						
1500	100	35	17	10	5	
1800	100	34	10	5	1	
2100	100	38	18	7	5	
2400	100	39	16	6	4	
QUALITY:						
-0.1	100	41	18	12	7	
-0.3	100	37	16	7	3	
-0.5	100	36	16	8	5	
-0.7	100	32	16	—	–	Insufficient Data
-0.9	100	—	—	—	–	Insufficient Data
ALL	100	37	17	8	4	

similarity:

	Data Sets		
	1	2	3
First DNB	100	100	100
Second DNB	34	37	37
Third DNB	16	11	17
Fourth DNB	7	4	8
Fifth DNB	3	–	4

A further study of Tables 5a and 5b reveals that the frequency of occurrence of multiple DNB events generally decrease as the mass velocities increase which is in a good agreement with earlier results obtained for data set number 1. Furthermore, Table 5b indicates that for Westinghouse PWR test sections, the frequency of occurrence of multiple DNB events is lowest near 1800 psia and increases at lower and higher pressures which is in good agreement with Figure 8b for Combustion Engineering PWR test sections. The range of operating pressures for General Electric BWR test sections (Table 5a) is not sufficiently wide to demonstrate this characteristic. Finally, Tables 5a and 5b indicate that the frequency of occurrence of multiple DNB events is lowest near an inlet quality of -0.3 which confirms the results obtained earlier in Figure 8c.

The frequency distribution of the occurrence of the multiple DNB events on data set numbers 2 and 3 revealed a fairly similar pattern as compared to that of data set number 1. This similarity can be confirmed by comparing the overall relative cumulative frequency distribution plots for Combustion Engineering, General Electric and Westinghouse data sets in Figures 9a, 12 and 13 respectively.

The predictive correlation studies, using the Bowring correlation, were also performed on data set numbers 2 and 3. The result of these studies are summarized in Tables 6a and 6b for General Electric and Westinghouse test sections. A comparison

FIGURE 12 OVERALL RELATIVE CUMULATIVE FREQUENCY DISTRIBUTION FOR DATA SET # 2, GENERAL ELECTRIC BWR UNIFORM AXIAL HEAT FLUX

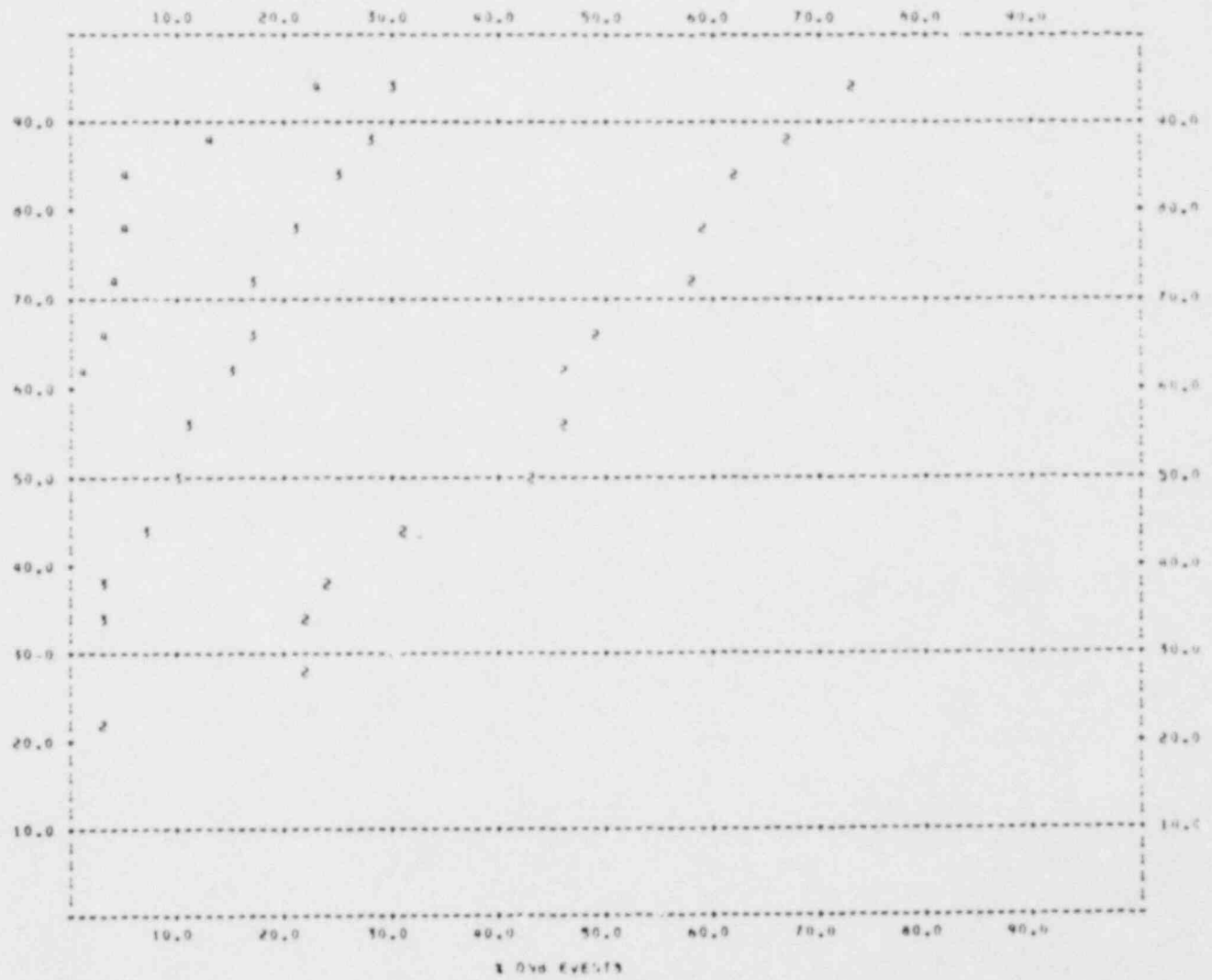

FIGURE 13 OVERALL RELATIVE CUMULATIVE FREQUENCY DISTRIBUTION FOR DATA SET # 3, WESTINGHOUSE PWR NON-UNIFORM AXIAL HEAT FLUX

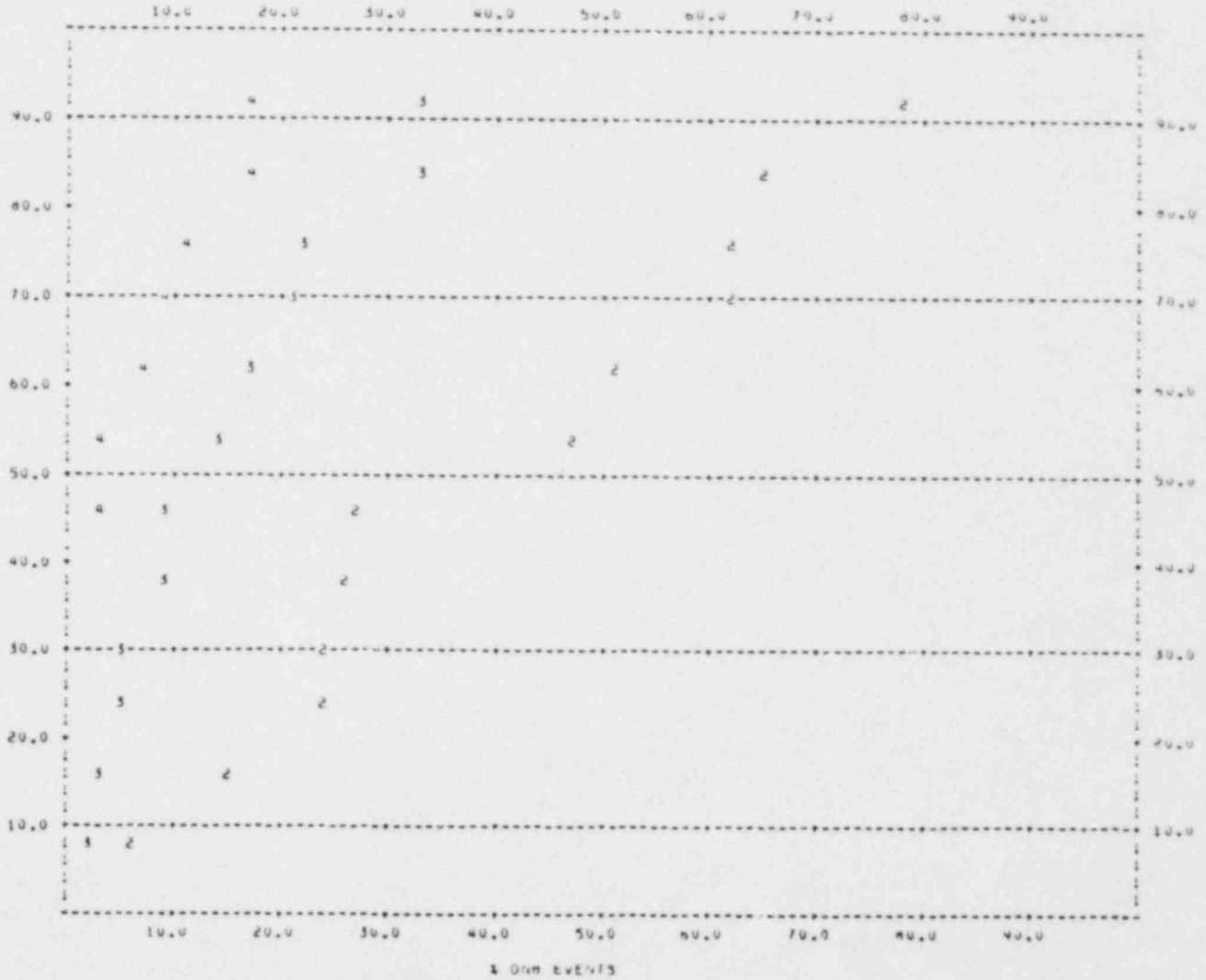

TABLE 6a STATISTICAL DATA ON DNB PREDICTIVE CORRELATION STUDIES FOR DATA SET # 2, GENERAL ELECTRIC BWR, UNIFORM AXIAL HEAT FLUX

	Average Ratio of Calculated To Observed DNB Heat Flux				Standard Deviation			
	DNB Rank				DNB Rank			
	1	2	3	4	1	2	3	4
MASS FLUX:								
0.25	1.017	.989	.984	.957	.058	.056	.064	.064
0.50	1.019	.988	.959	.924	.073	.048	.039	.026
0.75	1.055	1.011	.987	.978	.098	.082	.056	.081
1.00	1.079	1.025	1.017	1.012	.092	.070	.072	.014
1.25	1.081	.998	1.005	1.042	.108	.066	.091	.048
PRESSURE:								
1000	1.032	.982	.968	.957	.091	.052	.053	.059
1200	1.080	1.037	1.034	—	.080	.054	.045	—
1400	1.095	1.060	1.037	—	.076	.080	.068	—
QUALITY:								
-0.050	1.234	—	—	—	.040	—	—	—
+0.050	1.139	1.105	1.035	—	.088	.107	.075	—
+0.150	1.079	1.025	1.031	1.059	.082	.058	.060	.045
+0.250	1.012	.987	.973	.947	.066	.059	.062	.049
+0.350	1.000	.991	.965	.935	.058	.045	.036	.036
+0.450	1.989	.965	.971	.944	.058	.045	.056	.054
+0.550	.994	.989	.974	.957	.055	.058	.066	.068
ALL	1.050	1.002	.983	.964	.091	.064	.060	.063

- designates insignificant number of data points

TABLE 6b STATISTICAL DATA ON DNB PREDICTIVE CORRELATION STUDIES FOR DATA SET # 3, WESTINGHOUSE PWR, NON-UNIFORM AXIAL HEAT FLUX

	Average Ratio of Calculated To Observed DNB Heat Flux				Standard Deviation			
	DNB Rank				DNB Rank			
	1	2	3	4	1	2	3	4
MASS FLUX:								
1.50	1.059	1.102	1.126	1.107	.125	.148	.093	.135
2.00	.976	1.010	1.061	1.018	.134	.168	.137	.166
2.50	.934	.934	.942	.972	.118	.098	.095	.144
3.00	.913	.911	.967	.860	.115	.111	.151	.146
PRESSURE:								
1500	1.061	1.041	1.052	1.069	.186	.199	.140	.130
1800	1.018	1.057	1.077	1.101	.109	.139	.107	.069
2100	.913	.951	1.021	.971	.104	.105	.120	.147
2400	.852	.860	.881	.854	.099	.110	.137	.093
QUALITY:								
0.05	.971	.982	1.006	1.045	.154	.180	.129	.182
0.10	.933	.935	.978	.976	.124	.138	.162	.166
0.15	.968	1.003	1.008	1.019	.130	.120	.137	.170
0.20	.948	.940	1.036	1.039	.122	.145	.146	.162
0.25	.968	.943	.909	.975	.102	.038	.110	.074
ALL	.965	.966	1.003	1.005	.155	.155	.144	.160

of these tables with Table 3 confirms the previous results that: 1) the trends in DNB events of higher rank generally follow those of the first DNB; and 2) the DNB correlations based on local conditions at first DNB can predict the DNB events of higher rank with the same degree of accuracy as the first DNB. These comparisons also demonstrate the need for further predictive correlation studies based on local conditions as pointed our earlier.

Based on the average values and standard deviations presented in Tables 3, 6a and 6b, it is noteworthy to observe that the Bowring Correlation predicts the General Electric BWR data reasonably well. However, the performance of the correlation is less satisfactory for the prediction of Combustion Engineering and Westinghouse PWR data.

4. ANALYSIS OF FLOW DECAY MULTIPLE DNB EVENTS

As stated earlier, two types of DNB heat transfer tests are conducted at Columbia rod bundle test facility: 1) steady state DNB tests; and 2) transient DNB tests. The analysis of steady state multiple DNB events was conducted in the previous sections. A study of the transient multiple DNB events, under flow decay conditions, will be undertaken in this section.

The test section geometry, including the axial and radial flux distribution, is typically shown in Figure 4. The test conditions, including the bundle inlet temperature, initial average mass velocity, average heat flux and pressure as well as the time history of normalized flow decay are typically shown in Figure 5.

The normalized flow decay defined as the ratio of the instantaneous to the initial average bundle mass velocity, G/G_i, versus time is a ramp function typically shown in Figure 14.

In flow decay tests, all test conditions including the bundle inlet temperature, average heat flux and pressure are held constant, as closely as possible. The bundle average mass velocity is lowered as indicated by the flow decay time history. The rod thermocouples temperature excursions are recorded on the strip chart recorder and are also stored by the data acquisition computer system. Typical rod thermocouples temperature excursions, as recorded by the computer, are shown in Figures 15a, 15b, 15c, 15d and 15e for Exxon flow decay test run # FD003A for thermocouple numbers 3.6, 5.5, 5.6, 5.8 and 3.8 respectively. Based on these plots, the order of occurrence of the multiple DNB events are recorded and entered in Figure 5 and Table 7.

Further examination of these records reveals the following features:

1) The number of multiple DNB events for flow decay tests

FIGURE 14 NORMALIZED FLOW DECAY TIME HISTORY

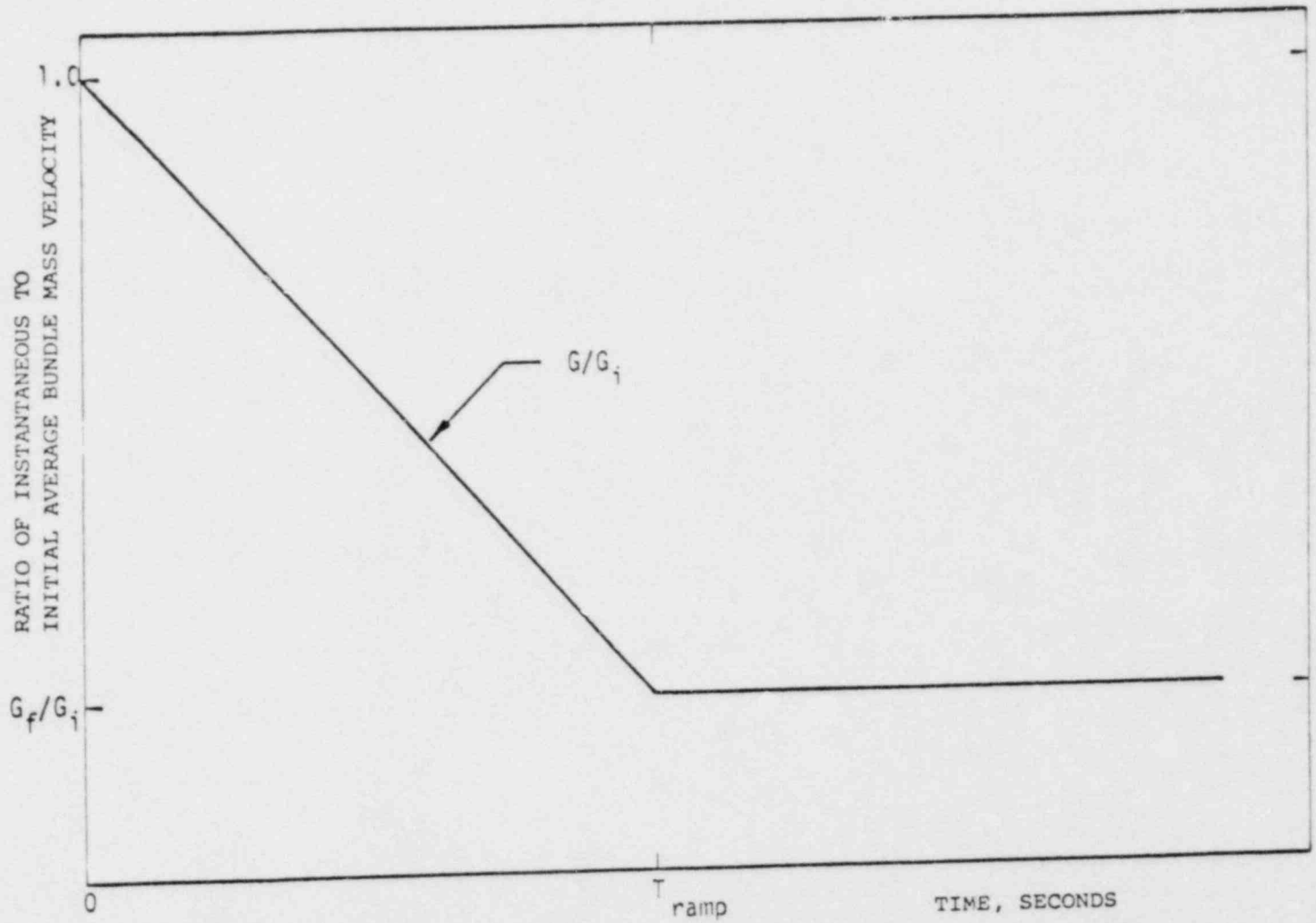

FIGURE 15a TEMPERATURE EXCURSION OF THERMOCOUPLE # 3.6

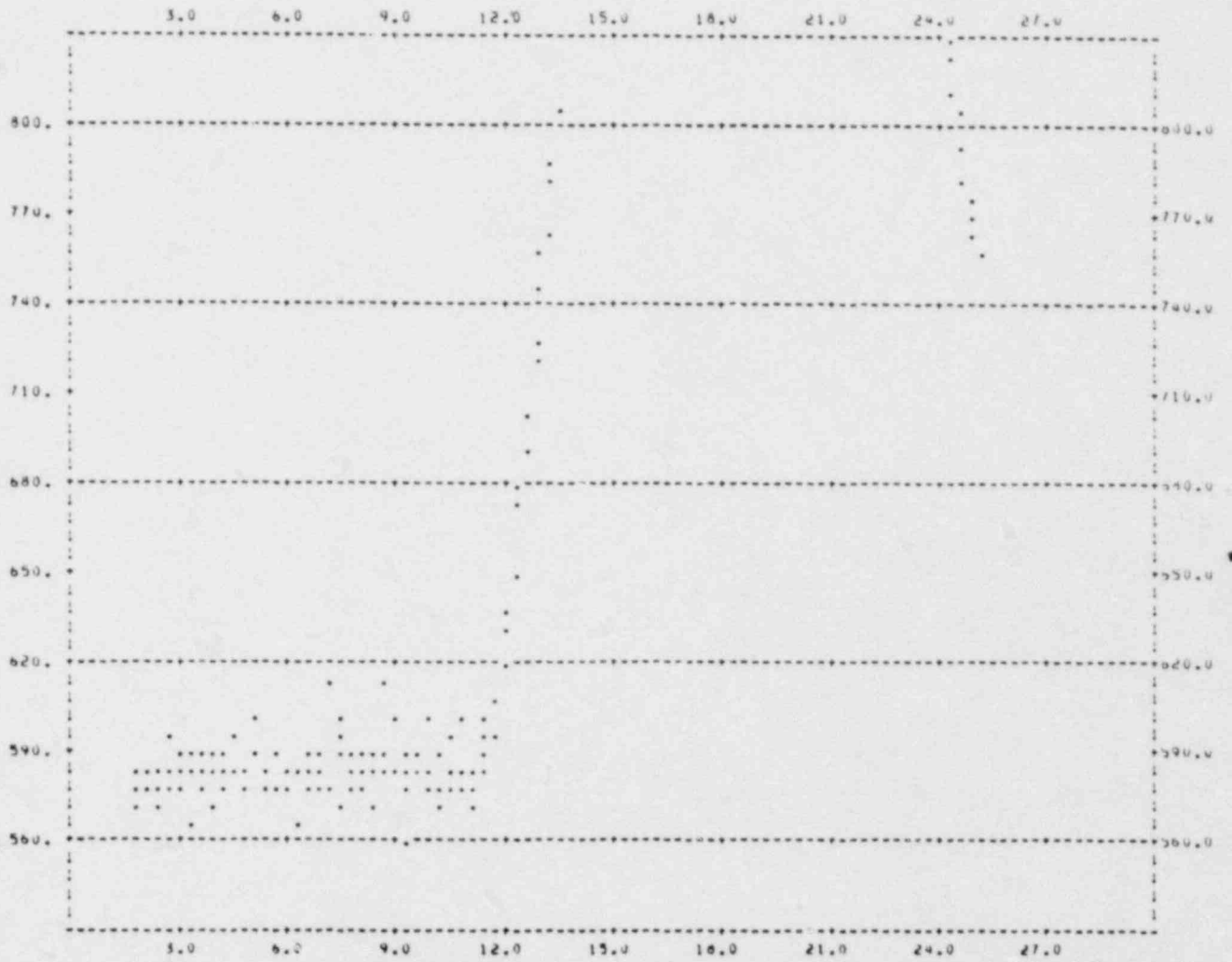

FIGURE 15b TEMPERATURE EXCURSION OF THERMOCOUPLE # 5.5

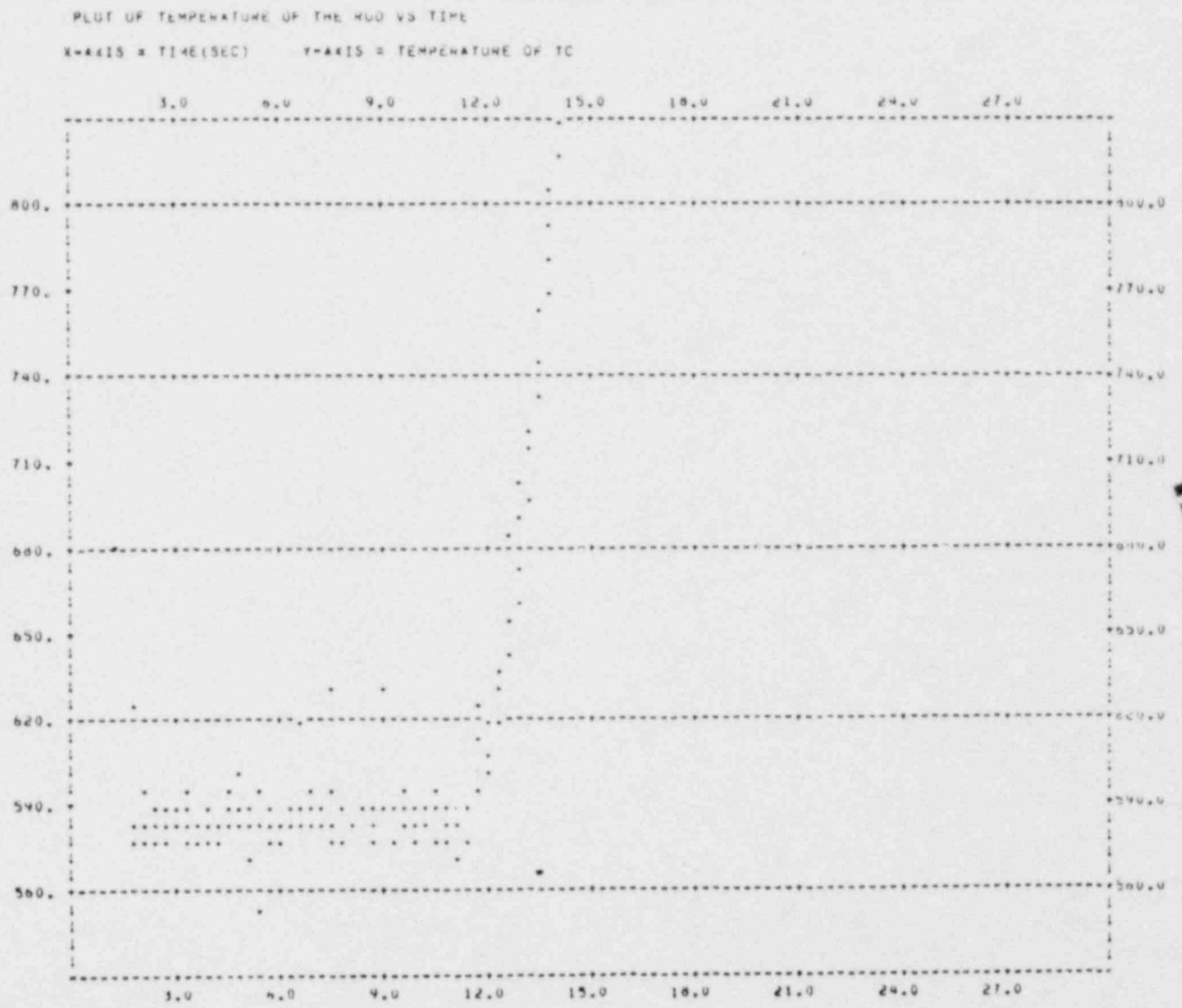

FIGURE 15c TEMPERATURE EXCURSION OF THERMOCOUPLE # 5.6

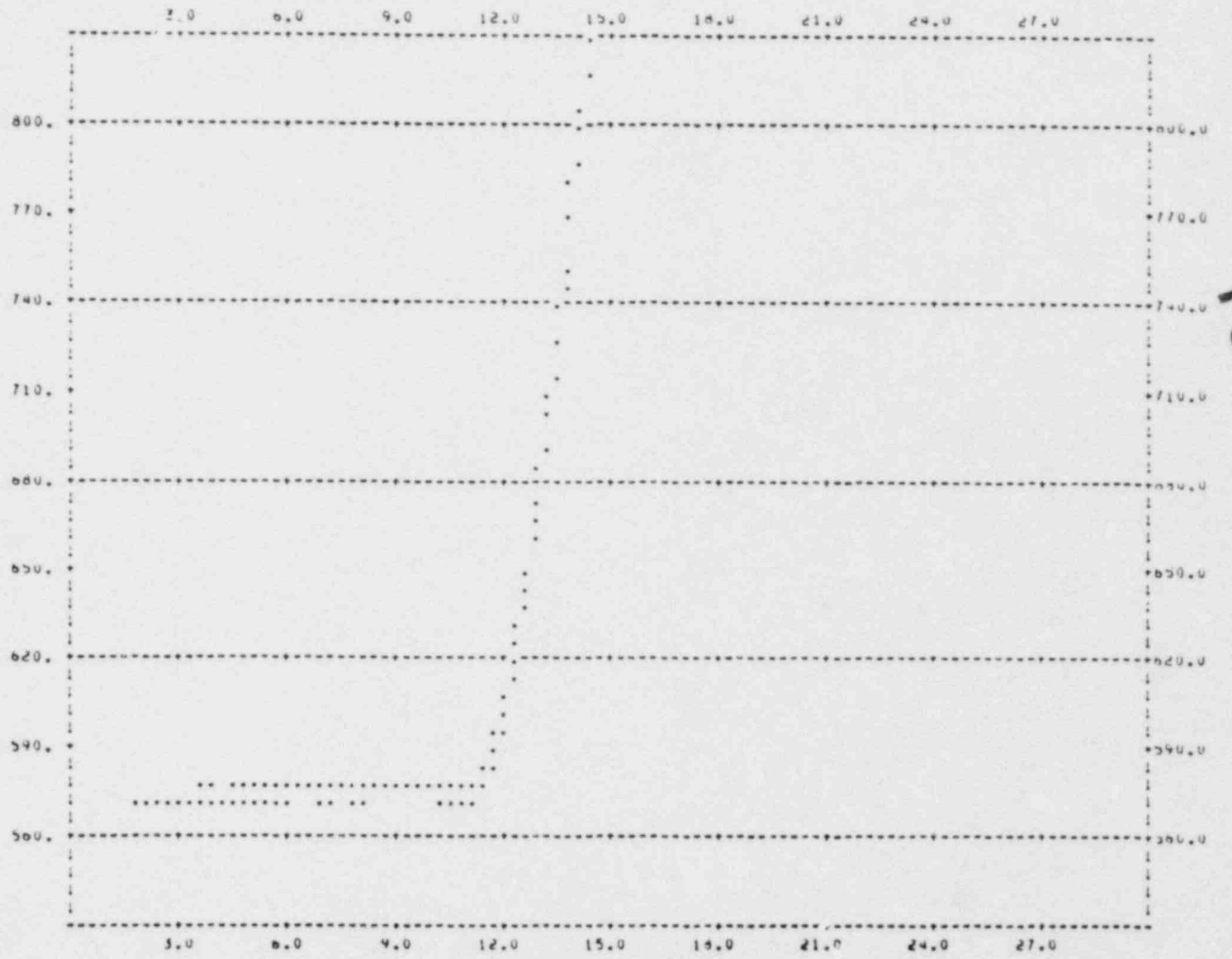

FIGURE 15d TEMPERATURE EXCURSION OF THERMOCOUPLE # 5.8

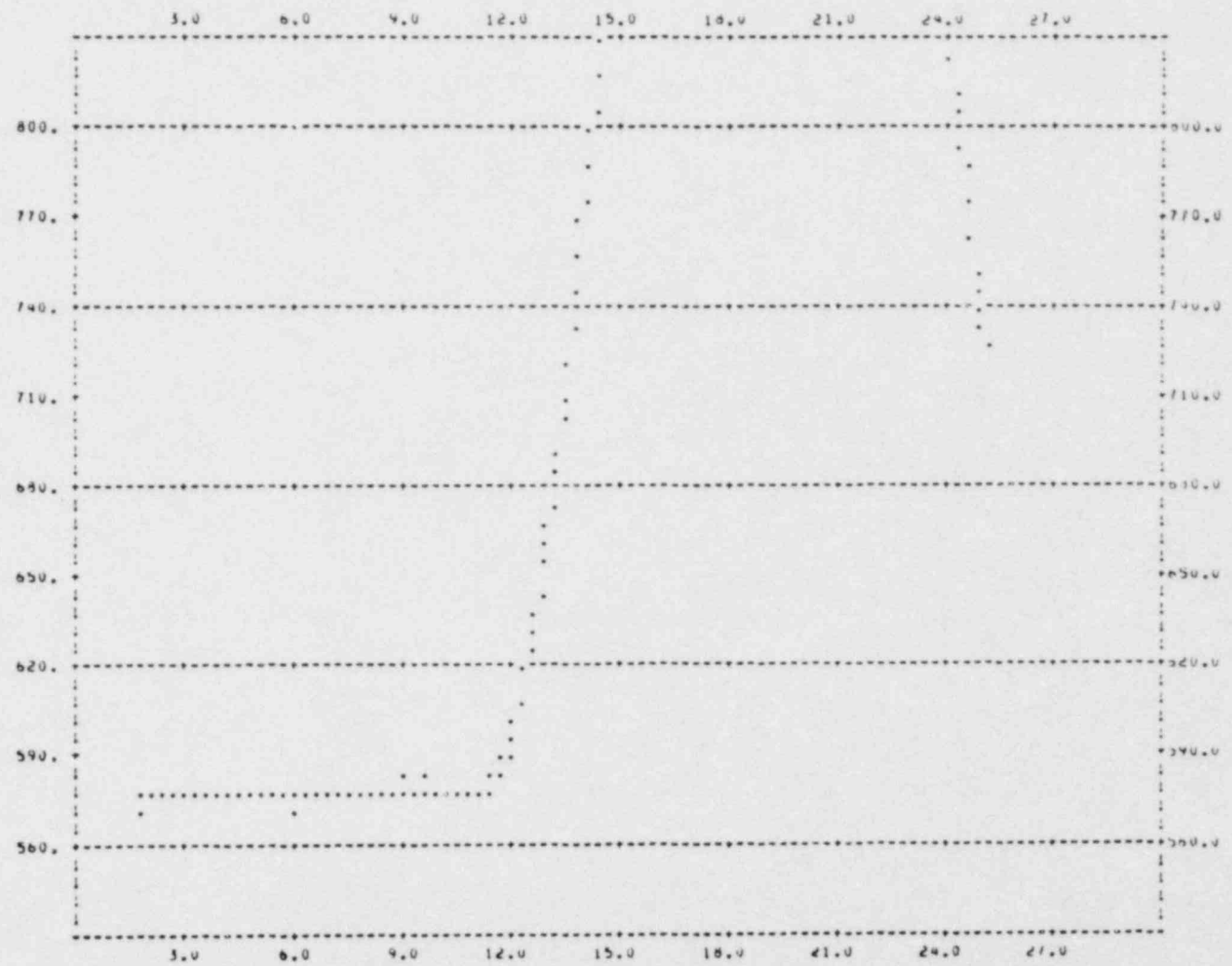

FIGURE 15. TEMPERATURE EXCURSION OF THERMOCOUPLE # 3.8

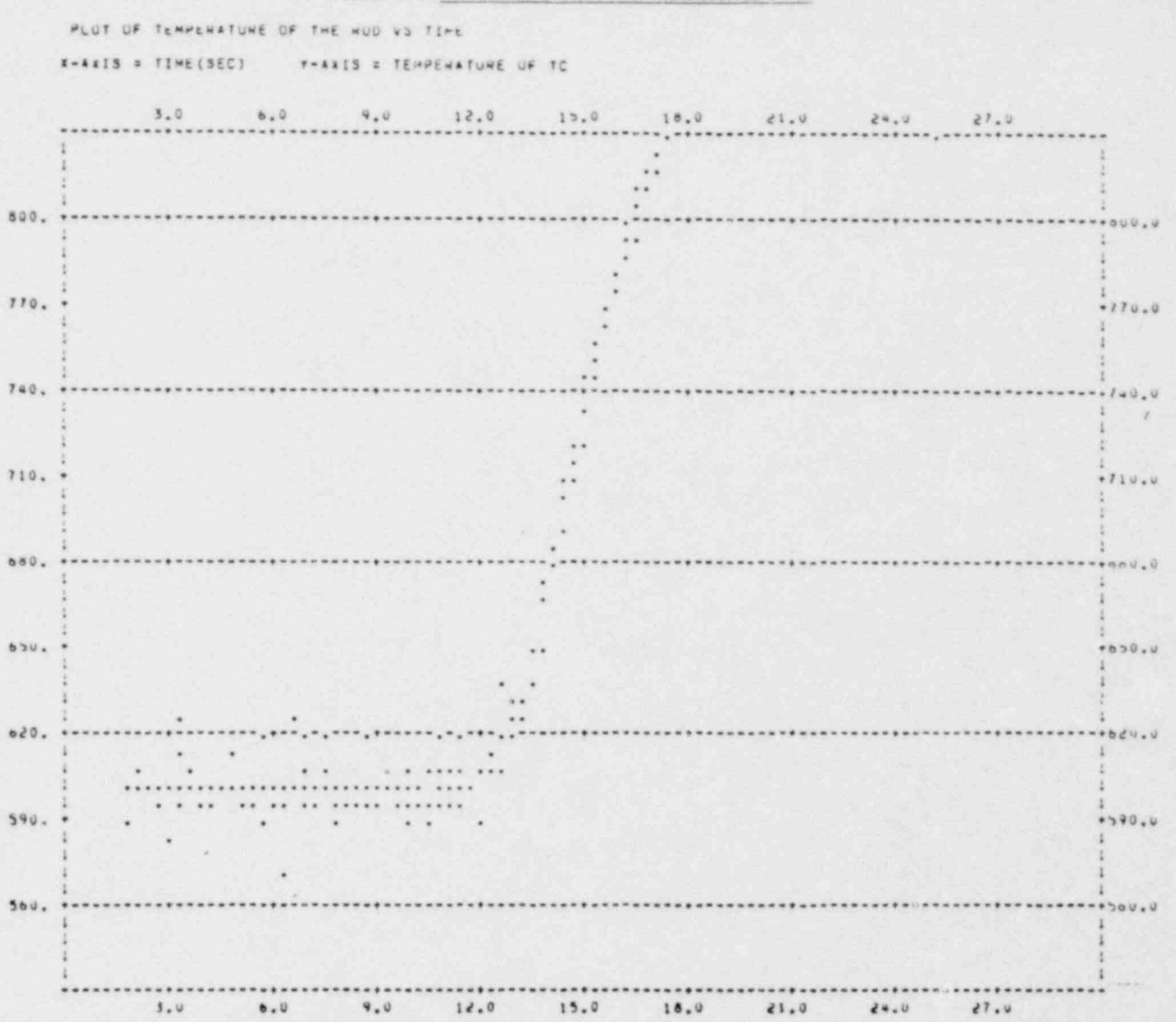

TABLE 7 MULTIPLE DNB EVENTS IN EXXON FLOW DECAY TESTS[1]

RUN NO.	SLOPE OF FLOW DECAY LINE	G_i	q	DNB RANKS FIRST	SECOND	THIRD	FOURTH	FIFTH	T_{ramp}	G_f	Percent DNB
FD001A[2]	.05	1.0	0.20	5.2	3.2*	5.3*	3.3**	1.2**	14.0	0.3	100
FD001A[2]	.05	1.0	0.20	5.2	1.2	5.3			14.0	0.3	60
FD002	.10	1.0	0.20	5.2	5.3*	3.2*	1.2*		7.0	0.3	80
FD003A	.05	0.8	0.20	3.6	5.5*	5.6*	5.8	3.8	12.5	0.3	100
FD004	.10	0.8	0.20	5.6	4.7*	7.5*	4.6*	2.5	6.25	0.3	100
FD006	.10	1.0	0.24	5.5	5.2	1.3	1.2*	5.3*	6.0	0.4	30
FD005A	.05	1.0	0.24	5.2	1.2*	1.3*	5.3**	7.2**	12.0	0.4	31

1. The following runs are conducted with bundle inlet temperature of 516°F and pressure of 1000 psia

2. This run was conducted twice.

NOTE 1) DNB events marked with asterisk (*) have occurred simultaneously.

NOTE 2) DNB events marked with double asterisk (**) have occurred simultaneously.

are much higher than those for steady state multiple DNB tests. In fact, the percent number of thermocouples experiencing DNB is inversely proportional to the final average bundle mass velocity. As shown in the last two columns of Table 7, for a final average bundle mass velocity of 0.4 M lbs/hr-ft^2 nearly one third of the thermocouples experienced DNB while for a final mass velocity of 0.3 M lbs/hr-ft^2, the number of thermocouples experiencing DNB increased dramatically to the range of 60 to 100 percent.

2) Many DNB events of higher rank than first occur almost simultaneously. This behavior is documented in Table 7. For example in Exxon run # FD003A the thermocouples temperature excursions shown in Figures 15b and 15c indicate that thermocouples 5.5 and 5.6, marked with asterisks, experienced DNB simultaneously. This fact renders the determination of the order of occurrence of multiple DNB events very difficult.

3) The information collected in this study, typically shown in Figures 4, 5, 15a to 15e and Table 7 will provide the needed input data for a subchannel computer code, such as COBRA-IIIC, for the determination of the rod bundle local conditions during flow decay tests. This information will further serve to ascertain the adequacy of steady state predictive correlations based on local conditions at first DNB, for the prediction of DNB events of higher rank during flow decay conditions.

5. CONCLUSIONS AND RECOMMENDATIONS

Three data sets of rod bundle heat transfer tests performed at Columbia University, Heat Transfer Research Facility, are examined for multiple DNB events. These data sets are comprised of:

1) 3800 data point for 60 Combustion Engineering test sections with uniform axial flux distribution simulating PWR reactor cores.

2) 871 data points for 21 General Electric test sections with uniform axial flux distribution simulating BWR reactor cores.

3) 838 data points for 23 Westinghouse Electric Corporation test sections with non-uniform axial flux distribution simulating PWR reactor cores.

A combination of parametric studies, statistical analyses and predictive correlation approach based on bundle average conditions are employed to compare the characteristics and the probabilities of occurrence of steady state DNB events of higher rank with the first DNB for the three data sets mentioned above. These studies have led to the following conclusions:

1) The number of multiple DNB events of higher rank than first are significant as compared to the first DNB.

2) The frequency of occurrence of multiple DNB events decrease at high mass velocities (2 to 3 M lbs/hr-ft^2), at intermediate operating pressures (1400 to 1800 psia), and at intermediate inlet subcooling (inlet quality = -0.3).

3) The characteristic behavior of DNB events of higher rank than first are essentially close to those of the first DNB. Similarity among the multiple DNB events is established by comparison of two noteworthy characteristics:

   a) The slope and the intercept of the pressure contours in the DNB heat flux versus steam energy flow plane.

b) The statistical results obtained from the application of the Bowring DNB predictive correlation.

4) The presently available DNB correlations for the first DNB, based on the bundle average conditions, are useful in the prediction of DNB events of higher rank. These correlations could predict the DNB events of higher rank with the same degree of accuracy as the first DNB. These accuracies, however, are inadequate for most design applications. To provide more accurate correlations, the predictive correlations should be based on local conditions.

To ascertain the adequacy of the predictive correlations based on local conditions at first DNB, for the prediction of DNB events of higher rank, it is recommended that the following studies be undertaken:

a) Employing the information collected in this study, for steady state and flow decay DNB tests and a subchannel computer code, such as COBRA-IIIC, the rod bundle local conditions at DNB should be determined.

b) The predictive correlations based on local conditions at first DNB, should then be applied for the prediction of DNB events of higher ranks and compared to the information compiled in the present study.

The recommended study will provide the accuracy and may prove the adequacy of the available predictive correlations in the prediction of the multiple DNB events.

6. REFERENCES

1) Hovemeyer, W,E., Sreepada, S.R., and Casterline, J.E., "Uprated DC Power System and Thermal-Hydraulic Facilities at Columbia University", NP-773 Project 345-1, 1978, Electric Power Research Institute, Palo Alto, California.

2) Bowring, R.W.,, "A New Mixed Flow Cluster Dryout Correlation for Pressures in the Range 0.6 - 15.5 MN/m^2 (90 - 2250 psia) - for Use in a Transient Blowdown Code", Institute of Mechanical Engineers, 1977, p. 175 - 179.

3) Foster, A.R., and Wright, Jr., R.L., Basic Nuclear Engineering, Allyn and Bacon, Inc. third edition, p. 399.

4) Levedahl, W.J., "Application of Steam Energy Flow to Reactor Design" Transactions of the Americal Nuclear Society, 5,1 (June 1962) pp. 149-150.

7. APPENDIX - A SUMMARY OF BOWRING CORRELATION

Bowring has developed a DNB correlation based on global test conditions in rod bundles. This correlation is appropriate for application in the range of the present analysis and is considered to be more accurate than the Macbeth and Barnett correlations (2).

In this correlation, the DNB heat flux q_{DNB} is given by

$$q_{DNB} = \frac{A - B\, h_{fg}\, x_{in}}{C + Z\, Y} \qquad \text{(A-1)}$$

where

h_{fg} = latent heat of evaporation, Btu/lb

x_{in} = steam quality at bundle inlet

Z = bundle heated length, in

Y = ratio of average heat flux over the heated length to local radially averaged heat flux at DNB point (Y = 1 for axially uniform heat flux)

A, B, C = parameters depending on the pressure range and defined as follows:

1) For $p \leq 1250$ psia

$$A = \frac{242.4\, F_1\, G\, D_h}{1 + \dfrac{1.52\,(F_p\, D_h)^2\, G}{F_2\, D_w^{1.3}\,[1 + G(0.8 F_p\, D_h / D_w - 1)]}} \qquad \text{(A-2)}$$

$$B = 0.25\, G\, D_h\, e^{-0.2G} \qquad \text{(A-3)}$$

$$C = 60\, D_w^{0.57}\, G^{0.27} \left\{ 1 + \frac{Y-1}{G+1} \right\} \qquad \text{(A-4)}$$

where

p = pressure, psia

G = bundle inlet mass velocity, M lbs/hr-ft^2

D_h = channel hydraulic diameter, in

D_w = channel heated diameter, in

F_p = radial heat flux peaking factor

F_1, F_2 = parameters defined hereunder:

$$p_T = p / 1000 \qquad \text{(A-5)}$$

$$F_1 = \left[1.0 - 0.04\, p_T \left(1 + 0.47\, p_T^2 \right)^{1/2} \right]^2 \qquad \text{(A-6)}$$

$$F_2 = (3.2 - p_T)(0.32 + 0.135\, p_T) \quad \text{For } p > 650 \text{ psia} \qquad \text{(A-7)}$$

2) For p > 1250 psia

$$A = A_2 + (2.250 - 0.001\, p)(A_1 - A_2) \qquad \text{(A-8)}$$

where

$$A_1 = \text{value of A obtained from equation (A-2) at } p = 1250,\ F_1 = 0.8726 \text{ and } F_2 = 0.953 \qquad \text{(A-9)}$$

$$A_2 = 18.0\ G + \frac{9.5\ GD_h}{0.1 + G} \qquad \text{(A-10)}$$

Values of B and C are to be obtained from equations (A-3) and (A-4) respectively.